

STUDIES IN THE SPOUTING
OF
MIXED PARTICLE SIZE BEDS

by

KANDULA VENKATA SUBBA REDDY

B. Sc., (Hons), Andhra University, Waltair, India, 1954
M. Sc., (Tech), Andhra University, Waltair, India, 1956

A THESIS SUBMITTED IN PARTIAL FULFILMENT OF
THE REQUIREMENTS FOR THE DEGREE OF
MASTER OF APPLIED SCIENCE

in the Department
of
Chemical Engineering

We accept this thesis as conforming to the
required standard.

THE UNIVERSITY OF BRITISH COLUMBIA

March, 1963

In presenting this thesis in partial fulfilment of the requirements for an advanced degree at the University of British Columbia, I agree that the Library shall make it freely available for reference and study. I further agree that permission for extensive copying of this thesis for scholarly purposes may be granted by the Head of my Department or by his representatives. It is understood that copying or publication of this thesis for financial gain shall not be allowed without my written permission.

Department of Chemical Engineering

The University of British Columbia,
Vancouver 8, Canada.

Date March 27, 1963

ABSTRACT

Correlations of minimum spouting velocity, with one or two exceptions, have been reported only for particles of uniform size. If spouting techniques are to be applied to fluid-solid contacting operations other than the drying of grains, the effect of particle size distribution must also be known.

In this work, spouting characteristics of a variety of materials over wide and narrow particle size distributions have been studied in a 6-inch diameter column fitted with a 60° conical bottom.

Air inlets used were of a special design which resulted in improved spoutability of materials and inlet orifice varied in size from 3/8-inch to 3/4-inch.

Mean particle diameters were varied from 0.0134 to 0.104 inches, solids density from 65.8 to 246.3 lb._m/ft.³ and static bed heights from 7.5 to 40 inches.

The minimum spouting velocity for all the runs has been correlated to within $\pm 10\%$ by using the arithmetic mean Tyler screen size for individual fractions of particulate materials; by assuming a geometric mean particle diameter as the characteristic diameter for individual grains of granular material and the length mean diameter as the representative diameter for mixtures of all materials.

Some qualitative measurements of solids attrition rates were also made.

ACKNOWLEDGEMENTS

The author wishes to express his sincere thanks to Dr. J. W. Smith for his very valuable guidance and encouragement throughout this investigation.

Thanks are also due to Dr. Norman Epstein for suggesting the problem and for his helpful discussions.

The author is deeply indebted to Professor J. S. Forsyth for his keen interest in this work and his invaluable assistance in design of the equipment.

Thanks are also due to Mr. R. Muelchen, Technical Supervisor, for his help in building the apparatus.

TABLE OF CONTENTS

		Page
CHAPTER I	INTRODUCTION	1
CHAPTER II	REVIEW OF LITERATURE AND THEORY	
II-1	General Description of Spouting Phenomenon	3
II-2	Explanation of Some Important Variables	
(a)	Incipient and Minimum Spouting Velocity	5
(b)	Static Bed Height	5
(c)	Maximum Spoutable Bed Depth (or Height)	6
(d)	Mean Particle Diameter	
(1)	General	7
(ii)	Characteristic Diameter of Single (or Uniform) size Fraction	7
(iii)	Definitions of Mean Diameters of Mixed Size Particles	8
(1)	Volume or Weight Mean Diameter	8
(2)	Surface Mean Diameter	9
(3)	Length Mean Diameter	9
(4)	Mean Volume or Weight Diameter	10
(5)	Mean Surface Diameter	10
(6)	Mean Length Diameter	11
(iv)	Usage of Characteristic/Mean Particle Diameters	11
II-3	Mathur-Gishler Correlation for Minimum Spouting Velocity	14
II-4	Madonna-Lama-Brisson Equation for Minimum Spouting Velocity	16
II-5	Becker's Analysis	17

TABLE OF CONTENTS Continued

		Page
II-6	Work of Buchanan and Manurung with Maxed size Coal Beds	19
II-7	Work of Koyanagi	21
II-8	Advantages of Spouting over Fluidization	22
II-9	Statement of the Problem	22
CHAPTER III	EXPERIMENTAL EQUIPMENT	
III-1	General	29
III-2	Air Supply	29
III-3	Entrainment Separator	30
III-4	Pressure Regulating Valve	30
III-5	Rotameters	
(a)	General	31
(b)	Air Flow Control	31
(c)	Air Flow Measurement	32
III-6	Experimental Test Column	
(a)	General	35
(b)	Conical-Cylindrical Base	36
(c)	Inlets	37
(d)	Auxiliaries	38
CHAPTER IV	EXPERIMENTAL PROCEDURE	
IV-1	Materials Used	55
IV-2	Determination of Physical Properties of Materials	
(a)	Sampling and Size Analysis	
(i)	Particulate Materials	55
(ii)	Granular Materials	57

TABLE OF CONTENTS Continued

		Page
	(b) Mean Particle Diameters	
	(i) Particulate Materials	58
	(ii) Granular Materials	58
	(c) Solid Density	62
IV-3	Experimental Runs	
	(a) General	62
	(b) Preparation of Bed Mixture	63
	(c) Feed to Column, Start and Control or Air Flow	65
	(d) Record of Measurements	66
	(e) Discharge of Material, Screening etc.	66
	(f) Change of Inlet	67
 CHAPTER V	 EXPERIMENTAL RESULTS	
V-1	Results of Spouted Beds of Alundum Mixtures	69
V-2	Results of Spouted Beds of Ottawa Sand, Silica Sand and Crystolon	
	(a) Ottawa Sand	77
	(b) Silica Sand	77
	(c) Crystolon	80
V-3	Results of Spouted Beds of Polystyrene A, Polystyrene B and Mixtures of Polystyrene A and B	80
V-4	Segregation of Fines in the Bed	
	(a) General	85
	(b) Time Dependence of the Segregation of Fines at the Top of the Bed	85
	(c) Segregation of Fines in Pockets	86

TABLE OF CONTENTS Continued

		Page
V-5	Radial Distribution of Solids During Spouting	86
V-6	Electrostatic Effects in Spouted Beds	87
V-7	Solids-Attrition in Spouted Beds	88
V-8	Pressure Drop — Air Flow Data	89
V-9	Minimum Spouting Velocity Observed Vs. Minimum Spouting Velocity Pre- dicted by Mathur-Gishler Correlations	89
CHAPTER VI	CORRELATION OF MINIMUM SPOUTING VELOCITY DATA	
VI-1	General	92
VI-2	Effect of Bed Height on Minimum Spouting Velocity	93
VI-3	Effect of Mean Particle Diameter on Minimum Spouting Velocity for Alundum Mixtures	95
VI-4	Effect of Mean Particle Diameter on Minimum Spouting Velocity for Polystyrene Mixtures	96
VI-5	Effect of Particle Density on Minimum Spouting Velocity	98
VI-6	Application of Dimensional Analysis	99
VI-7	Correlation of Slope m with $\frac{D_1}{D_c}$	102
VI-8	Correlation of Intercept A with $\frac{D_1}{D_c}$	102
VI-9	Dimensionless Correlation	103
VI-10	Dimensional Correlation	104

TABLE OF CONTENTS Continued

		Page
CHAPTER VII	DISCUSSION OF RESULTS	
VII-1	Minimum Spouting Velocity Measurements	126
VII-2	Comparison of Correlation, Equation VI-14, with the Mathur-Gishler Correlation, Equation II-8	127
VII-3	Comparison of V_s Predicted by Equation VI-14 with Previous Data	
(a)	Data of Buchanan and Manurung	130
(b)	Data of Mathur and Gishler	130
VII-4	Critical Ratio of $\frac{D_i}{D_c}$	131
VII-5	Effect of Column Diameter on Minimum Spouting Velocity	133
VII-6	Effect of Inlet Design	135
VII-7	Some Characteristics of the Spouted Beds of Mixed-Size Particles	136
CHAPTER VIII	CONCLUSIONS AND RECOMMENDATIONS	139
NOMENCLATURE		142
REFERENCES		145
APPENDIX 1	EQUIPMENT DETAILS	
(a)	Pressure Regulating Valve	147
(b)	Rotameter-1	148
(c)	Rotameter-2	148
APPENDIX 2	CALIBRATION DATA	
(a)	Rotameter-1	149
(b)	Rotameter-2	150
APPENDIX 3	CALCULATED DATA	
(a)	Data of 3/4" Inlet	151
(b)	Data of 5/8" Inlet	154
(c)	Data of 1/2" Inlet	155
(d)	Data of 3/8" Inlet	157

TABLE OF CONTENTS Continued

		Page
APPENDIX 4	DATA OF PREVIOUS WORKERS	
(a)	Data of Buchanan and Manurung	159
(b)	Data of Mathur and Gishler	160
APPENDIX 5	SAMPLE CALCULATIONS	
(a)	Minimum Spouting Velocity	161
(b)	Length Mean Diameter	163
(c)	Minimum Spouting Velocity by Equations VI-14 and VI-15	163

LIST OF FIGURES

Figure		Page
II-1	A Typical Air Flow — Pressure Drop Diagram for a Spouted Bed System	25
II-2	An Illustration of the Difference Between the Various Mean Diameters Defined by Equations II-2 to II-7	26
II-3	Variation of the Ratio of Observed V_s to V_s Calculated by Equation II-8: Data of Buchanan and Manurung (14) and Koyanagi (21)	28
III-1	Schematic Diagram of Apparatus	40
III-2	Entrainment Separator	42
III-3	Calibration Chart for Rotameter-1	43
III-4	Calibration Chart for Rotameter-2	44
III-5	Comparison of the Volume Calculated using Figure III-3 and Equation III-10 for Rotameter-1, with the Volume Measured	45
III-6	Comparison of the Volume Calculated using Figure III-4 and Equation III-10 for Rotameter-1, with the Volume Measured	46
III-7	Sectional Drawing of the Column Assembly	47
III-8	Conical-Cylindrical Base to the Column	48
III-9	Inlet Set-up Used by Mathur-Gishler (1), and Thorley, Mathur, Klassen et al (15)	49
III-10	Schematic Diagrams Showing the Inlet-Design Development of Buchanan and Manurung (14)	50
III-11	3/8-inch Orifice-Diameter Inlet	51
III-12	1/2-inch Orifice-Diameter Inlet	52
III-13	5/8-inch Orifice-Diameter Inlet	53
III-14	3/4-inch Orifice-Diameter Inlet	54
VI-1	Minimum Spouting Velocity — Bed Height Relationship for Alundum Mixtures	106

LIST OF FIGURES Continued

Figure		Page
VI-2	Minimum Spouting Velocity — Bed Height, Relationship for Alundum B, Crystolon, Silica Sand and Polystyrene A	107
VI-3	Minimum Spouting Velocity — Bed Height Relationship for Alundum Mixtures, Ottawa Sand and Polystyrene A	108
VI-4	Minimum Spouting Velocity — Bed Height Relationship for Polystyrene A, B and Mixtures of Polystyrene A and B	110
VI-5	Minimum Spouting Velocity — Bed Height Relationship for Alundum B, Ottawa Sand Polystyrene A and B	111
VI-6	Minimum Spouting Velocity — Bed Height Relationship for Alundum Mixtures and Polystyrene A	112
VI-7	Effect of Mean Particle Diameter of Alundum Mixtures on Minimum Spouting Velocity	113
VI-8	Effect of Mean Particle Diameter of Polystyrene on Minimum Spouting Velocity	114
VI-9	Effect of Solid Density on Minimum Spouting Velocity	116
VI-10	Plot of Y Against $\frac{H}{D_c}$ for 3/4-inch Inlet	117
VI-11	Plot of Y Against $\frac{H}{D_c}$ for 5/8-inch Inlet	118
VI-12	Plot of Y Against $\frac{H}{D_c}$ for 1/2-inch Inlet	119
VI-13	Plot of Y Against $\frac{H}{D_c}$ for 3/8-inch Inlet	120
VI-14	Correlation of Slope m with $\frac{D_i}{D_c}$	121
VI-15	Plot of Intercept A Against $\frac{D_i}{D_c}$	122
VI-16	Correlation of Intercept A with $\frac{D_i}{D_c}$	123

LIST OF FIGURES Continued

Figure		Page
VI-17	Correlation of Minimum Spouting Velocity Data	124
VI-18	Ratio of Predicted to Observed Minimum Spouting Velocity Against Bed Height	125

LIST OF TABLES

Table		Page
II-1	Characteristic/Mean Particle Diameter — Correlations Applicable	12
II-2	Key to Figure II-2	27
III-1	Key to Figure III-1	41
IV-1	Physical Properties of Materials Used	56
IV-2	Calculated Values of Mean Particle Diameters of Particulate Materials	59
IV-3	Calculated Values of Mean Particle Diameters of Granular Materials	60
V-1	Data for Minimum Spouting Velocity of Alundum A, B, C and Mixtures of A, B and C	71
V-2	Data for Minimum Spouting Velocity of Ottawa Sand	78
V-3	Data for Minimum Spouting Velocity of Silica Sand	79
V-4	Data for Minimum Spouting Velocity of Crystolon	81
V-5	Data for Minimum Spouting Velocity of Polystyrene A, B and Mixtures of A and B	82
V-6	Comparison of Values of Experimental Minimum Spouting Velocity of Runs A-10(a) to A-10(i) with Values Predicted by Equation II-8 and II-9.	90
VI-1	List of Variables	92
VI-2	Slope m, Intercept A and $\frac{D_c}{D_1}$	102
VI-3	Key to Figure VI-3	109
VI-4	Key to Figure VI-8	115

LIST OF TABLES Continued

Table		Page
VII-1	Deviations of V_s Predicted by Equations II-8 and VI-14 from the Experimental: Runs A-10(a) to A-10(i) and Runs P-13(a) to P-13(g)	128
VII-2	Comparison of Values of V_s at $\frac{D_i}{D_c} = 0.284$ with V_{mf}	132
VII-3	Comparison of V_s Predicted by Equation VI-14 with Koyanagi's (21) Data	134

CHAPTER I

INTRODUCTION

The spouted bed technique for contacting fluid and uniform, coarse particles was developed in 1955 by Mathur and Gishler (1), following preliminary experiments on fluidization of wheat. Later, Mathur and Gishler (2) and Becker and Sallans (3) made studies on the drying of wheat as a possible application of this new and novel fluid-solid contacting operation. Publications have also appeared on heat transfer (4,5), wood chip drying (6,7) and on flow characteristics in the spouted bed (8,9,10,11). Commercial spouted bed pea driers are already in operation in Canada (12). Thus, the spouted bed technique appears to be an effective means of contacting fluid and uniform, coarse particles, particularly cereals such as peas, wheat and lentils.

However, the commercially available particulate materials like coal, sand, gravel and catalysts are non-uniform and exhibit a wide range of particle sizes. Fluidization is an established fluid-solid contacting operation for such particles.

Fluid-solid contacting in the spouted beds appears as effective as in the fluidized beds. Moreover, power requirements for operating the spouted beds are less and the operation is easily controllable. Due to these features, application of the spouted bed technique as a contacting operation for non-uniform particulate materials might be preferred to fluidization. If so, a knowledge of the effect of particle size distribution on spouting is desirable.

Data on spouting of narrow size fractions of Ottawa sand, gravel, alundum and catalysts have been reported by Mathur and Gishler (1).

Buchanan and Manurung (13,14) have investigated the effect of size distribution in spouted beds of coal in their study of the possible application of the spouting technique to coal carbonization. Their data is, however, sparse and limited to only one material.

Correlations for predicting the superficial minimum spouting velocity have been proposed by Mathur and Gishler (1) and by Becker (9). These do not appear to apply to all systems and particularly to beds of non-uniform size solids.

The present work has been carried out to measure the superficial minimum spouting velocity for mixed-size beds and to correlate the data using a suitable mean particle diameter of mixtures, covering a wide range of solid densities, bed heights and inlet diameters.

CHAPTER II

REVIEW OF LITERATURE AND THEORY

II-1. GENERAL DESCRIPTION OF SPOUTING PHENOMENON

The phenomenon of spouting has attracted increasing interest since it was first described by Mathur and Gishler (1) in 1955.

Coarse and uniform materials such as wheat, rice, beans are not easily amenable to fluidization due to their tendency towards slugging. But Mathur and Gishler (1) found that contacting of such coarse and uniform materials with fluid could be easily effected using a new technique which they termed "spouting".

Spouting may be achieved by subjecting a bed of solid particles contained in a vertical circular-cylindrical column to an upward flow of fluid — generally air — through a central inlet to a cone at the base of the column as shown in Fig. III-7, which is a sectional drawing of the assembly of the test column used in the present investigation.

At low fluid velocities, the bed behaves as a packed bed. If the air velocity is gradually increased beyond a point, the particles at the base of the cone are lifted and an internal channel or spout is formed. With further increase in the air velocity, the height of the internal spout increases and an expansion of the bed takes place. At greater air flows, the spout breaks through the upper bed boundary. Above the bed, the solids fall back into the annular space around the spout and travel downwards by gravity as a moving packed bed. The solids enter the spout mainly in the conical section. However, there will also be an appreciable lateral movement

of solids into the spout from the annular space throughout the entire height of the bed. The spout can be considered as a dilute phase, central core solid-air jet moving upwards and the annulus a downward moving dense phase. Thus, the coexistence of these two phases in a spouted bed produces a characteristic fluid-solid contact different from that in a fluidized bed. The air distribution in a spouted bed is also highly non-uniform unlike that in a fluidized bed.

Spouting may be illustrated further by consideration of a typical air flow-pressure drop curve in Fig. II-1. In this example, pressure drops across the bed ($-\Delta P$), in inches of water were measured for a 24.5-inch high bed of coarse size polystyrene pellets ($D_p = 0.104''$) contained in the test column with the $1/2''$ inlet used in the present investigation. The pressure drop is plotted against air flow rate in standard cubic feet per minute (S.C.F.M.). As shown in Fig. II-1, ($-\Delta P$) increases with increase in air flow and reaches a maximum at b. According to Madonna and Lama (11) an internal spout has begun to form at a velocity lower than that corresponding to the maximum pressure drop at b, and at b the internal spout has experienced a considerable development whereas the bed is just beginning to expand. Further increase in air flow rate beyond point b brings a decrease in pressure drop until point c (Fig. II-1). A very slight further increase in air flow beyond point c causes a sudden and sharp decrease in pressure drop (as shown by cd, Fig. II-1) due to the spout breaking through the top of the bed. Beyond d, pressure drop remains almost constant and the spout rises higher in the column.

If the air flow is then gradually decreased, the bed stays in the spouted condition until an air velocity corresponding to point f (Fig. II-1)

is reached which is lower than the velocity at point d. At f the spout is about to collapse. A very slight decrease in air flow causes the spout to disappear and the pressure drop rises suddenly to g. On further decrease of air flow, ($-\Delta P$) decreases and follows the path gh. The pressure drop for decreasing air flow is slightly lower than that for increasing air flow since the particles are more loosely packed.

II-2. EXPLANATION OF SOME IMPORTANT VARIABLES

(a) INCIPIENT AND MINIMUM SPOUTING VELOCITIES

The superficial velocity corresponding to d (Fig II-1) where the spout first breaks through the top of the bed as the air flow is being increased is termed the "incipient spouting velocity". The superficial velocity at this point is not exactly reproduceable because the 'yield shear strength' depends upon the degree of compaction of the bed.

But, on the other hand, the superficial velocity corresponding to f (Fig. II-1) where the spout is at its minimum condition, i.e., at the point of extinction, is not subject to initial packing conditions and is a precisely determineable quantity which Mathur and Gishler (1) call the "minimum spouting velocity". As will be seen in latter sections, it is this quantity for which correlations have been developed.

(b) STATIC BED HEIGHT

The static bed height is the height measured from the air inlet-orifice to the top of the bed after the bed has been spouted and air flow gradually and gently stopped. Again, this is a reproduceable quantity whereas the initial height of the randomly packed bed is variable. The static bed depth is used in the correlations for minimum spouting velocity defined in section II-2 (a) above.

(c) MAXIMUM SPOUTABLE BED DEPTH (OR HEIGHT)

Mathur and Gishler (1) have found that for a given system of column geometry, gas and particles, there is a maximum bed height that can be spouted. At greater heights, the bed directly fluidizes or slugs.

At lower bed heights, gas velocity can be increased far beyond the incipient spouting velocity without causing instability of the spout. In these cases, the spout pierces as a jet through the bed, the gas being largely accommodated in the spout. At slightly higher bed depths, noticeable expansion of the bed takes place. Fractional expansion of the beds increases with increasing bed heights and reaches a maximum at heights near the maximum spoutable bed heights. Therefore, near the maximum spoutable bed heights, the spouting becomes unstable with respect to changes in the gas flow rate. The gas distribution is more nearly uniform at these bed heights and the condition of the beds approximates that of aggregative fluidization. The minimum spouting velocity near the maximum spoutable bed heights is thus approximately equal to the velocity for the onset of aggregative fluidization.

A correlation of experimental data on maximum spoutable bed height H_m , with fluid, particle and column properties due to Becker (9) is given below:

$$\left(\frac{H_m}{D_p}\right) \left(\frac{D_p}{D_c}\right)^{1.76} \left(12.2 \frac{D_i}{D_c}\right)^n \left[22 + \frac{2600}{Re_m}\right] \times f(\theta)^{2/3} \times Re_m^{1/3} = 42$$

where $n = 1.6 e^{-0.0072 Re_m}$

As explained later in III-6 (c), the experimentally obtained maximum spoutable bed height in a particular system is very sensitive to modifications in the construction of the inlet to the column. Therefore, the above correlation for calculating the maximum spoutable bed heights cannot be generally applied.

(d) PARTICLE DIAMETERS

(i) GENERAL

The solid particles are generally non-uniform in size and irregular in shape. A representative sample of any material, can be separated by any suitable means into a number of fractions. All the particles in a single fraction are then assumed to have approximately the same size and shape. The particle size of each one of these uniform fractions can be denoted by a characteristic diameter.

(ii) CHARACTERISTIC DIAMETER OF SINGLE (OR UNIFORM) SIZE FRACTION

The selection of a characteristic diameter of a single size fraction is arbitrary and depends upon the method of determination, relative size, shape etc. Commonly used characteristic diameters are: given below:

- (1) The diameter of an equivolumed sphere — mostly for particles larger than about 0.125" in size,
- (2) The diameter of a sphere with the same surface area as the particle,
- (3) The diameter of a circle of area equal to the projected area of the particle in its most stable position,
- (4) The arithmetic mean of the mesh sizes of a Standard Testing Sieves (usually Tyler sieves) that define the fraction, and
- (5) The geometric mean of the width and thickness or the geometric mean of the width, thickness and length.

Of all the characteristic diameters mentioned above, the Tyler screen size (4 above) is the one most commonly used for particulate materials such as sand, catalysts, coal and gravel.

The geometric mean diameter, on the other hand, describes adequately the size of large granules like rice, wheat and manufactured pellets.

(iii) DEFINITIONS OF MEAN DIAMETERS OF MIXED-SIZE PARTICLES

Mean diameters which are based on weight, surface or length and which are characteristic of all the particles can be defined to express the average size of a group of particles. Suppose a unit mass of material contains n_1 particles of characteristic diameter d_1 constituting a mass fraction x_1 , n_2 particles of characteristic diameter d_2 constituting a mass fraction x_2 etc. Assuming that all the particles in the sample have the same shape, the volume v_1 and surface s_1 of any single particle of diameter d_1 can be represented by

$$v_1 = k_v d_1^3$$

$$s_1 = k_s d_1^2$$

$$\therefore x_1 = n_1 k_v d_1^3 e_s \quad (II-1)$$

similarly $x_2 = n_2 k_v d_2^3 e_s$

$$n_1 s_1 = n_1 k_s d_1^2$$

$$\sum n_1 s_1 = \sum n_1 k_s d_1^2$$

(1) VOLUME OR WEIGHT MEAN DIAMETER

If a relationship between mass fraction x and diameter d can be represented by a continuous curve, mean diameter D_w is given by

$$D_w = \frac{\sum d \cdot dx}{\sum dx}$$

or differentially,

$$D_w = \frac{\int_0^1 d \cdot dx}{\int_0^1 dx} = \frac{\int_0^1 d \cdot dx}{\sum x_1} = \frac{\sum d_1 x_1}{\sum x_1}$$

Substituting the values of x_1 from Equation II-1,

$$D_w = \frac{\sum n_1 k_v d_1^4 e_s}{\sum n_1 k_v d_1^3 e_s} = \frac{\sum n_1 d_1^4}{\sum n_1 d_1^3} = \sum x_1 d_1 \quad (\text{II-2})$$

The mean evaluated by this relation is called the weighted mean or volume mean diameter.

(2) SURFACE MEAN DIAMETER

Following a similar analysis to that given above and considering the relationship between the surface area and diameter, the surface mean diameter D_s , can be shown to be

$$D_s = \frac{\sum n_1 d_1^3}{\sum n_1 d_1^2} = \frac{1}{\sum \frac{x_1}{d_1}} \quad (\text{II-3})$$

It is to be noted from Equation II-3, that the surface mean diameter is proportional to the ratio of total volume to total surface of the mixture and therefore the size of a particle with the same specific surface as the mixture. This is also known as volume-surface mean diameter.

(3) LENGTH MEAN DIAMETER

The length or linear mean diameter is equivalent to the total surface area of all the particles divided by the summation of the diameters and is given by

$$D_v = \frac{\sum n_1 d_1 d_1}{\sum n_1 d_1} = \frac{\sum n_1 d_1^2}{\sum n_1 d_1} = \frac{\sum \frac{x_1}{d_1}}{\sum \frac{x_1}{d_1^2}} \quad (\text{II-4})$$

(4) MEAN VOLUME OR WEIGHT DIAMETER

The mean volume or weight diameter is quite different from the volume mean or weight mean diameter defined above. The mean volume diameter D'_v is the size that each particle would have to be to make the total volume of the particles the same as in the mixture and thus

$$k_v D'_v{}^3 \sum n_1 = \sum n_1 k_v d_1^3$$

or $D'_v{}^3 = \frac{\sum n_1 d_1^3}{\sum n_1}$
 or $D'_v{}^3 = \frac{\sum n_1 d_1^3}{\sum n_1}$

$$D'_v = \sqrt[3]{\frac{\sum n_1 d_1^3}{\sum n_1}} = \sqrt[3]{\frac{1}{\sum \frac{x_1}{d_1^3}}} \quad (\text{II-5})$$

(5) MEAN SURFACE DIAMETER

The mean surface diameter D'_s is the size that each particle would have to be to make the total surface as that of mixture and therefore,

$$k_s D'_s{}^2 \sum n_1 = \sum n_1 k_s d_1^2$$

$$D'_s = \frac{\sum n_1 d_1^2}{\sum n_1} = \frac{\sum \frac{x_1}{d_1}}{\sum \frac{x_1}{d_1^2}} \quad (\text{II-6})$$

(6) MEAN LENGTH DIAMETER

The mean length diameter D' is equivalent to the sum of the diameters of all the particles divided by the number of particles and is thus given by

$$D'_L = \frac{\sum n_1 d_1}{\sum n_1} = \frac{\sum \frac{x_1}{d_1^2}}{\sum \frac{x_1}{d_1^3}} \quad (\text{II-7})$$

Mean diameter is hereafter written as the weight mean D_p , surface mean D_p , length mean D_p etc as the case may be.

The difference between the values of various mean diameters for a sample of known particle size distribution is illustrated in Fig. II-2, in which the mean diameters of mixtures of alundum A and B used in the present investigation have been plotted against % of alundum B in alundum A. (See Table IV-1 for the differential screen analyses of alundum A and B, Table IV-2 for the values of different mean diameters of mixtures of alundum A and B).

(iv) USAGE OF CHARACTERISTIC/MEAN PARTICLE DIAMETERS

Various workers, as shown in Table II-1 below, have used different definitions to evaluate the parameter D_p — characteristic or mean — in correlating their experimental data.

TABLE II-1

CHARACTERISTIC/MEAN PARTICLE DIAMETER —

CORRELATIONS APPLICABLE

Characteristic/Mean Particle Diameter	Correlations Applicable
1) a) Tyler screen size for narrow size fractions. b) Surface mean diameter for wide size fractions.	i) Generalized correlation of Leva et al (16) for predicting the minimum fluidization velocity. ii) Correlations of heat and mass transfer data (18) in fixed and fluidized beds. iii) Generalized correlation of Leva et al (19) for pressure drop through packed beds.
2) Equivolumed sphere diameter for particles larger than 0.125" in size.	i) Ref. (19) quoted above.

TABLE II-1 Continued

3) Geometric mean of width and thickness for rice, wheat etc.	Applicable for Leva's generalized correlation (16) according to Liang-Tseng Fan and Charles J. Swartz (17).
4) Length mean diameter for mixed size particles.	Rausch's correlation (20) for weight rate of flow of solids by gravity through delivery orifices of tubular columns fitted with conical bottoms.
5)a) Smaller dimension for wheat.	
b) Tyler screen size for narrow cut fractions of sand, gravel etc.	Mathur-Gishler correlation (1) for minimum spouting velocity.
c) Weight mean diameter for mixed size particles.	
6) Equivolumed sphere diameter diameter for all materials, like wheat, sand, peas and barley.	Correlations of Becker (9) for the dependent variables in spouted beds.

TABLE II-1 Continued

<p>7) Geometric mean diameter e.g. $3\sqrt{\text{width} \times \text{thickness} \times \text{length}}$ for wheat, barley, peas and lentils.</p>	<p>Correlation of Peterson (12) for the solids temperature in spouted bed driers.</p>
--	---

It appears that the length mean diameter as used by Rausch (20) in correlating the data on weight rate of flow by gravity will be suitable for correlating the spouted bed data. On the other hand, for uniform granular materials, the geometric mean diameter as used by Peterson (12) is likely to be most suitable since this takes into account the effect of all the three principal dimensions of the particles.

II-3. MATHUR -- GISHLER CORRELATION FOR MINIMUM SPOUTING VELOCITY

Mathur and Gishler (1) -- the originators of the technique of spouting -- have proposed a dimensionless correlation for predicting the minimum spouting velocity necessary to spout a given bed of material. This is given below:

$$V_s = \left(\frac{D_p}{D_c} \right) \left(\frac{D_i}{D_c} \right)^{1/3} \sqrt{\frac{2gH (e_s - e_f)}{e_f}} \quad (\text{II-8})$$

The range of variables covered by Mathur and Gishler (1) is:

D_p : from 0.023 to 0.25 inches

D_i : from 1/16 to 2 1/8 inches

D_c : from 3 to 12 inches

e_s : from 69 to 464 lb._m/ft.³

H : from 3 1/2 to 106 inches

e_f : 0.073 and 62.4 lb._m/ft.³

An 85° cone was used at the base of each column.

The bulk of the work carried out by Mathur and Gishler was with beds of uniform sized cereal grains such as wheat, peas, mustard, rape, sunflower seeds, coffee beans etc. Narrow cut fractions of gravel, Ottawa sand etc., were also used as bed material.

In arriving at the correlation, (Equation II-8), these researchers used the smaller diameter as the representative dimension for wheat and the average Tyler screen opening for all other materials. For mixtures, weight mean diameter was used. (See section II-2(d)iii for a discussion of mean diameters).

Limited experiments conducted by Mathur and Gishler (1) on wheat beds in 24" diameter column using 45° and 85° cones indicated that air velocity required for minimum spouting was less with a 45° cone than with an 85° cone. However, in the 6" diameter column the cone angle (85°, 60° and 45°) apparently did not influence the minimum spouting velocity.

Based upon the data obtained with beds of wheat in a 24" diameter column, Thorley, Mathur et al (15) have modified Equation II-8 as follows:

$$v_s = \left(\frac{D_p}{D_c} \right) \left(\frac{D_i}{D_c} \right)^n \sqrt{\frac{2gH(e_s - e_f)}{e_f}} \quad (\text{II-9})$$

$$n = 0.23 \quad \text{for } 45^\circ \text{ cone}$$

$$= 0.13 \quad \text{for } 85^\circ \text{ cone}$$

The exponent n on the group $\frac{D_i}{D_c}$ is, thus, a function of cone angle.

The range of D_i used by Thorley, Mathur et al (15) was from 1.78 to 4 inches.

The exponent n on the group $\frac{D_i}{D_c}$ for 60° cone has not been mentioned but

it appears from their results (15) that the air flow required with 60° cone is just about the same as with 45° cone for a given material (wheat) in a 24" diameter column for constant bed height and inlet diameter.

II-4. MADONNA-LAMA-BRISSEON EQUATION FOR MINIMUM SPOUTING VELOCITY

Assuming the phenomenon of spouting to be analogous to a jet mechanism, Madonna, Lama and Brisson (10) have derived the following equation for minimum spouting velocity:

$$V_s = C_s \left(\frac{D_i}{D_c} \right)^{\frac{5}{2}} \sqrt{\frac{2gH(1-\epsilon)(\rho_s - \rho_f)}{\rho_f}} \quad (\text{II-10})$$

Equation II-10 has been derived by applying the mechanical energy balance equation between the air inlet section and the top of the bed and making the following simplifying assumptions:

- (i) The specific volumes of air at the inlet and the top of the bed are approximately constant i.e., no density change,
- (ii) The fluid expands through the bed,
- (iii) The average velocity at the top of the bed is negligible when compared to the velocity through the inlet,
- (iv) The bed depth in feet of the flowing fluid e.g., air is small compared to the kinetic and frictional terms, and

- (v) The pressure drop in a spouting bed at the incipient spouting condition is equal to the fluidizing pressure drop, namely

$$\Delta P = H(1 - \epsilon)(e_s - e_f) \quad (\text{II-11})$$

The constant C_s in Equation II-10 is believed to be a complex function of several variables such as D_p , D_c , D_1 , ϵ , θ and α where ϵ , θ and α are bed porosity, cone angle and coefficient of friction between solids and column respectively. In addition, the assumption (v) above is likely to affect the complexity of the term C_s , since the pressure drop at spouting is not equal to the fluidization pressure drop. There is no simple relationship between these two pressure drops. The nature of the term C_s in Equation II-11 has not yet been determined by Madonna, Lama and Brisson (10).

II-5. BECKER'S ANALYSIS

Becker, (9), during an extensive investigation to develop and present correlations for predicting the more important of dependent variables such as frictional pressure drop $(-\Delta P)_c$, minimum spouting velocity V_s , maximum of the minimum spouting velocity, maximum spoutable bed depth etc. involved in spouted beds, proposed a similarity principle of spouted beds which is given below:

"Beds of given particles spouted with a given gas in geometrically similar columns behave similarly when the reduced bed heights $\frac{H}{H_m}$, i.e., the ratios of static bed heights H to maximum spoutable bed heights H_m , are the same".

In the case of minimum spouting velocity, the above similarity principle predicts that for a given particle and gas and geometrically similar columns

$$\frac{V_s}{V_m} = f\left(\frac{H}{H_m}\right) \quad (\text{II-12})$$

where V_m is the minimum spouting velocity at maximum spoutable bed height.

Based on data obtained with wheat in geometrically similar columns

($D_c = 0.50$ to 2 feet, $\frac{D_1}{D_c} = 0.172$), Becker obtained an explicit form of

Equation II-12 as

$$\frac{V_s}{V_m} = 1 + s \ln\left(\frac{H}{H_m}\right) \quad (\text{II-13})$$

The coefficient s in Equation II-13 is correlated as

$$s = 0.0071 \left(\frac{D_c}{D_1}\right)^{2/3} f(\theta) \text{Re}_m^{0.295} \quad (\text{II-14})$$

Combining Equations II-13 and II-14, Becker has obtained an equation of minimum spouting velocity which is

$$\frac{V_s}{V_m} = 1 + 0.0071 \left(\frac{D_c}{D_1}\right)^{2/3} f(\theta) \text{Re}_m^{0.295} \ln\left(\frac{H}{H_m}\right) \quad (\text{II-15})$$

In Equation II-15, $f(\theta)$ is an experimental shape factor of the particle defined by (9)

$$C_D f(\theta) = 22.4 \frac{2600}{\text{Re}_m} \quad (\text{II-16})$$

Re_m is the particle Reynolds Number at maximum spoutable bed depth.

Equation II-15 is said to be generally valid at $\text{Re}_m > 100$, while at $10 < \text{Re}_m < 100$, it is valid only if inlet Reynolds Number

$$\frac{D_1 V_1 \rho}{\mu} > 30,000.$$

Equation II-15 is not valid for low bed heights where $\frac{H}{D_c} < 1$.

A correlation for minimum spouting velocity applicable to very low bed depths is given by Becker (9) as

$$\frac{V_s}{V_m} = 1.2 \left(\frac{H}{D_c} \right)^{-0.058} \left(\frac{D_c}{D_1} \right) \quad (\text{II-17})$$

Equation II-17 correlates data on particles spouted in 0.50' diameter column with cone angle of 180° and $\frac{D_1}{D_c} = 0.172$.

It is to be noted that all the materials spouted by Becker (9) are uniform and particle diameters are expressed as equivalent sphere diameter.

In order to make use of Equation II-15 to calculate V_s , one should have reliable data on experimental shape factors of the particles and data on maximum spoutable bed depth or alternately an accurate means of calculating the same. As already mentioned in section II-2(c), the correlation for maximum spoutable bed depth cannot be generally applied. Further, the applicability of Equation II-15 to beds of mixed size particles is doubtful since it is derived from data obtained with uniform materials only.

II-6. WORK OF BUCHANAN AND MANURUNG WITH MIXED SIZE COAL BEDS

Buchanan and Manurung (13,14), during their investigation into the possibilities of applying the spouted bed technique to the low temperature carbonization of coal, have conducted preliminary work on the effect of size distribution on spouting and minimum spouting velocity. Beds of coal of narrow and wide cut coal fractions were investigated in a 5.75" I.D.,

four foot high industrial pyrex column fitted with a 45° cone and 1/2" I.D. air inlet at the bottom.

The results of Buchanan and Manurung on the effect of particle size distribution on spouting can be summarized as follows:

- i) Coal fraction of Tyler sieve size range -6 +16 will spout very well up to 33" high,
- ii) If the proportion of -16 mesh fines is increased, the spoutable bed depth decreases and
- iii) With beds containing 40% or more of -16 mesh fines spouting cannot be produced.

Minimum spouting velocity data obtained with narrow and wide size range coal fractions (Tyler sieve sizes ranges (a) -6 +10, (b) -8 +12, (c) -10 +28 including 6.8% of -28 mesh fines and (d) mixtures of (a) and (c) above) have been compared with the values calculated from the Mathur-Gishler correlation Equation II-8. A plot made by Buchanan and Manurung (14) with the ratios of the observed and calculated minimum velocities and bed height as ordinates is reproduced in Figure II-3. Figure II-3 shows that the calculated values based on $D_p = \sum x_1 d_1$ show greater deviation from the observed values than those calculated values based on $D_p = \frac{1}{\sum \frac{x_1}{d_1}}$.

Thus the definition of $D_p = \frac{1}{\sum \frac{x_1}{d_1}}$ for calculating the mean particle diameter

appears to be better suited than the definition $D_p = \sum x_1 d_1$. However, both the lines are parallel and neither of them correspond with the line

given by $\frac{V_s \text{ (obs)}}{V_s \text{ (cal)}} = 1$. This graph clearly shows that the relationship

between the minimum spouting velocity V_s and bed height H is not the same as that given by the Mathur-Gishler correlation.

II-7 WORK OF KOYANAGI

Koyanagi (21) has investigated the effect of particle size distribution on spouting and minimum spouting velocity in a 4" I.D. column fitted with a 60° cone and 1/4" Schedule-40 pipe as inlet ($D_i = 0.364"$, $\frac{D_i}{D_c} = \frac{1}{11}$) using Ottawa sand as the bed material. The sizes of Ottawa sand used by Koyanagi (21) were -20 +30 mesh ($D_p = 0.028"$) and -40 + 60 mesh ($D_p = 0.014"$) and mixtures of these two fractions.

The results of the work of Koyanagi on spouting can be summarized as follows:

- i) -20 +30 mesh Ottawa sand can be spouted up to a height of about 24",
- ii) -40 +60 mesh sand cannot be spouted in this system, and
- iii). The maximum spoutable bed depth decreases somewhat linearly with increasing proportion of -40 +60 mesh sand in -20 +30 mesh sand from 24" with 0% of -40 +60 mesh sand to 14" with 20% of -40 +60 mesh sand. Beds containing more than about 25% of -40 +60 mesh sand cannot be spouted at all in the system.

The minimum spouting velocity data of Koyanagi also showed deviations from the Mathur-Gishler correlation. The ratio of minimum spouting velocity observed to that calculated by the latter correlation, Equation II-8, was also

plotted against bed height in Figure II-3. This plot shows the variation of minimum spouting velocity with bed height is not in agreement with the Mathur-Gishler correlation.

II-8. ADVANTAGES OF SPOUTING OVER FLUIDIZATION

Measurements of Madonna and Lama (11) show that the pressure drop in spouted beds is always less than the fluidization pressure drop. As explained earlier in II-2(c), the minimum spouting velocity is also less than the fluidization velocity except at higher bed heights where it is almost equal to the fluidization velocity. Thus the operating power costs of spouted beds are generally less.

In addition, due to the characteristic solid circulation pattern obtainable in the spouted beds, gas-solid contacting and mixing — particularly at higher bed depths — might be more effective.

The application of spouting technique to the beds of uniform and coarse particles which are difficult to fluidize is definitely advantageous.

Non-uniform and finer particles are, however, easily fluidizable. The application of spouting technique, if possible, to the beds of particles in the fluidizable size range may prove more economical and easier to operate.

II-9. STATEMENT OF THE PROBLEM

Originally, the phenomenon of spouting had received attention as a more suitable means of gas-solid contacting beds of coarse and uniform materials such as wheat, rice, peas and beans which are difficult to fluidize. The particulate materials such as coal, catalysts — either uniform or non-uniform — in a size range that render them fluidizable could also be spouted. By virtue of lower power and gas requirements, gas-solid contacting operations in spouted beds might be preferable to fluidization. Then, quantitative

measurements of the limits of spoutability especially when mixing fine non-spoutable size particles with coarse spoutable fractions of the same material are necessary.

The work on this problem, started by Koyanagi-Epstein (21), was to some extent continued in the present study. But the major emphasis of the present investigation was with the effect on spouting behaviour of mixing particles of different sizes each of which was usually in the spoutable range.

As explained earlier, in Chapter II-2(d)(iii), different workers in the related fields of study have used different definitions to evaluate the particle diameters of uniform and non-uniform size particles. The main purpose of the present work was to study the effect of particle size distribution on minimum spouting velocity and find a suitable mean particle diameter to correlate the data. The effect of solid density — another important physical property of the materials — on minimum spouting velocity also needed to be investigated.

The trend of the deviation of data of Koyanagi (21) and Buchanan and Manurung (14) from the Mathur-Gishler correlation (1) for minimum spouting velocity indicated that the effect of bed height on minimum spouting velocity needs further clarification.

It was also felt that the effect of inlet diameter — an important design variable — on minimum spouting velocity should be investigated.

Thus, the present programme of experimental work was undertaken to study the effect of particle size distribution, solid density, bed height and inlet diameter on minimum spouting velocity.

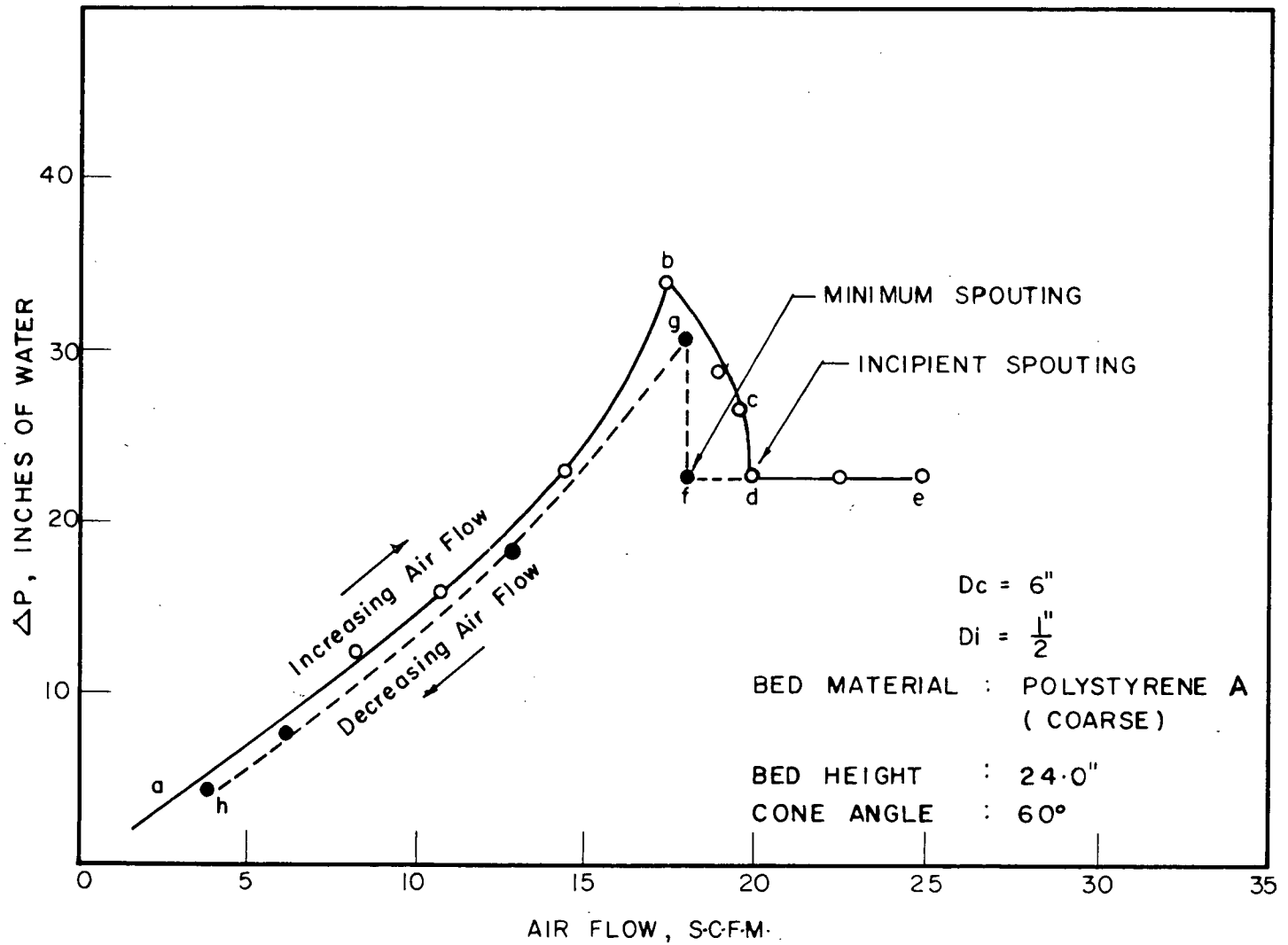


FIGURE II-1. A TYPICAL AIR FLOW — PRESSURE DROP DIAGRAM FOR A SPOUTED BED SYSTEM

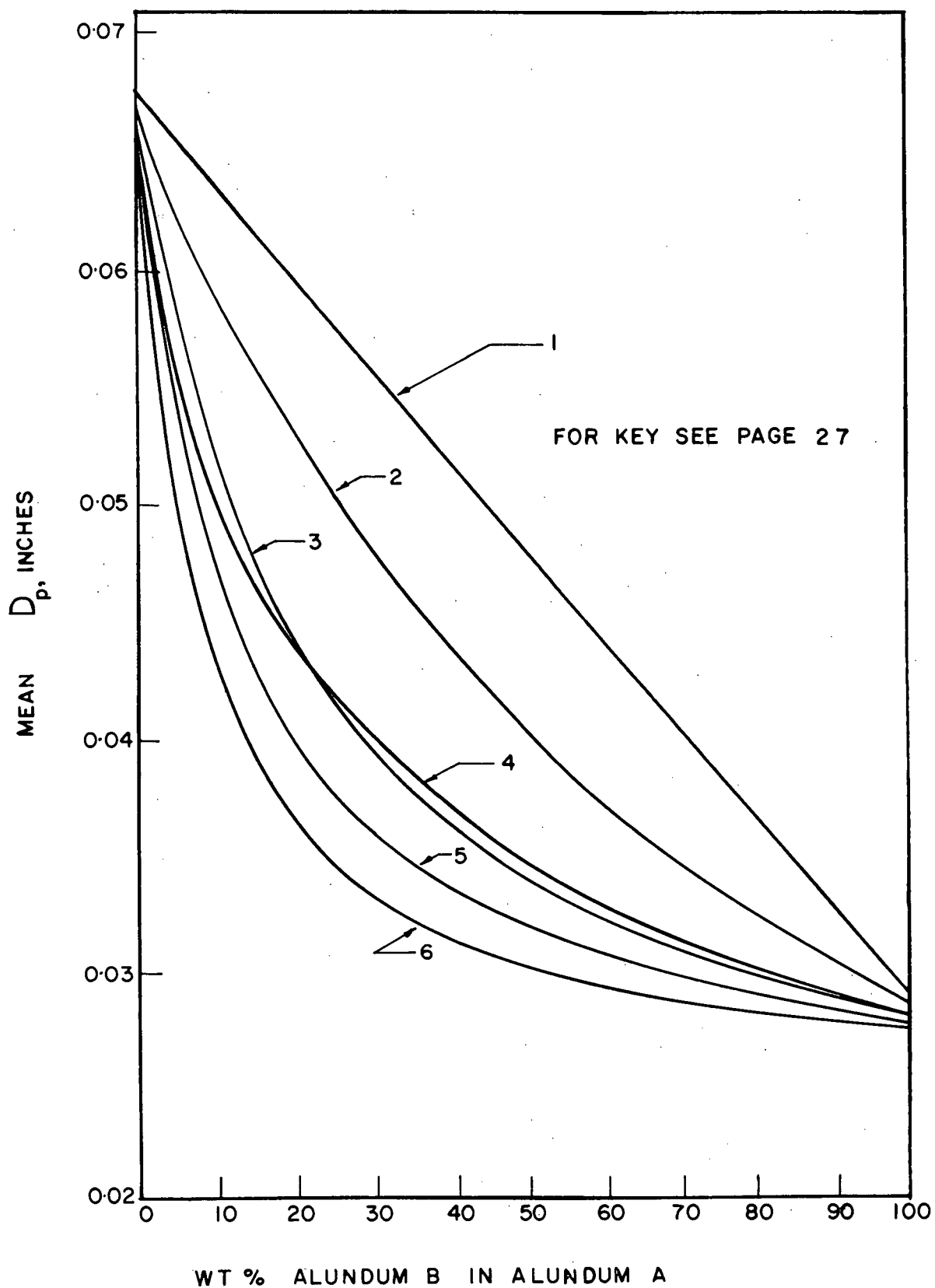


FIGURE II-2. AN ILLUSTRATION OF THE DIFFERENCE BETWEEN THE VARIOUS MEAN DIAMETERS DEFINED BY EQUATIONS II-2 TO II-7

TABLE II-2

KEY TO FIGURE II-2

<u>Line</u>	<u>Ordinate</u>	
1	Weight Mean D_p	(Equation II-2)
2	Surface Mean D_p	(Equation II-3)
3	Length Mean D_p	(Equation II-4)
4	Mean Weight D_p	(Equation II-5)
5	Mean Surface D_p	(Equation II-6)
6	Mean Length D_p	(Equation II-7)

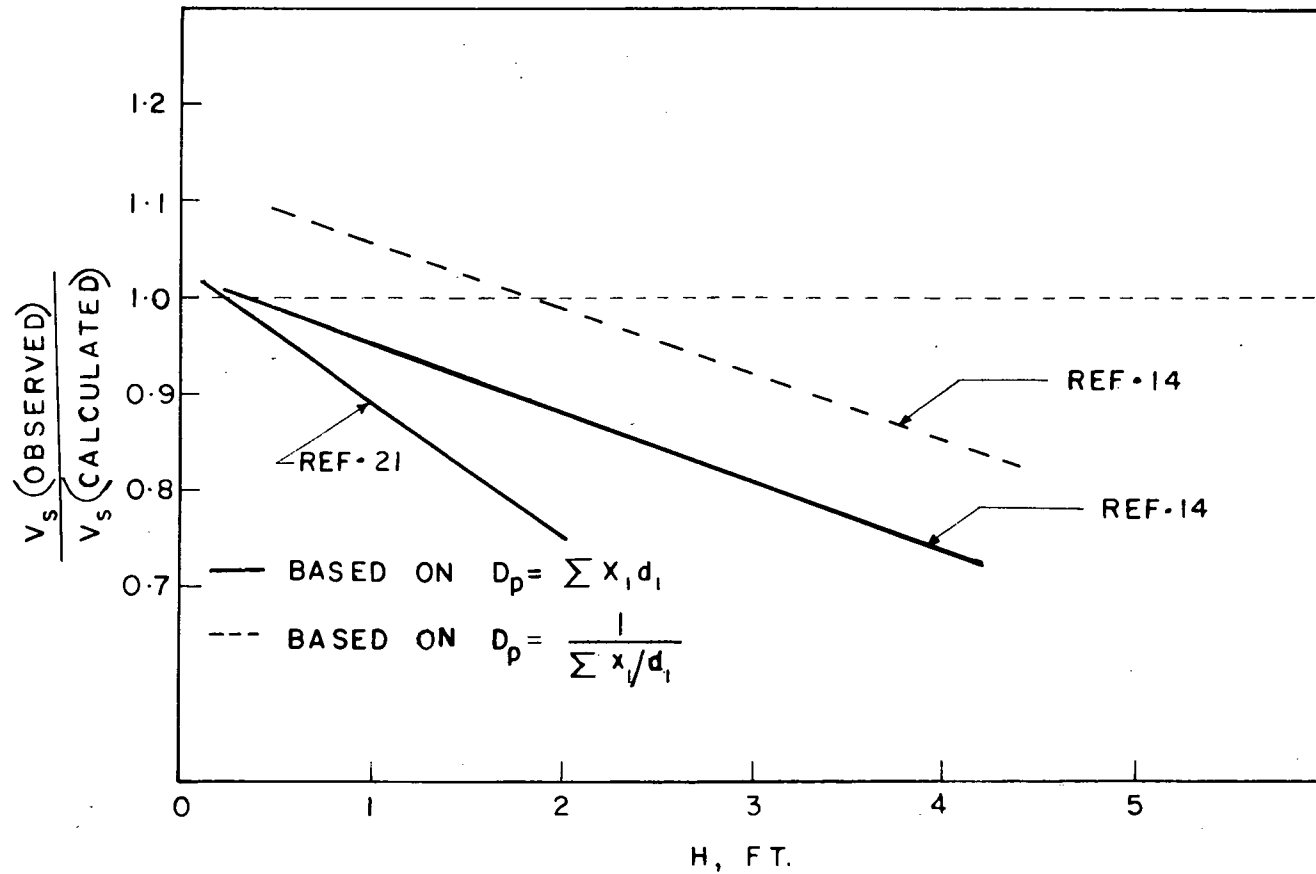


FIGURE II-3. VARIATION OF THE RATIO OF OBSERVED V_s TO V_s CALCULATED BY EQUATION II-8: DATA OF BUCHANAN AND MANURUNG (14) AND KOYANAGI (21)

CHAPTER III

EXPERIMENTAL EQUIPMENT

III-1. GENERAL

The experimental equipment used in this investigation is illustrated schematically in Figure III-1.

The experimental test column consisted of a 6" I.D., 5' long pyrex glass column fitted with a brass cylindrical-conical base with an included angle of 60° and an air inlet of special design.

Air, which was used as the spouting medium, was obtained from the building process air supply and flowed through a water entrainment separator and a pressure regulating valve, was metered in one of the two rotameters and from thence flowed to the test column through the inlet. The air pressure downstream from the rotameter was measured with either a 30" Meriam U-tube vertical mercury manometer or a calibrated pressure gauge (0 - 60 p.s.i.g.) and the temperature of the air was measured with a thermometer reading from 0°F to 220°F . The pressure drop across the spouted bed was measured with a 48-inch vertical carbon-tetrachloride-air manometer. 1-inch Schedule-40 steel piping was used throughout.

A more detailed description of individual parts of the apparatus is given below.

III-2. AIR SUPPLY

The air was drawn from the process air supply in the building. The source of this air is a Nash Hytor compressor, driven by 40 HP Induction motor, with a rated capacity of 120 standard cubic feet per minute at a

maximum delivery pressure of 50 p.s.i.g. The air from the compressor is led to a storage tank. The delivered air pressure in the tank is in the range of 40 - 45 p.s.i.g. From the tank the compressed air passes through a pressure reducing valve and thence to the building process air lines. The outlet pressure of the pressure reducing valve is maintained at approximately 35 p.s.i.g. The maximum amount of air that could be obtained in the test column was only about 75 standard cubic feet per minute, because of resistances in the air lines and equipment.

III-3. ENTRAINMENT SEPARATOR

An orifice-impact type entrainment separator (22) was installed in the line coming from the process air supply to remove any entrained water in the air. The design details of the separator are given in Figure II-2. The average velocity of air through the orifices at normal estimated flow rates is about 100'/sec. at which velocity the entrained water, if any, will separate from air (22). Periodic checks of the stop cocks connected to the separator (Figure III-2) showed that the process air was entirely free of entrained moisture. Further confirmation is provided by the fact that water droplets were never observed in the rotameters or the glass column.

III-4 PRESSURE REGULATING VALVE

Air from the entrainment separator passes through a pressure regulating valve. The pressure regulating valve was installed to reduce the air pressure before it is metered and to reduce possible fluctuations in pressure. The pressure regulating valve used is a Masoneilan 1 1/4" size, direct operated diaphragm type spring-loaded valve. A special feature of this valve is that an outlet pressure range of 10 - 40 p.s.i.g. could be maintained with a single spring under an inlet pressure of 50 p.s.i.g. The specifications of the valve are appended in Appendix 1 (a).

III-5. ROTAMETERS

(a) GENERAL

The air flow rates were measured by means of one of two rotameters connected in parallel on the discharge side of the pressure regulating valve. These rotameters were supplied by Rotameter Manufacturing Company of England. The maximum air capacity of rotameter-1 is 32 cubic feet per minute at 14.7 p.s.i.a. pressure and 59°F and that of Rotameter-2 is 124 cubic feet per minute at 14.7 p.s.i.a. pressure and 59°F. The minimum flow measuring capacity of each one of these meters is one-tenth of its maximum capacity. The manufacturing tolerances of the tube and float of each rotameter while being used to measure the flow rates of gases are 1 and 2 respectively expressed as per cent of full scale reading.

The specifications of the rotameter-1 and 2 are given in Appendices 1(b) and 1(c) respectively. Calibration of the meters is described in Chapter III-5 (c).

(b) AIR FLOW CONTROL

The flow rate through the rotameter was controlled by valves on the upstream side. In each of the two upstream lines leading to the rotameters, one standard globe valve and one standard gate valve were installed and the two lines were cross-connected as shown in Figure III-1. The globe valve in the line leading to the rotameter-1 is 1/2" standard whereas all the others are 1" size. Depending upon the flow rate required, only one of the meters was used at a time. During operation, the gate valve was fully closed. The 1" globe valve was then used for coarse adjustment of the air flow rate and the 1/2" globe valve for fine control.

(c) AIR FLOW MEASUREMENT

Calibration charts for air for the rotameters used in this work were provided by the manufacturer. These are reproduced in Figures III-3 and III-4. In these figures, air flow rate in cubic feet per minute at standard conditions (59°F temperature and 14.7 p.s.i.a. pressure) is plotted against rotameter tube reading. Since the air flow conditions are different from standard, these calibration charts cannot be used directly to obtain the volumetric flow rate from the observed tube reading. A working equation which enables calculation of air flow rate from the observed rotameter downstream air pressure and temperature and tube reading is developed as follows:

(i) From the calibration chart, let the volume read corresponding to a particular rotameter tube reading be v_1 , standard cubic feet per minute. Converting to mass rate of flow, this becomes

$$W_1 = v_1 \rho_{f1} \quad (\text{III-1})$$

Where ρ_{f1} is the density of air in lb._m/ft.³ at standard conditions.

(ii) Mass rate of flow of fluid W , through a rotameter, in terms of meter constants, properties of the flowing fluid and discharge coefficient, is given by (23)

$$W = C_D A_2 \sqrt{\frac{2gV_F(\rho_F - \rho_f)\rho_f}{A_F \left[1 - \left(\frac{A_2}{A_1} \right)^2 \right]}} \quad (\text{III-2})$$

The discharge coefficient C_D of the rotameter depends upon shape of the float and Reynolds Number (based on the velocity through annulus and mean hydraulic diameter of annulus) for the flow through the annular

space between the float and tube. For the type of floats provided with the rotameters used in the present investigation, the discharge coefficient at Reynolds Numbers greater than 10^4 is constant and approximately equals to 0.98, according to Linford (24). For all air flow rates used in this investigation, the Reynolds Number was always greater than 10^4 . Therefore, because e_f is very much smaller than e_F , it may be neglected in the $(e_F - e_f)$ term. Substituting 0.98 for C_D in Equation III-1, one gets

$$W = 0.98 \left[A_2 \sqrt{\frac{2gV_F e_F}{A_F \left\{ 1 - \left(\frac{A_2}{A_1} \right)^2 \right\}}} \right] \sqrt{e_f} \quad (\text{III-3})$$

The properties of the float, i.e., V_F , A_F , e_F , are all constants and the function within the square brackets of Equation III-3 depends on A_2 and $\frac{A_2}{A_1}$, or in other words, tube reading only. For any tube reading, therefore,

the mass rate of flow W can be written as

$$W = k \sqrt{e_f} \quad (\text{III-4})$$

where k is a function of tube reading.

Equation III-4 applied to standard flow conditions becomes

$$W_1 = k \sqrt{e_{f_1}} \quad (\text{III-5})$$

If the temperature and pressure of air metered were T_2 and P_2 and density e_{f_2} , the mass rate of flow corresponding to a particular meter reading becomes

$$W_2 = k \sqrt{e_{f_2}} \quad (\text{III-6})$$

Dividing Equation III-6 by Equation III-5, one gets

$$\frac{W_2}{W_1} = \sqrt{\frac{\rho_{f_2}}{\rho_{f_1}}} \quad (\text{III-7})$$

But, from Equation III-1, $W_1 = v_1 \rho_{f_1}$. On substituting $v_1 \rho_{f_1}$ for W_1 , Equation III-7 becomes

$$W_2 = v_1 \rho_{f_1} \sqrt{\frac{\rho_{f_2}}{\rho_{f_1}}}$$

or

$$\frac{W_2}{\rho_{f_1}} = v_1 \sqrt{\frac{\rho_{f_2}}{\rho_{f_1}}}$$

$$v_2 = v_1 \sqrt{\frac{\rho_{f_2}}{\rho_{f_1}}} \quad (\text{III-8})$$

The left hand side of Equation III-8 is the actual mass rate of flow W_2 , divided by the density of air at standard condition ρ_{f_1} . So, it is equal to the volumetric flow rate of air expressed as standard cubic feet per minute. From ideal gas law,

$$\frac{\rho_{f_2}}{\rho_{f_1}} = \frac{P_2}{P_1} \frac{T_1}{T_2} \quad (\text{III-9})$$

Combination of Equation III-8 and III-9 results in

$$v_2 = v_1 \sqrt{\frac{P_2 T_1}{P_1 T_2}} \quad (\text{III-10})$$

In order to check the accuracy of calibration charts supplied by the manufacturer and the applicability of Equation III-10, actual flow measurement of metered air were made with a diaphragm type gas meter and vane anemometer. The flow rate measured by diaphragm meter or vane

anemometer expressed in standard cubic feet per minute was compared with flow rate calculated by Equation III-10, from the observed rotameter tube reading, rotameter downstream pressure and temperature. Such a comparison is shown in Figure III-5 and III-6 for rotameter-1 and rotameter-2 respectively. An excellent agreement was found, the maximum deviation being $\pm 3\%$ between the calculated and measured values at any flow rate. Therefore, it was decided to use Equation III-10 to calculate air flow rates from the observed rotameter tube reading, downstream air pressure and temperature. Calibration data of rotameters is given in Appendix 2.

III-6 EXPERIMENTAL TEST COLUMN

(a) GENERAL

One test column was used. Provision was also made for setting up a half column, (i.e., a column which would appear in plan as a semi-circle); but this was not installed due to shortage of time.

The test-column consists of:

(i) A 5' high, 6" I.D. 'Double Tough' Pyrex brand glass pipe, provided with a 6" Corning style-1 Aluminum flange and an asbestos insert to serve as a cushion between the flared end of the glass and the flange,

(ii). A brass conical-cylindrical base with an included angle of 60° designed to be joined to (i) above, and

(iii). A brass inlet to the column designed to fit in the flange at the apex of the cone of part (ii) above.

The assembly details of these three parts are shown in detail in a sectional drawing of the test column, Figure III-7. The approach pipe section was also shown in Figure III-7.

Type R-2, style 1-2, Corning 6" Neoprene gasket was used as interfacial gasket between glass and brass portions of the column.

As shown in Figure III-7, cone and approach pipe flanges were connected by bolts with a rubber interfacial gasket. A 20 mesh steel wire screen was held between the inlet and pipe flange to prevent solids falling into and clogging the approach pipe.

(b) CONICAL-CYLINDRICAL BASE

The design details of the base of the column are given in Figure III-8. This was made of brass. The cylindrical portion is 2 1/2" high and the inside diameter of the cylinder is 6". The included angle of the cone is 60°. The upper flange on this was designed to mate with 6" style-1 Corning Aluminum flange. The flange at the base of the cone was designed to mate with standard 1" ASME flange.

At 60° cone-angle was chosen because of geometrical symmetry and simplicity in construction.

The two pressure taps were located at the base of cone and at the join of conical and cylindrical sections of the column, respectively, as shown in Figure III-8. Both pressure taps were inclined at an angle of 45° to the horizontal to reduce the possibility of pressure leads being blocked during runs by the material in the column. The brass cylindrical portion of the column was provided to make this arrangement feasible. The pressure tap at the base of the cone was, however, closed after a few runs since erratic and inconsistent pressure drops were observed. Thorley, Saunby et al (15) have also found erratic behavior of pressure drop across the bed when the

pressure tap was located in the region of inlet. This was, perhaps, due to a Vena Contracta effect. Therefore, pressure drops were measured only through the tap at the join of conical and cylindrical portions of the column, which gave consistent and reproduceable readings.

As shown in Figure III-8, a 1/2" brass outlet pipe with a 1/2" gate valve screwed to its discharge end was soldered to the cone to enable the discharge the bed materials.

(c) INLETS

The design of inlet to the column has an important effect on spouting. The set-up used by Mathur and Gishler (1), Thorley, Saunby et al (15) is illustrated schematically in Figure III-9. The entrance pipe, as shown in Figure III-9, could serve as inlet. Thorley, Saunby et al (15) have reported that the size of inlet or orifice size was changed by insertions between the flanges connecting the column and the approach pipe as shown in Figure III-9.

Buchanan and Manurung (14) have conducted experiments with varying inlet constructions to determine an optimum design. The types of constructions used by them are illustrated in Figure III-10. With the type of construction shown in Figure III-10A, the feed (-6 +14 mesh coal) being introduced from top of the column, it was found that spouting could not be produced. However, if the feed was introduced from the bottom with the spouting air, (without gauze on the inlet), spouting was found to be stable. With the arrangement as shown in Figure III-10B, the spouted bed was found to be stable and a 24" high bed composed of -6 +16 mesh coal including and up to 10% of -16 mesh fines could be spouted. Removing the gauze on the inlet, it was reported (14), improved the spouting appreciably and beds up to 28" height were spoutable.

The construction shown in Figure III-10C in which the tube protrudes $1/8$ " above the flanged surface, gave better spouting with maximum bed heights considerably in excess of 28". The presence of gauze with this type has little effect on spouting.

The modification of a lip proposed by Buchanan and Manurung as well as a nozzle-like entrance configuration has been incorporated in the design of the inlets used in the present investigation. (Figures III-11 to 14) Four inlets, viz., $3/8$ ", $1/2$ " $5/8$ " and $3/4$ " orifice diameter, the details of which are shown in Figures III-11, III-12, III-13 and III-14, were used. Each one of these inlets can be fitted into the lower flange of the cone as shown in assembly drawing, Figure III-7. The entrance of each inlet is machined in the shape of a flow-nozzle.

During the initial experimental runs, difficulty was experienced in removing the inlets from the cone flange due to the collection of fine dust in the space between the inlet and the cone flange. This difficulty was overcome by polishing the outside surface of the inlet and the inside surface of the flange smooth, thoroughly cleaning these surfaces and applying grease each time a change of inlet was made.

(d) AUXILIARIES

A sheet metal cone of approximately 20" high (included angle of about 20°) was attached to the top of column so that solids which, were, during spouting, carried higher than the top of the column would fall back into the column. (See item 12, Figure III-1).

During operation, fine particles are likely to fall into the entrance pipe through the screen held between the flanges connecting the cone and the entrance pipe. As shown in Schematic Diagram, Figure III-1, a branch line with a gate valve was installed to allow any such material to be blown out of the system.

A considerable amount of dust is created during spouting due to attrition of particles. The entrained dust was removed via a flexible hose through an exhaust system in the building.

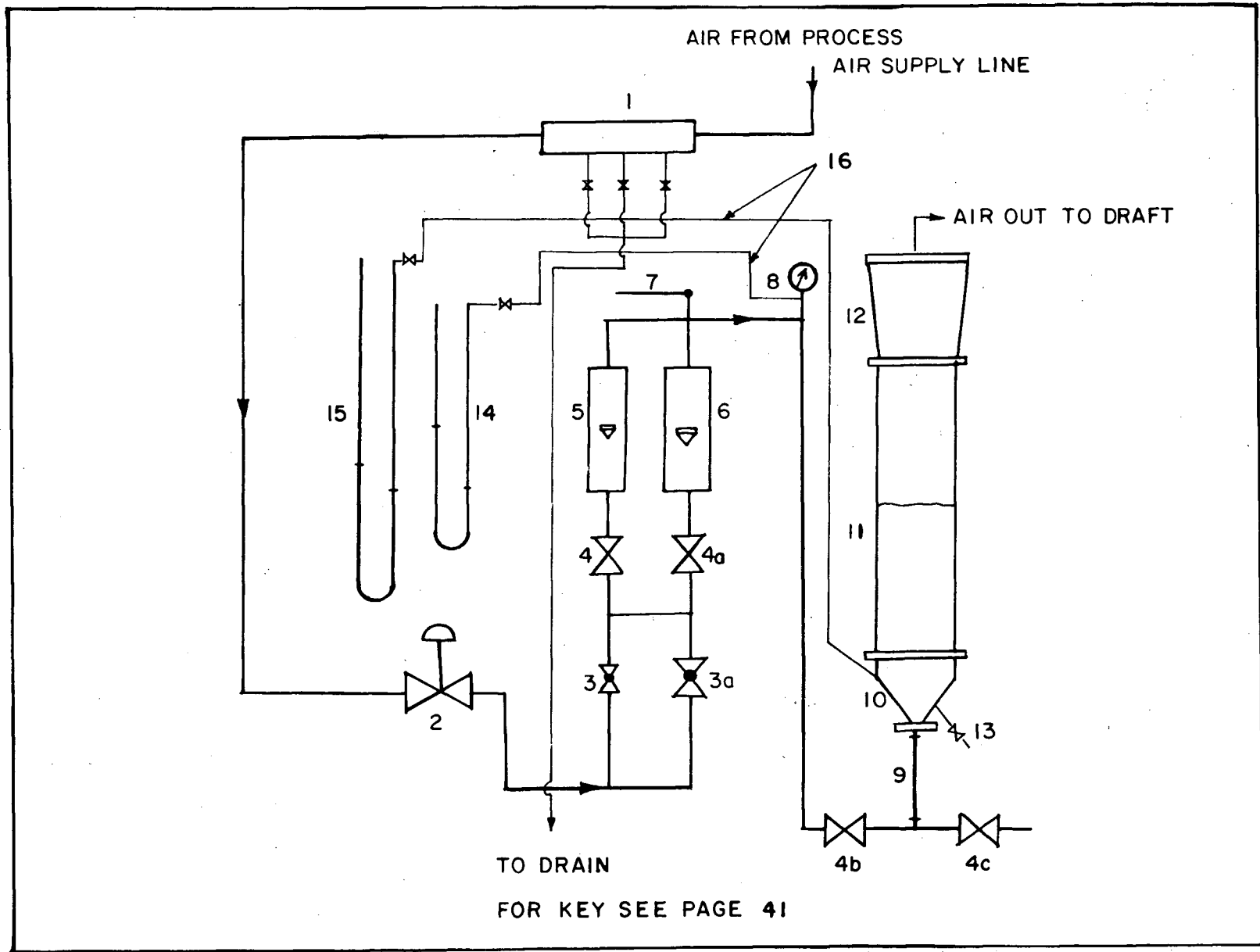
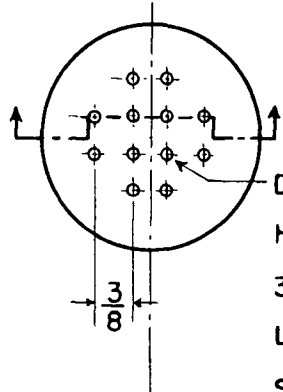


FIGURE III-1. SCHEMATIC DIAGRAM OF APPARATUS

TABLE III-1

KEY TO FIGURE III-1

1. Entrainment Separator
2. Pressure Regulating Valve
3. 1/2" Globe Valve
- 3a. 1" Globe Valve
- 4, 4a, 4b, 4c. 1" Gate Valves
5. Rotameter-1
6. Rotameter-2
7. Thermometer (0 to 212^oF)
8. Pressure Gauge (0 to 60 p.s.i.)
9. 1" Flexible Rubber Hose Pipe
10. Conical-Cylindrical Base (Brass)
11. 6" I.D., 5' high, Double-Tough Pyrex Glass Column.
12. Conical Attachment to the Column
13. 1/2" Discharge Valve
14. A Mercury-Air Manometer
15. Carbon Tetrachloride — Air Manometer
16. Pressure Leads to the Manometers.



DRILL 1/8" DIA.
HOLES (12),
3/8" PITCH,
LOCATION AS
SHOWN

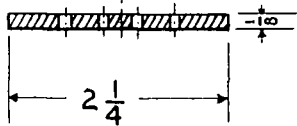
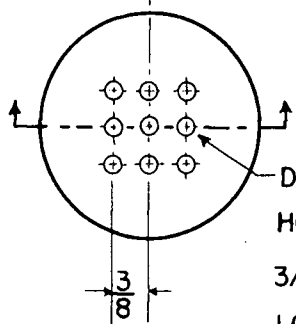


PLATE-1
(COPPER)



DRILL 3/16" DIA.
HOLES (9),
3/8" PITCH,
LOCATION AS
SHOWN

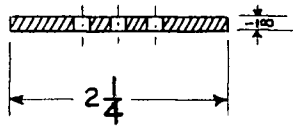


PLATE-2
(COPPER)

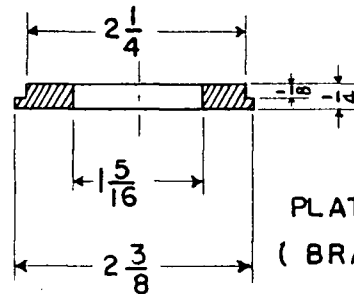
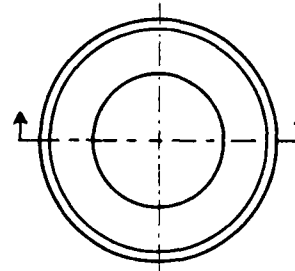
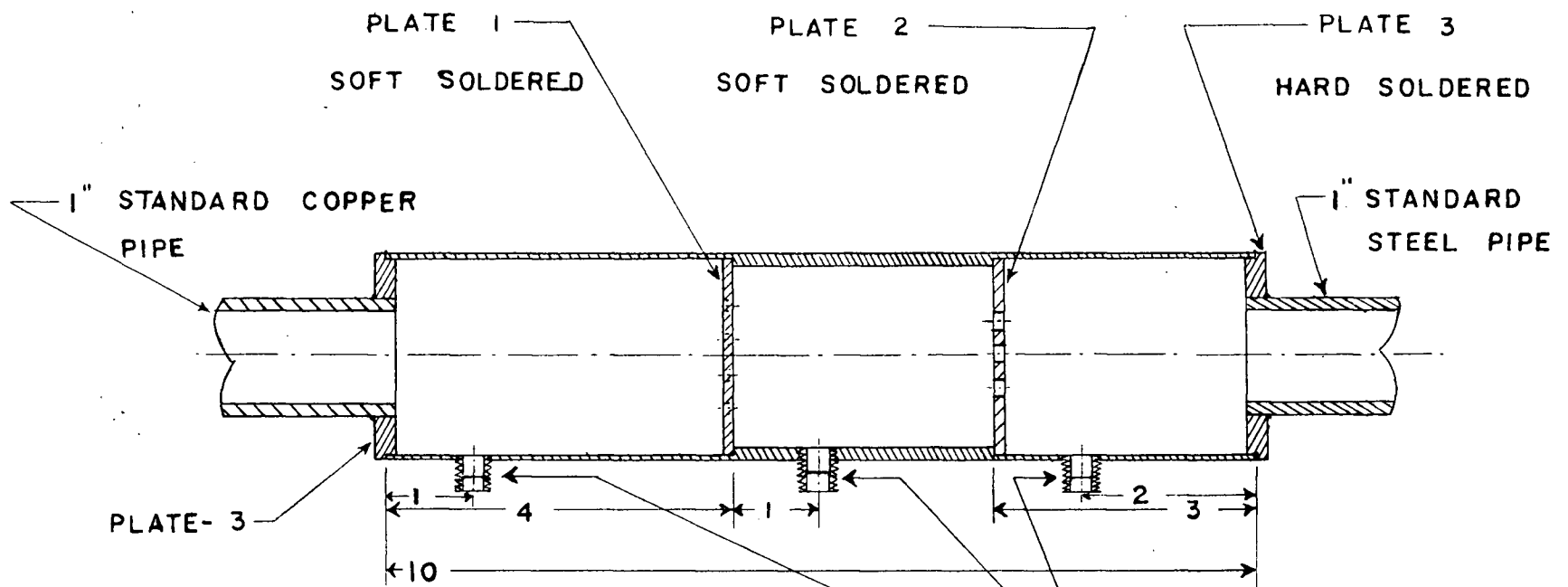


PLATE-3
(BRASS)

NO. OF PIECES: 2



TO ACCEPT 1/4" FEMALE
COMPRESSION FITTING

SECTIONAL VIEW

SCALE: HALF
DIMENSIONS: INCHES
MAIN BODY: COPPER

FIGURE III-2 ENTRAINMENT SEPARATOR

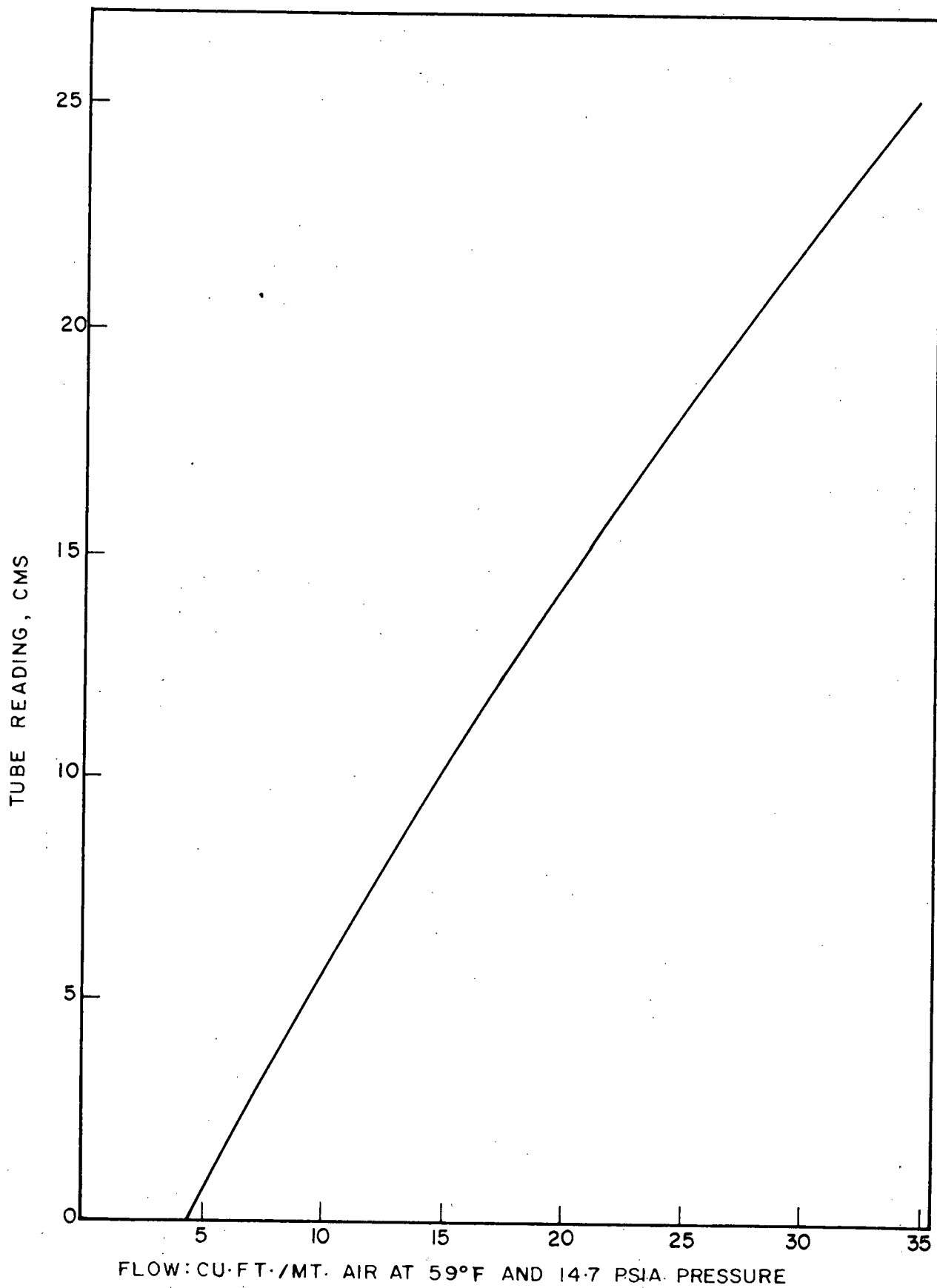


FIGURE III-3. CALIBRATION CHART FOR ROTAMETER-1

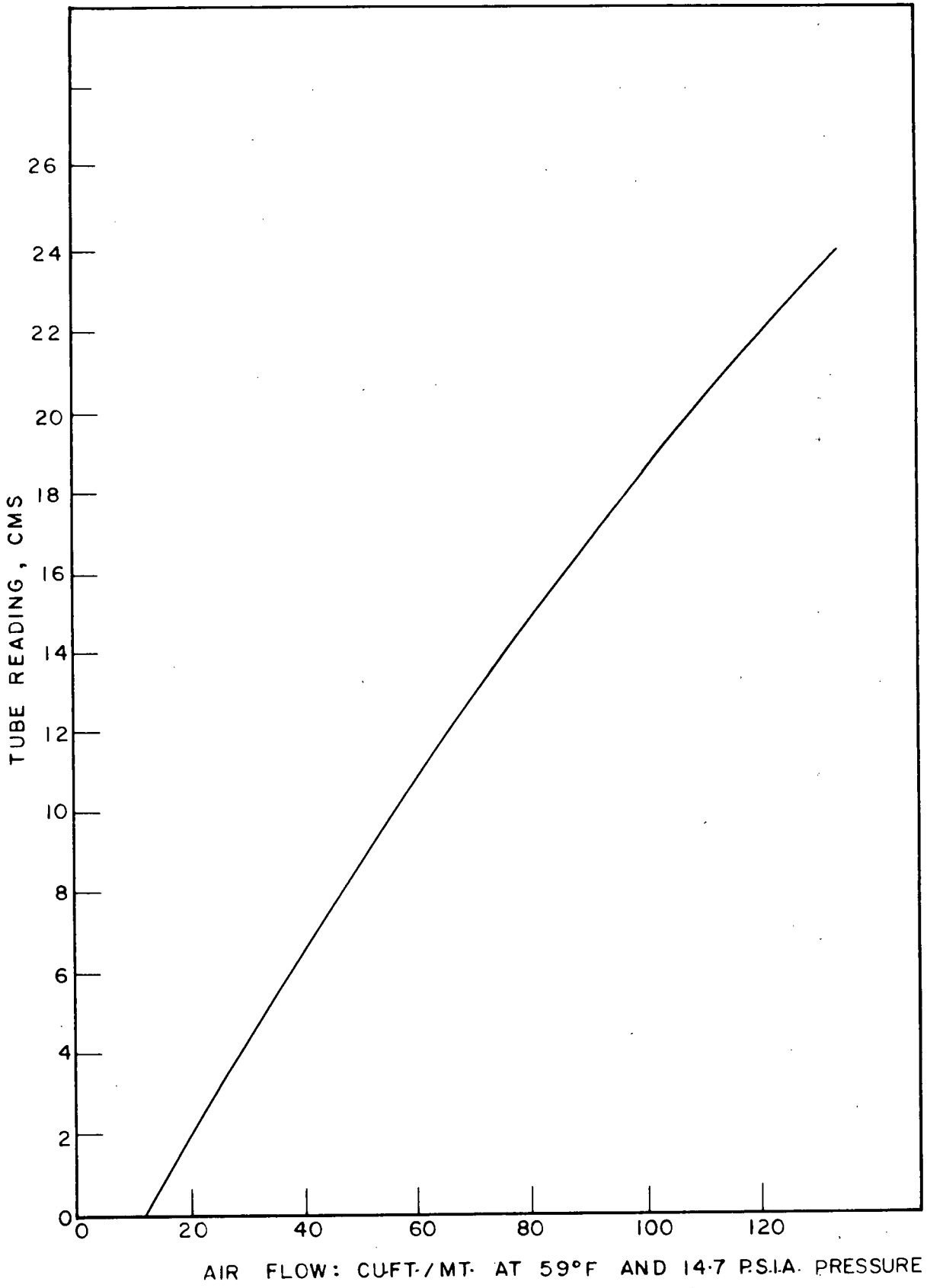


FIGURE III-4. CALIBRATION CHART FOR ROTAMETER-2

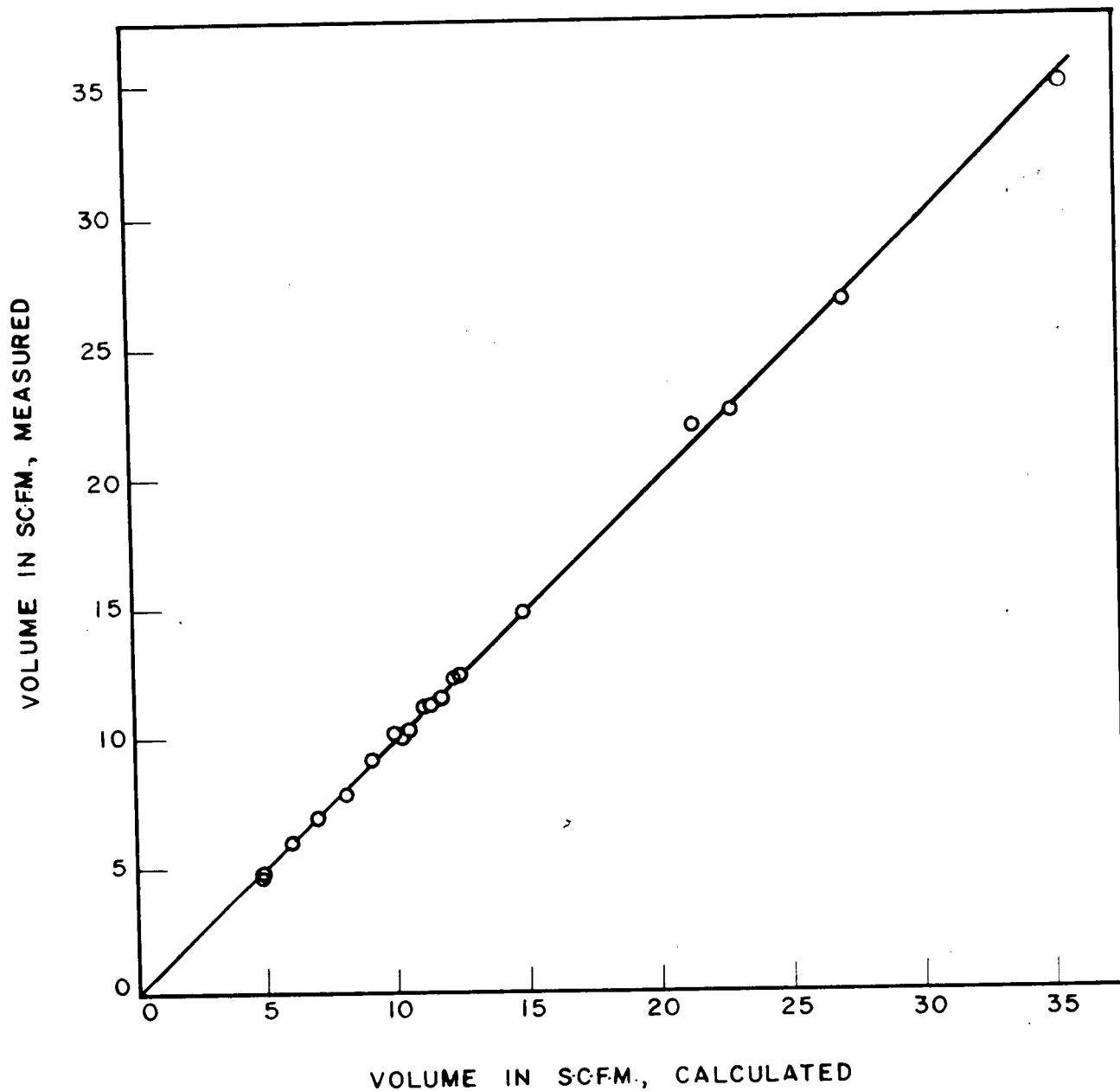


FIGURE III-5. COMPARISON OF THE VOLUME CALCULATED USING FIGURE III-3 AND EQUATION III-10 FOR ROTAMETER-1, WITH THE VOLUME MEASURED

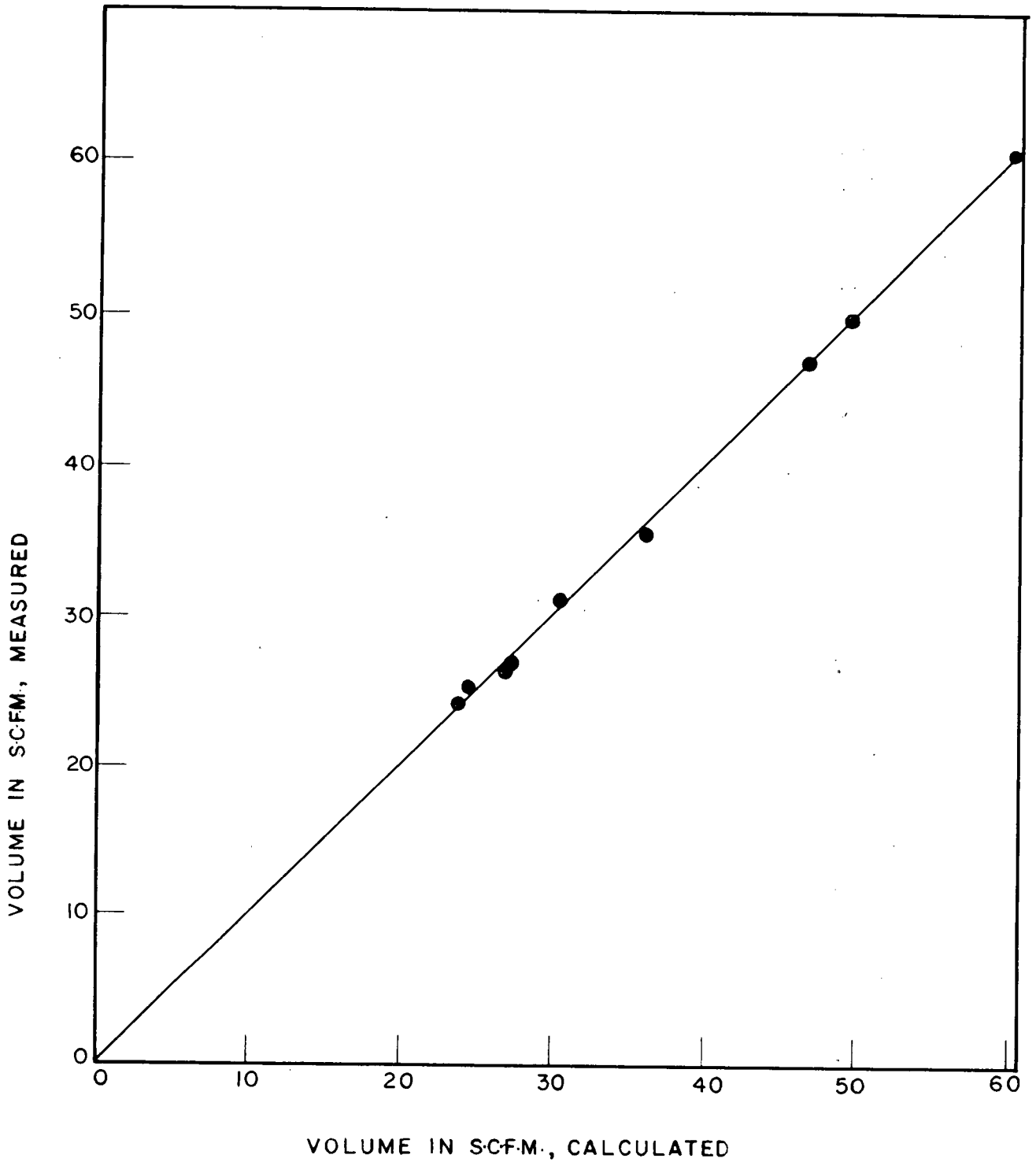


FIGURE III-6. COMPARISON OF THE VOLUME CALCULATED, USING FIGURE III-4 AND EQUATION III-10 FOR ROTAMETER-1, WITH THE VOLUME MEASURED

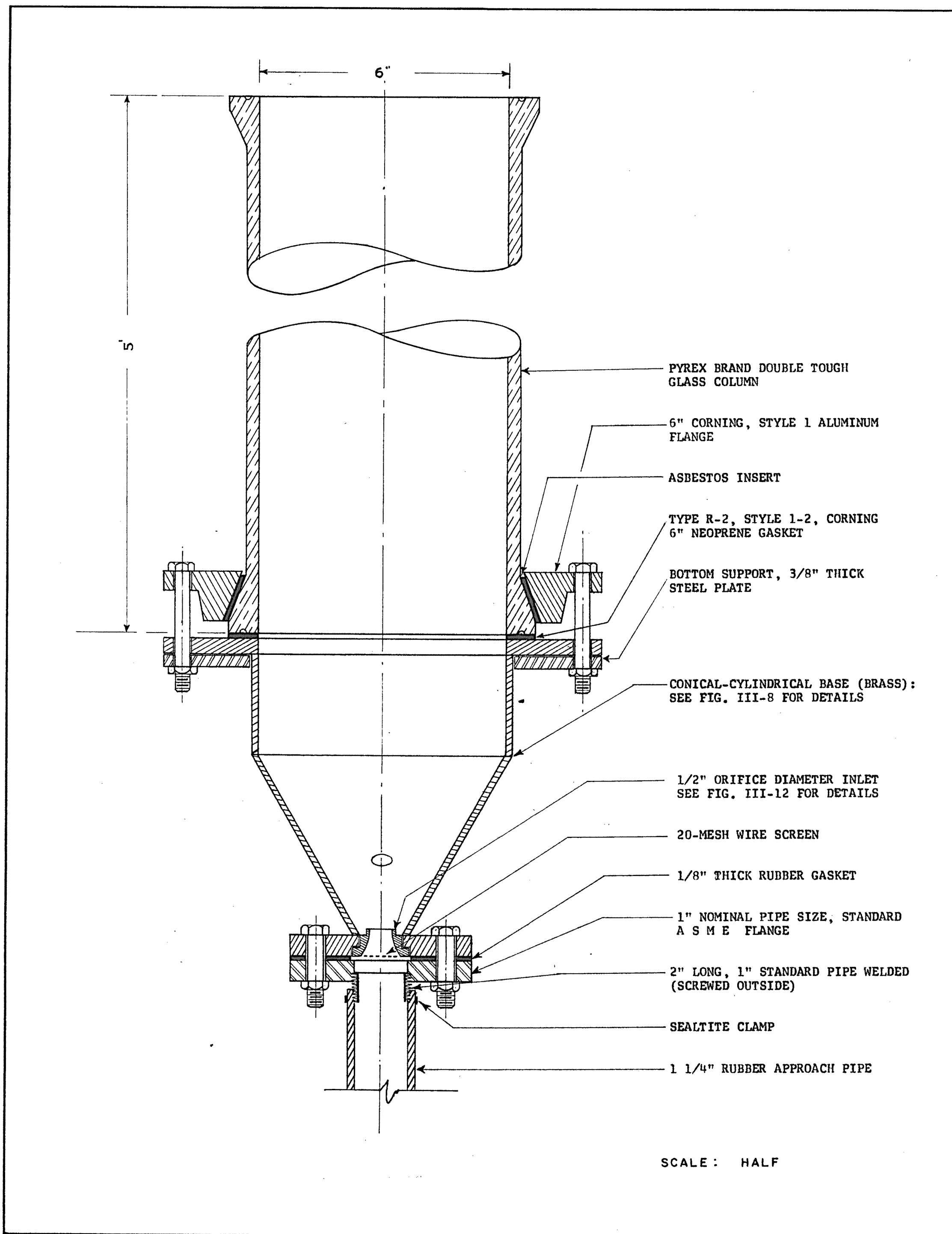


FIGURE III-7. SECTIONAL DRAWING OF THE COLUMN ASSEMBLY

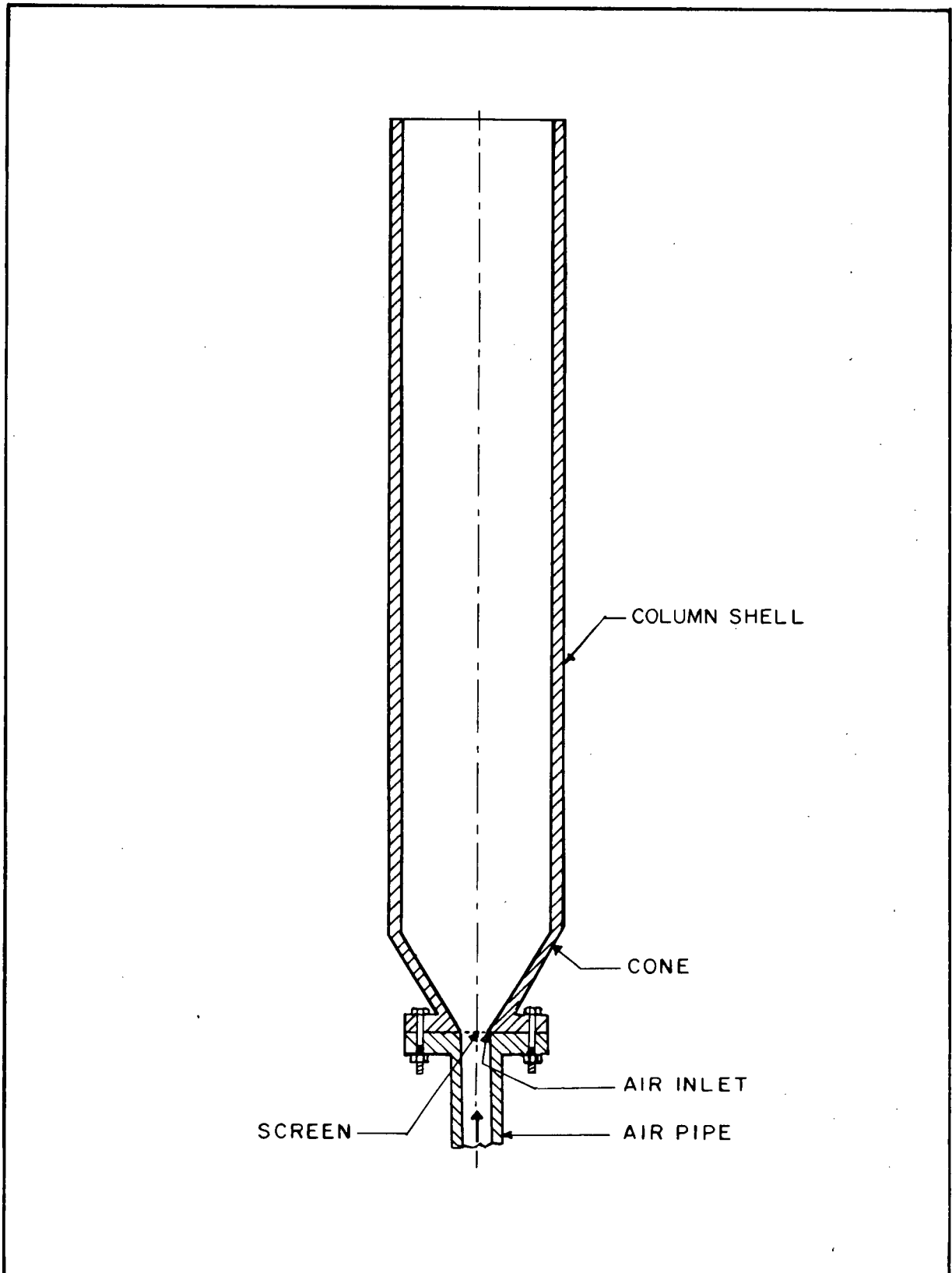


FIGURE III-9. INLET SET-UP USED BY MATHUR-GISHLER (1), AND THORLEY, MATHUR, KLASSEN ET AL (15)

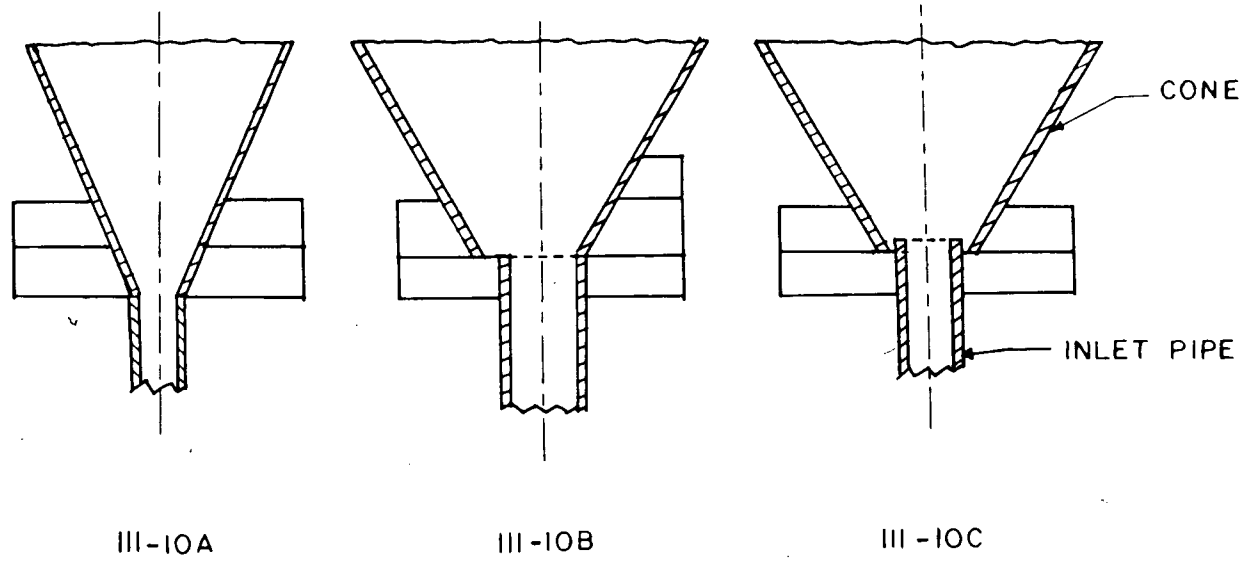
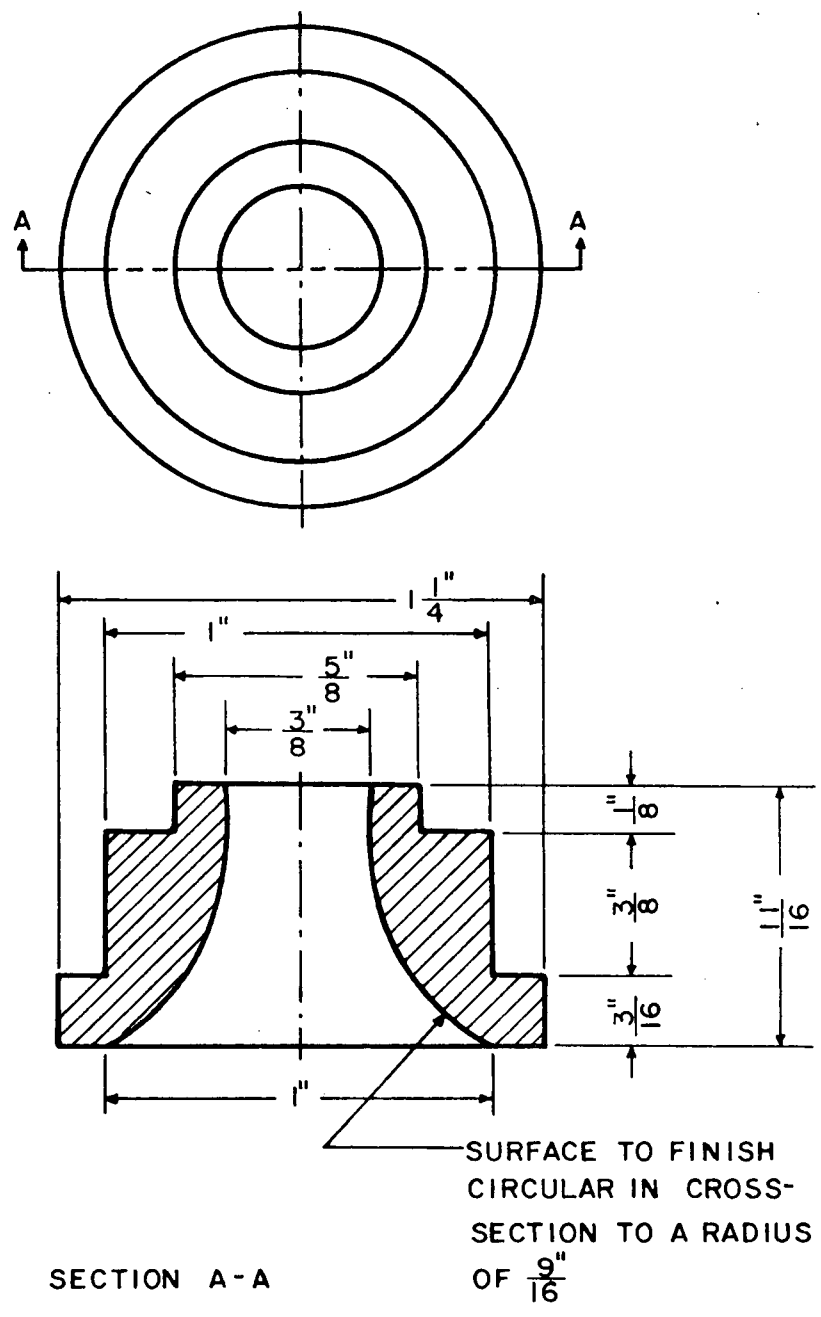


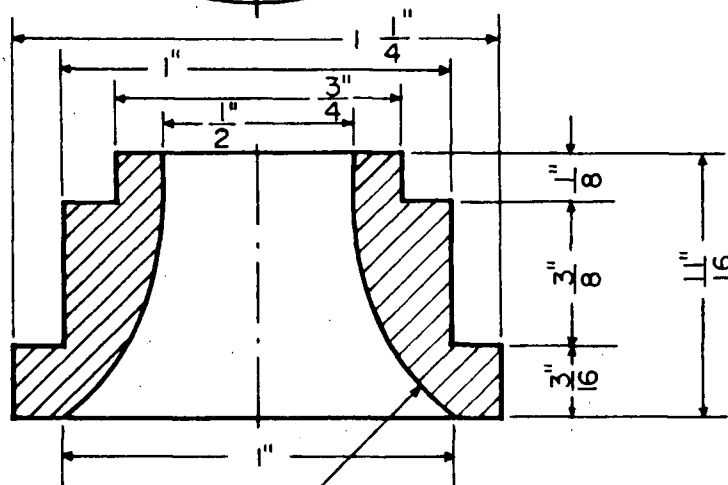
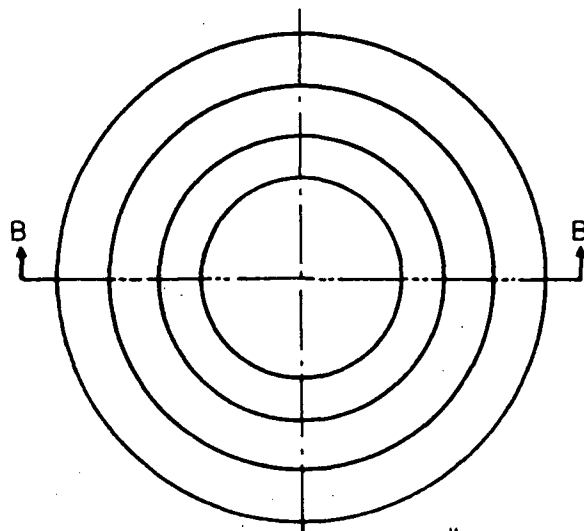
FIGURE III-10. SCHEMATIC DIAGRAMS SHOWING THE INLET-DESIGN DEVELOPMENT OF BUCHANAN AND MANURUNG (14)



MATERIAL : BRASS

SCALE : DOUBLE

FIGURE III-11. 3/8-INCH ORIFICE-DIAMETER INLET



SECTION B-B

SURFACE TO FINISH
CIRCULAR IN CROSS-
SECTION TO A RADIUS
OF ABOUT $\frac{5}{8}$ "

MATERIAL : BRASS

SCALE : DOUBLE

FIGURE III-12. 1/2-INCH ORIFICE-DIAMETER INLET

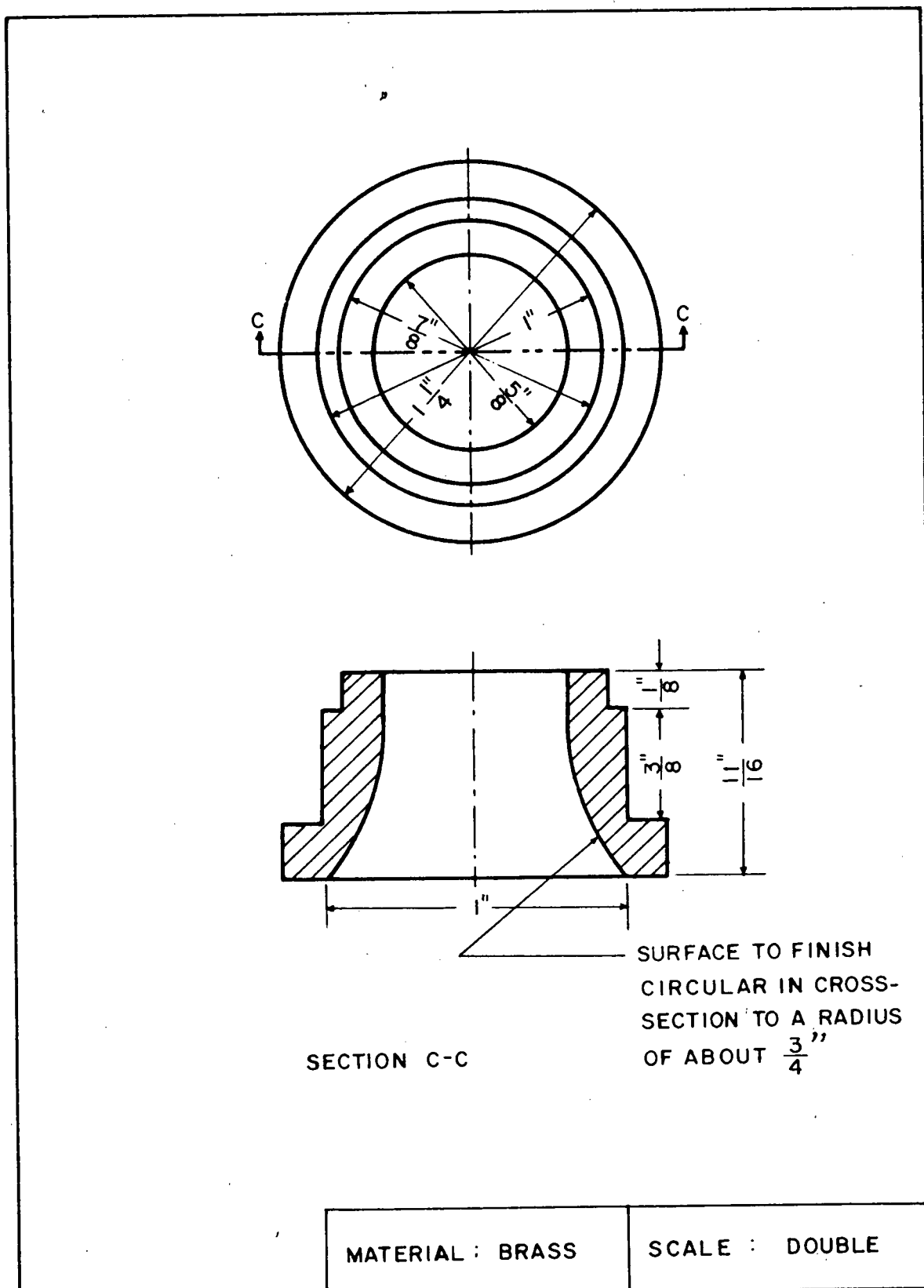
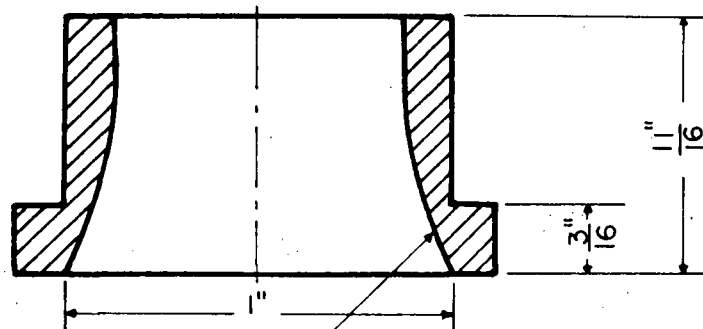
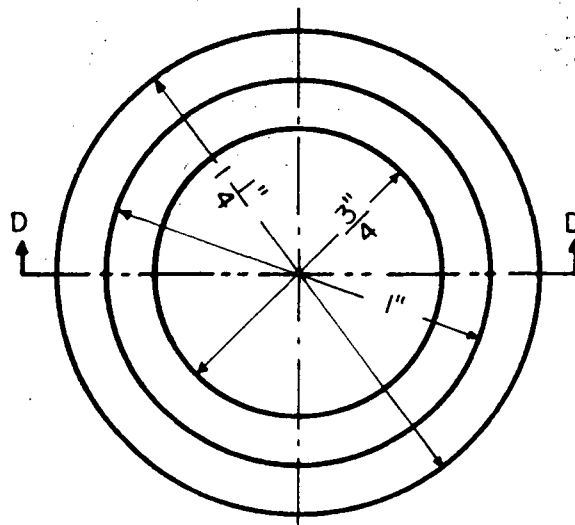


FIGURE III-13. 5/8-INCH ORIFICE-DIAMETER INLET



SECTION D-D

SURFACE TO FINISH
CIRCULAR IN CROSS-
SECTION TO A RADIUS
OF $\frac{7}{8}$ "

MATERIAL : BRASS

SCALE : DOUBLE

FIGURE III-14. $\frac{3}{4}$ -INCH ORIFICE-DIAMETER INLET

CHAPTER IV

EXPERIMENTAL PROCEDURE

IV-1. MATERIAL USED

The solid materials used in the experiments, alundum A, alundum B, alundum C, crystolon, silica sand, Ottawa sand, polystyrene A and polystyrene B were selected because their physical properties — particle size and distribution and density as shown in Table IV-1 — covered a wide range.

All the materials used, except polystyrene A and B, are particulate and each individual particle of these materials is approximately isometric in shape. These are referred as particulate materials.

On the other hand, polystyrene A and B are granular and pellet shaped. All the particles in either polystyrene A or B are nearly uniform. Polystyrene A and B are referred as granular materials.

IV-2. DETERMINATION OF PHYSICAL PROPERTIES OF MATERIALS

(a) SAMPLING AND SIZE ANALYSIS

(1) PARTICULATE MATERIALS

Each one of these materials was thoroughly hand mixed in a container and a random sample was drawn from each material.

All the samples were carefully hand sieved into fractions using Tyler standard sieves and the differential screen analysis of each was determined. Since the materials undergo certain degree of attrition during spouting resulting in size distribution different from initial distribution, the screen analysis of each one of these materials was again determined after all the experimental runs were over. The screen analyses recorded in Table IV-1 are the arithmetic averages of the initial and final analyses of each material.

TABLE IV-1

PHYSICAL PROPERTIES OF MATERIALS USED

Material	Sieve Range (Tyler)	Mean Opening d, in.	Weight Fraction x	Density ₃ lb. _m /ft. ³
Alundum A	- 9 +10	0.0718	0.619	246.3
	-10 +12 2	0.060	0.356	
	-12 +14	0.0505	0.025	
Alundum B	-16 +20	0.0359	0.101	
	-20 +24 4	0.0302	0.550	
	-24 +28	0.0254	0.295	
	-28 +32	0.0214	0.054	
Alundum C	-35 +42	0.0515	0.345	
	-42 +48	0.0127	0.055	
Crystolon	-16 +20	0.0359	0.052	199.6
	-20 +24	0.0302	0.420	
	-24 +28	0.0254	0.295	
	-28 +32	0.0214	0.233	
Silica Sand	-10 +12	0.060	0.091	165.0
	-12 +14	0.0505	0.263	
	-14 +16	0.0425	0.221	
	-16 +20	0.0359	0.163	
	-20 +24	0.0302	0.110	
	-24 +28	0.0254	0.152	
Ottawa Sand	-20 +24	0.0302	0.205	166.4
	-24 +28	0.0254	0.647	
	-28 +32	0.0214	0.148	
	Width in.	Breadth in.	Length in.	
Polystyrene A	0.073	0.107	0.144	65.8
Polystyrene B	0.0427	0.054	0.0813	

(ii). GRANULAR MATERIALS

Polystyrene A and B, as mentioned earlier, are granular and have a pellet-like shape. Therefore, mesh dimensions for these materials are not believed sufficient to express their sizes adequately.

The three principal dimensions, i.e., width d_1 , breadth d_2 and length d_3 of polystyrene A and B were determined as follows:

25 grains were taken as a sample from each fraction. Width d_1 and breadth d_2 were measured by a micrometer. The length d_3 being somewhat irregular is not determinable by micrometer. Average volume of a grain of each fraction was then determined by pycnometric method using methanol as displacement liquid.

If each grain is considered as a pellet with an elliptical base having d_1 and d_2 as minor and major axes and length d_3 , the volume V of the grain is given by

$$V = \pi \frac{d_1 d_2}{4} d_3$$

$$\text{or } d_3 = \sqrt[4]{\frac{4V}{\pi d_1 d_2}} \quad (\text{IV-1})$$

The average length d_3 of a grain of each fraction was calculated from Equation IV-1, using the average values of d_1 , d_2 and V (based on 25 particles for each) of a grain of the corresponding fraction.

Similar procedure was adopted to determine d_1 , d_2 and d_3 of each fraction of polystyrene after the experimental runs were over. The dimensions recorded in Table IV-1 are the averages of the respective initial and final dimensions.

(b) MEAN PARTICLE DIAMETERS

(i) PARTICULATE MATERIALS

The mean particle diameters — weight mean, surface mean, length mean, mean weight, mean surface and mean length — defined by Equations II-2 to II-7 were calculated for alundum A, alundum B, alundum C, crystolon, silica sand and Ottawa sand from their screen analyses shown in Table IV-1.

It will be noted, that by mixing alundum A (Tyler sieve range -9 +14) and B (Tyler sieve range -16 +32), or alundum A, B and alundum C (Tyler sieve range -35 +48), or alundum A and C in different weight proportions, size distributions and thereby mean particles diameters can be varied. Mean particle diameters for all such mixtures of alundum A and B, alundum A, B and C, and alundum A and C used in the present investigation together with the mean particle diameters of individual cuts of alundum A, alundum B, alundum C, crystolon, Ottawa sand and silica sand are tabulated in Table IV-2.

(ii) GRANULAR MATERIALS

Either the geometric mean of the two smaller dimensions, i.e., $\sqrt{d_1 d_2}$ ($\sqrt{\text{width} \times \text{breadth}}$), or the geometric mean of the three dimensions, i.e., $\sqrt[3]{d_1 d_2 d_3}$ ($\sqrt[3]{\text{width} \times \text{breadth} \times \text{length}}$), can be considered as the characteristic diameter of the individual fractions of the granular materials, polystyrene A and B.

Considering $\sqrt{d_1 d_2}$ as the characteristic diameter of either fraction of polystyrene, mean particle diameters defined by Equations II-2 to II-7 were calculated for mixtures composed of varying proportions of polystyrene A and B. These are tabulated in Table IV-3.

TABLE IV-2

CALCULATED VALUES OF MEAN PARTICLE DIAMETERS OF PARTICULATE MATERIALS

(Alundum A, B, C, Mixtures of Alundum A, B and C, Crystolon, Silica Sand and Ottawa Sand)

Material			Mean Particle Diameter (Inches)					
			Weight Mean	Surface Mean	Length Mean	Mean Weight	Mean Surface	Mean Length
Alundum								
%A	%B	%C						
100			0.0671	0.0665	0.658	0.0658	0.0654	0.0651
	100		0.0289	0.0285	0.0280	0.0280	0.0278	0.0275
		100	0.0135	0.0134	0.0134	0.0134	0.0133	0.0133
90	10		0.0633	0.0586	0.0515	0.0506	0.0470	0.0430
83 1/3	16 2/3		0.0607	0.0545	0.0460	0.0457	0.0418	0.0380
75	25		0.0576	0.0516	0.0414	0.0415	0.0378	0.0345
66 2/3	33 1/3		0.0544	0.0471	0.0381	0.0385	0.0352	0.0325
50	50		0.0480	0.040	0.0338	0.0344	0.0319	0.0302
25	75		0.0385	0.0332	0.0302	0.0306	0.0293	0.0285
10	90		0.0327	0.0302	0.0287	0.0289	0.0283	0.0278
90	5	5	0.0625	0.0526	0.0348	0.0336	0.0268	0.0217
75	20	5	0.0568	0.0454	0.0314	0.0312	0.0259	0.0214
50	25	25	0.0442	0.0286	0.0192	0.0204	0.0172	0.0154
Crystolon			0.0270	0.0264	0.0258	0.0258	0.0255	0.0252
Silica Sand			0.0412	0.0383	0.0356	0.0356	0.0343	0.0331
Ottawa Sand			0.0258	0.0255	0.0253	0.0253	0.0251	0.0250

(i) For a discussion on "Mean Particle Diameter", see Chapter II-2(d)(iii).

(ii) Arithmetic mean of the screen opening was used as the representative diameter of a Tyler screen fraction.

TABLE IV-3

CALCULATED VALUES OF MEAN PARTICLE DIAMETERS OF GRANULAR MATERIALS

(Polystyrene A, B and Mixtures of Polystyrene A and B)

Material		Mean Particle Diameter (Inches)					
		Weight Mean	Surface Mean	Length Mean	Mean Weight	Mean Surface	Mean Length
Polystyrene							
%A	%B						
100	0	0.0884	0.0884	0.0884	0.0884	0.0884	0.0884
		0.104	0.104	0.104	0.104	0.104	0.104
90	10	0.0844	0.0816	0.0774	0.0768	0.0746	0.0718
		0.0993	0.0961	0.0914	0.0909	0.0883	0.0853
80	20	0.0803	0.0757	0.0699	0.0696	0.0668	0.0638
		0.0976	0.0894	0.0828	0.0824	0.0793	0.0759
50	50	0.0682	0.0622	0.0572	0.0576	0.0554	0.0536
		0.0806	0.0738	0.0680	0.0684	0.0660	0.0639
25	75	0.0580	0.0542	0.0516	0.0519	0.0508	0.050
		0.0689	0.0645	0.0615	0.0618	0.0606	0.0597

TABLE IV-3 Continued

<u>Polystyrene</u>		Weight Mean	Surface Mean	Length Mean	Mean Weight	Mean Surface	Mean Length
%A	%B						
10	90	0.0520	0.0503	0.0493	0.0494	0.0490	0.0487
		0.0619	0.0599	0.0587	0.0589	0.0584	0.0580
0	100	0.0480	0.0480	0.0480	0.0480	0.048	0.048
		0.0572	0.0572	0.0572	0.0572	0.0572	0.0572

- (i) The values in the upper half of each box are those obtained when $\sqrt{\text{width} \times \text{thickness}}$ was taken as the characteristic diameter of either polystyrene.
- (ii) The values in the lower half of each box are those obtained when $\sqrt[3]{\text{width} \times \text{breadth} \times \text{length}}$ was taken as the characteristic diameter of either polystyrene.
- (iii) For a discussion on "Mean Particle Diameters", see Chapter II-2(d)(iii).

Similarly, considering $\sqrt[3]{d_1 d_2 d_3}$ as the characteristic diameter of either fraction of polystyrene, mean particle diameters defined by Equations II-2 to II-7 were calculated for mixtures composed of varying weight proportions of polystyrene A and B. These are also tabulated in Table IV-3.

(c) SOLID DENSITY

Absolute solid densities of all the materials were determined pycnometrically. Water was used as displacement liquid for all the materials except polystyrene. Methanol was used as displacement liquid for polystyrene.

The reported values of densities (Table IV-1) are the averages of 6 determinations for alundum (2 for each alundum sample), 2 determinations for crystolon, 2 for silica sand, 2 for Ottawa sand and 4 for polystyrene (2 for each polystyrene fraction).

The density of alundum C (Alundum C is finer than either alundum A or B) is consistently higher by about 0.5% than that of alundum A or B although all the three samples are of the same chemical composition. Since this difference is not large, average value of the 6 determinations (2 for each sample) was used as the density of alundum for all size distributions.

IV-3. EXPERIMENTAL RUNS

(a) GENERAL

The two rotameters and the test column were installed so that they are perfectly vertical. All the piping and flange joints were tested for air leaks with soapy water at 35 p.s.i.g. pressure and all air leakages corrected. One of the inlets was then inserted at the base of the cone

(see Figure III-7 for a sectional assembly drawing of the test column) and the approach section was connected to the test column. The outlet valves (items 13 and 4c, Figure III-1) were always kept closed except when they were under use to discharge the material from the column.

A typical run for measuring the minimum spouting velocity consists of feeding to the column a weighed amount of material of known size distribution, bringing the bed to minimum spouting condition and recording the rotameter tube reading, rotameter downstream air pressure and temperature, pressure drop across the bed and the static bed height.

The barometric pressure was also noted. The air flowing in the column was assumed to be at the room temperature.

The method of calculating the minimum spouting velocity from the observed readings is detailed in "Sample calculations" (Appendix 5).

A more detailed description of the experimental runs is given below.

(b) PREPARATION OF BED MIXTURE

In a single set of runs at different bed heights, it is necessary to maintain the same average size distribution of material at each run. This can be achieved only if material of the same size distribution is fed to the column each time the bed height is increased.

The size distribution cannot be expected to be uniform everywhere within the bulk of a solid material composed of different size fractions. It can, however, be reasonably assumed that if the material is a narrow cut fraction, approximately uniform size distribution can be obtained by a

thorough mixing. But it is not possible to obtain the same degree of uniformity if the material is a wide cut fraction.

Alundum A, alundum B and alundum C used in the present investigation are, as shown in Table IV-1, in the Tyler screen size ranges of -9 +14, -16 +32 and -35 +48 respectively. Since each one of them is a narrow cut fraction, it is assumed that a certain amount of material removed from any one of them will be representative of the original bulk fraction.

If the bed were to be composed of, say 50% alundum A, 25% alundum B and 25% alundum C, thus giving a wide size range, one of the two following methods can be adopted, viz.,

- (i) Mix, say 40 lbs. of alundum A, 20 lbs. of alundum B and 20 lbs. of alundum C. Take the required amount of material, say 16 lbs., from this mixture to feed to the column. Remove and add, say another 10 lbs. of material from the rest of the mixture to increase the bed height. This procedure can be continued. Or,
- (ii) Take 8 lbs. from alundum A, 4 lbs. from alundum B and 4 lbs. from alundum C, mix and feed these 16 lbs. of material to the column. For an additional amount of 10 lbs., take 5 lbs. from alundum A, 2.5 lbs. from alundum B and 2.5 lbs. from alundum C, mix and add to the column. The same procedure can be continued further.

The principle of method (ii) described above was adopted in the present work wherever necessary. For any single set of runs at different bed heights, this is more likely to give the same size distribution at each run than method (i).

(c) FEED TO COLUMN, START AND CONTROL OF AIR FLOW

The description of operation can best be done with reference to a particular run with material of a known size distribution as follows:

The bed material was to consist of 50% alundum A and 50% of alundum B. 8 lbs. of alundum A were weighed out from a thoroughly mixed bulk of alundum A and another 8 lbs. from alundum B. Both these were mixed and fed to the test column from the top in a slow current of air obtained by opening slightly the 1" globe valve (item 5, Figure III-1) in order that the material oriented itself to offer least resistance to the flow of air later. Abnormally high resistance to the flow of air indicated by a high pressure drop across the bed was observed if the air flow through the column was completely closed while the material was being fed to the column.

After the material was fed to the column, the flow of air was gradually increased by opening the 1" globe valve. (item 3a, Figure III-1). The gate valve (item 4, Figure III-1), leading to the rotameter-1, was kept fully open and the gate valve (item 4a, Figure III-1), leading to the rotameter-2, was kept completely closed. Initially the 1/2" globe valve (item 3, Figure III-1) was also kept closed.

Just before the incipient spouting, the 1/2" globe valve was partially open for fine control of air flow. The air flow was thus increased until the incipient spouting occurred.

The air flow was then increased slightly beyond the incipient condition, the bed was allowed to stay in spouting condition for about 2 minutes and the air flow was then gradually and carefully decreased by closing the 1/2" globe valve until the spout was just about to collapse. This is the minimum spouting point as defined in Chapter II-2(a).

Air flow rates over and above 30 S.C.F.M. were measured with rotameter-2.

(d) RECORD OF OBSERVATIONS

At the minimum spouting condition of the bed obtained as described above, the following readings were taken:

- (i) The rotameter tube reading
- (ii) The rotameter downstream pressure
- (iii) The rotameter downstream temperature
- (iv) The pressure drop across the spouted bed
- (v) The bed height

The bed height at minimum spouting recorded in many runs was not, however, used in the present correlation developed for minimum spouting velocity.

After the above readings were taken, the flow of air was gradually stopped and the bed was brought to static condition. The static bed height — referred to hereafter sometimes simply as bed height — was then noted.

The bed height was then increased by feeding to the column an additional 10 lbs. of material (5 lbs. of alundum A plus 5 lbs. of alundum B) and exactly the same procedure was followed to bring the bed to minimum spouting condition and again all the observations were recorded. Further increase of bed heights was obtained by feeding additional amounts of alundum A and alundum B in the same proportions.

(e) DISCHARGE OF MATERIAL, SCREENING, ETC.

After the readings were taken at different bed heights, the material was discharged through the discharge valve (item 13, Figure III-1).

The material was then separated into the original narrow cut fractions, alundum A and B, by sieving through Tyler 14-mesh screen. The material retained on the 14-mesh screen is alundum A and the material passed through 14-mesh screen is alundum B. Alundum B was also run through Tyler 32-mesh screen to screen off any material finer than 32-mesh, produced during the above runs. This was done because the original alundum B does not contain material finer than 32-mesh. This alundum B used again in further runs will, thus, have material in the same size range (-16 +32, see Table IV-1). Any change that would have occurred in the weight distributions of either cuts (alundum A or B) during a set of runs was not taken into account. But as mentioned earlier IV-2(a) the size analysis of each material was again taken after all the experimental runs were over and the average of the initial and final analyses has been reported in each case (Table IV-1).

A similar procedure was followed to prepare beds of alundum of various size distributions — by mixing alundum A,B,C in different proportions and the experiments were repeated.

Similar runs were made with beds of crystolon, silica sand and Ottawa sand in the test column.

Minimum spouting velocity data was also obtained for beds of polystyrene A, B and mixtures of polystyrene A and B in a similar way.

(f) CHANGE OF INLET

Inlets of different sizes (orifice diameters 3/4", 5/8", 1/2" and 3/8") were used. The change of inlet to the column was accomplished as follows:

- (i) The approach section was disconnected from the column (See Figure III-7);

- (ii) The inlet was removed from the cone;
- (iii) The inside surface of the cone flange was thoroughly cleaned and greased;
- (iv) Another inlet of desired size — the outside surface of which was thoroughly cleaned, polished and greased — was inserted into the cone flange; and
- (v) The approach section was reconnected to the column.

All the experimental data obtained to measure the minimum spouting velocity and other measurements and observations made were included in the next chapter.

CHAPTER V

EXPERIMENTAL RESULTS

By following the procedure detailed in the preceding chapter, extensive data on the minimum spouting velocity were obtained. The characteristics of the spouted beds of narrow and wide size range fractions were also observed.

V-1. RESULTS OF SPOUTED BEDS OF ALUNDUM MIXTURES

All the experimental data obtained with the beds of alundum mixtures is given in Table V-1. In this table, the minimum spouting velocities calculated from the observed readings are also recorded.

As detailed in Table V-1, alundum B was spouted in the test column fitted with the 5/8", 3/4", 1/2" and 3/8" diameter inlets. Measurements were made at various bed heights. Stable spouting was obtained up to a bed height of about 35" beyond which the bed tended to fluidize or slug.

Beds of alundum A were spouted in the test column fitted with a 3/8" and a 3/4" diameter inlet. Since the alundum A is coarse, stable spouting was obtained during all the runs.

Minimum spouting velocity data for the beds composed of the following proportions of alundum A and B was obtained. In all these cases, the 3/4" diameter inlet was used.

<u>% Alundum A</u>	<u>% Alundum B</u>
83 1/3	16 2/3
66 2/3	33
50	50
25	75
90	10
75	25
10	90

Alundum C was spouted in the column fitted with a 3/8" diameter inlet. Beds up to 23" high were spouted.

Beds made by mixing 90% alundum A, 5% alundum B and 5% alundum C were spouted with the 3/8" diameter inlet. Beds up to 28" high were spoutable.

With mixtures composed of 50% alundum A, 25% alundum B and 25% alundum C, beds up to 16" high only could be spouted with the 3/8" diameter inlet.

When the proportion of alundum C was increased beyond 25% (with 50% A and the balance alundum B), spouting was not produced at all.

Even though either alundum A, B or C — each of which a narrow size fraction — could be spouted individually in the column with the 3/8" inlet, the spoutability of mixtures of these fractions decreased with increasing proportions of the fine material, i.e., alundum C. In the mixtures of alundum A, B and C, the size of the finest fraction (0.0127") is about 1/6 the size of the coarsest fraction (0.0718").

Thus, it appears that the spoutability of non-uniform materials, in which the size of the coarsest fraction is more than 5 times that of the finest fraction, is less than that of any of the single fractions.

A mixture of 10% alundum A and 90% alundum C could not be spouted with 3/8" inlet. Thus, the addition of a small proportion of coarse material (alundum A) to a large proportion of the fines (alundum C) completely destroyed the spoutability of the fines.

Alundum C could not be spouted with any inlet larger than 3/8" in diameter.

TABLE V-1

DATA FOR MINIMUM SPOUTING VELOCITY OF ALUNDUM A, B, C

AND MIXTURES OF A, B AND C

$$D_c = 6''$$

$$\text{Cone Angle} = 60^\circ$$

(See Table IV-1 For Physical Properties of the Material)

Run No.	Material	Weight lb.	Flow Metering Section				Test Column Section			Air Flow Rate		V_s ft./sec.
			Inlet Dia. D_1 , in.	Rotameter [@] Tube Reading cm.	Down- stream Air Pres. in. Hg.	Down- stream Air Temp. °F.	Static Bed Height H, in.	Bed Ht. at Min. Spouting in.	Pressure Drop Across Bed in. CCl_4 .	S.C.F.M.	C.F.M. at Average Bed Pres. and Temp.	
A-1 (a)	Alundum B	19.0	0.625	8.1	75	1.1	11.5	5.7	12.50	12.32	1.088	
A-1 (b)		25.3		9.5		1.55	14.5	8.8	14.25	14.53	1.233	
A-1 (c)		32.3		11.2		2.0	17.8	11.6	16.36	16.58	1.407	
A-1 (d)		43.75		12.0		2.7	23.2	17.0	17.54	17.59	1.493	
A-1 (e)		56.7		12.6		3.4	29.3	22.9	18.48	18.33	1.556	
A-1 (f)		65.1		13.4		4.0	33.25	27.3	19.67	19.35	1.642	
A-1 (g)		70.5		13.7		4.25	35.8	29.7	20.16	19.75	1.676	
A-1 (h)		77.5		13.9		4.7	39.1	33.4	20.55	19.99	1.697	
A-2 (a)		18.8	0.75	9.0		1.3	11.4	6.2	13.6	13.92	1.182	
A-2 (b)	31.9	11.5		2.2	11.75	15.2	16.78	16.96	1.44			
A-2 (c)	39.7	12.3		2.7	21.5	16.6	17.8	17.86	1.516			
A-2 (d)	46.6	13.0		3.1	24.75	20.4	18.9	18.84	1.599			
A-2 (e)	56.3	13.4		3.5	29.0	24.4	19.52	19.29	1.637			
A-2 (f)	63.1	14.0		4.1	32.2	28.5	20.51	20.13	1.709			
A-2 (g)	68.8	14.4		4.5	35.0	31.6	21.2	20.69	1.756			
A-3 (a)		30.6	0.50	9.6		1.7	17.0	8.9	14.71	14.97	1.271	
A-3 (b)	58.1	12.6		3.4	29.6	23.6	18.47	18.36	1.558			
A-3 (c)	71.4	13.2		3.8	36.25	27.5	19.49	19.13	1.624			

TABLE V-1 Continued

Run No.	Material	Weight lb.	Flow Metering Section				Test Column Section			Air Flow Rate					
			Inlet Dia. D _i , in.	Rotameter [®] Tube Reading cm.	Down- stream Air Pres. in. Hg.	Down- stream Air Temp. °F.	Static Bed Height H, in.	Bed Ht. at Min. Spouting in.	Pressure Drop Across Bed in. CCl ₄ .	S.C.F.M.	C.F.M. at Average Bed Pres. and Temp.	V _s ft./sec.			
A-4 (a)	Alundum B	29.0	0.375	8.6	1.5	75	16.2		10.1	13.09	13.36	1.134			
A-4 (b)		56.3		11.9					2.9	29.0	24.6	17.47	17.47	1.483	
A-4 (c)		70.5		12.8					3.3	35.75	29.1	18.71	18.45	1.566	
A-5 (a)	Alundum A		0.375	18.0	7.4	72	11.0		3.9	27.24	27.81	2.36			
A-5 (b)				20.0					9.5	14.0	6.4	30.49	30.97	2.63	
A-5 (c)				22.5					13.6	20.2	10.7	36.53	36.8	3.12	
A-5 (d)				23.7					15.3	25.3	15.0	38.6	38.55	3.27	
A-5 (e)				5.1*					18.5	31.0	19.0	42.1	41.76	3.55	
A-5 (f)				5.3*					21.4	36.3	25.3	44.5	43.54	3.70	
A-6 (a)			0.75	5.5*	3.3	71	11.2		6.2	36.65	37.26	3.163			
A-6 (b)				6.2*					4.6	16.5	11.1	40.6	40.88	3.47	
A-6 (c)				7.0*					5.8	22.75	16.6	44.67	44.46	3.774	
A-6 (d)				7.1*					6.5	24.25	19.3	45.72	45.36	3.85	
A-6 (e)				7.55*					8.8	30.0	25.7	49.29	48.27	4.097	
A-6 (f)				7.75*					10.3	34.8	31.5	51.25	49.57	4.208	
A-7 (a)	83 1/3% Alundum A +16 2/3% Alundum B	28.0	0.75	20.4	3.2	70	15.0	15.3	9.8	28.97	29.06	2.467			
A-7 (b)		34.0		21.5					3.7	17.7	18.2	12.7	30.77	30.7	2.606
A-7 (c)		46.0		23.3					4.7	22.9	23.6	18.7	33.83	33.36	2.832
A-7 (d)		58.0		24.5					5.7	28.3	29.75	25.2	35.98	35.05	2.975
A-7 (e)		70.0		25.5					6.8	33.4	35.0	31.8	38.12	36.68	3.112
A-7 (f)		82.0		6.2*					8.0	38.8	41.0	38.6	42.2	40.1	3.404

TABLE V-1 Continued

Run No.	Material	Weight lb.	Flow Metering Section				Test Column Section			Air Flow Rate		
			Inlet Dia. D _i , in.	Rotameter [®] Tube Reading cm.	Down- stream Air Pres. in. Hg.	Down- stream Air Temp: °F.	Static Bed Height H, in.	Bed Ht. at Min. Spouting in.	Pressure Drop Across Bed in. CCl ₄ .	S.C.F.M.	C.F.M. at Average Bed Pres. and Temp.	V _s ft./sec.
A-8 (a)	66 2/3% Alundum A +33 1/3% Alundum B	15.0	0.75	15.9	1.7	74	9.5	9.8	4.8	22.29	22.73	1.929
A-8 (b)		27.0		16.8	2.4		14.25	14.5	10.4	23.76	23.97	2.034
A-8 (c)		39.0		17.5	3.2		19.25	19.75	16.2	24.97	24.92	2.115
A-8 (d)		51.0		18.6	4.0		24.25	25.25	22.2	26.72	26.35	2.237
A-8 (e)		63.0		19.55	4.9		29.25	30.5	28.5	28.42	27.7	2.351
A-8 (f)		69.0		19.95	5.4		31.75	33.25	31.8	29.28	28.37	2.408
A-8 (g)		75.0		20.8	5.8		34.25	35.75	35.1	30.66	29.53	2.507
A-9 (a)	50% Alundum A +50% Alundum B	16.0	0.75	14.0	1.5	72	9.9	10.1	5.4	19.77	20.06	1.703
A-9 (b)		26.0		14.8	2.2		13.9	14.25	10.3	21.04	21.15	1.795
A-9 (c)		36.0		15.7	2.9		18.0	18.6	15.2	22.45	22.35	1.897
A-9 (d)		46.0		16.4	3.4		22.25	22.75	20.2	23.6	23.28	1.976
A-9 (e)		51.0		16.8	3.8		24.2	25.0	22.8	24.28	23.83	2.023
A-9 (f)		57.0		17.1	4.2		26.6	28.0	25.9	24.79	24.19	2.053
A-9 (g)		67.0		17.5	4.8		30.8	32.0	31.6	25.56	24.67	2.094
A-10(a)	25% Alundum A +75% Alundum B	16.0	0.75	11.3	1.3	73.5	9.8	9.9	5.4	16.34	16.65	1.413
A-10(b)		24.0		12.5	1.85		13.3	13.6	9.0	17.96	18.17	1.542
A-10(c)		32.0		13.6	2.3		16.6	17.25	12.9	19.49	19.58	1.662
A-10(d)		40.0		14.0	2.7		19.9	20.75	16.5	20.11	20.06	1.703
A-10(e)		48.0		14.4	3.3		23.3	24.25	21.1	20.85	20.62	1.75
A-10(f)		52.0		14.7	3.6		25.0	26.0	23.3	22.06	21.72	1.844
A-10(g)		60.0		15.4	4.1		28.75	29.6	27.5	22.39	21.89	1.958
A-10(h)		64.0		15.5	4.3		30.3	31.5	29.7	22.62	22.0	1.867
A-10(i)		72.0		16.2	5.0		34.0	35.25	34.6	23.82	22.96	1.949

TABLE V-1 Continued

Run No.	Material	Weight lb.	Flow Metering Section				Test Column Section			Air Flow Rate		
			Inlet Dia. D ₁ , in.	Rotameter [®] Tube Reading cm.	Down- stream Air Pres. in. Hg.	Down- stream Air Temp. °F.	Static Bed Height H, in.	Bed Ht. at Min. Spouting in.	Pressure Drop Across Bed in. CCl ₄ .	S.C.F.M.	C.F.M. at Average Bed Pres. and Temp.	V _g ft./sec.
A-11(a)	90% Alundum A + 5% Alundum B + 5% Alundum C	15.0	0.625	12.8	2.3	75	9.75	10.0	3.2	18.23	18.74	1.59
A-11(b)		20.0		13.1	2.7		11.75	12.0	5.2	19.08	19.55	1.66
A-11(c)		25.0		13.7	3.0		13.75	14.5	6.2	19.81	20.26	1.72
A-11(d)		30.0		14.7	3.4		16.0	16.8	8.3	21.54	21.94	1.863
A-11(e)		40.0		15.6	4.1		20.5	21.4	11.4	22.74	22.97	1.95
A-11(f)		45.0		16.0	4.3		22.8	23.75	13.1	23.23	23.44	1.99
A-12(a)	75% Alundum A +20% Alundum B + 5% Alundum C	20.0	0.625	14.0	2.2	75	11.25	11.6	5.4	20.42	20.9	1.775
A-12(b)		28.0		16.4	2.6		14.25	15.25	8.1	22.98	23.4	1.99
A-13(a)	Alundum C		0.375	1.5	1.1	75	13.0	13.1	5.9	5.41	5.533	0.47
A-13(b)				2.2	1.6		16.75	16.9	8.9	6.156	6.259	0.531
A-13(c)				2.6	1.9		20.75	20.9	11.6	6.614	6.691	0.568
A-13(d)				2.9	2.0		22.7	23.0	13.5	6.914	6.968	0.591
A-14(a)	90% Alundum A + 5% Alundum B + 5% Alundum C	15.0	0.375	9.4	2.5	75	9.4	9.5	2.6	14.34	14.77	1.254
A-14(b)		25.0		11.9	4.0		13.5	13.75	4.7	17.69	18.14	1.54
A-14(c)		40.0		15.8	7.1		19.75	20.75	7.9	23.92	24.38	2.07
A-14(d)		50.0		18.0	9.4		24.5	25.7	10.5	27.76	28.15	2.39
A-14(e)		55.0		19.4	11.3		27.75	28.5	11.0	30.65	31.06	2.637

TABLE V-1 Continued

Run No.	Material	Weight lb.	Flow Metering Section				Test Column Section				Air Flow Rate	
			Inlet Dia. D _i , in.	Rotameter [®] Tube Reading cm.	Down- stream Air Pres. in. Hg.	Down- stream Air Temp. °F.	Static Bed Height in. CCl ₄ .	Bed Ht. at Min. Spouting in.	Pressure Drop Across Bed in. CCl ₄ .	S.C.F.M.	C.F.M. at Average Bed Pres. and Temp.	V _s ft./sec.
A-15(a)	50% Alundum A +25% Alundum B +25% Alundum C	15.0	0.375	4.8	1.4	75	9.3	9.5	3.3	8.79	9.03	0.767
A-15(b)		25.0		5.5	2.0		13.25	13.5	7.4	9.79	9.98	0.843
A-15(c)		35.0		6.0	2.3		17.0	17.5	11.4	10.39	10.51	0.892
A-16(a)	90% Alundum A +10% Alundum B	18.75	0.75	21.0	2.5	67	11.0	11.25	6.0	29.63	29.9	2.54
A-16(b)		21.25		21.5	2.75		12.0	12.5	7.1	30.4	30.6	2.6
A-16(c)		26.25		22.5	3.25		14.1	14.75	9.2	32.0	32.1	2.72
A-16(d)		31.25		23.2	3.8		16.25	17.0	11.1	33.3	33.3	2.82
A-16(e)		36.25		24.4	4.4		18.5	19.25	13.2	35.19	35.0	2.97
A-16(f)		41.25		25.2	4.7		20.75	21.5	15.6	36.63	36.2	3.07
A-16(g)		46.25		5.2*	5.1		22.75	23.75	19.1	37.21	36.58	3.11
A-16(h)		51.25		5.4*	5.95		25.0	25.0	21.1	38.24	37.5	3.18
A-16(i)		56.25		5.6	6.6		27.2	28.5	23.8	38.98	37.98	3.22
A-17(a)	75% Alundum A +25% Alundum B	12.0	0.75	13.8	1.5	72	8.0	8.0	3.0	19.51	19.95	1.693
A-17(b)		16.0		15.8	2.0		9.6	9.75	4.8	22.26	22.69	1.926
A-17(c)		20.0		16.6	2.3		11.25	11.5	6.5	23.48	23.85	2.024
A-17(d)		24.0		17.3	2.5		12.8	13.25	8.0	24.45	24.76	2.102
A-17(e)		28.0		17.8	2.8		14.25	15.0	10.0	25.23	25.45	2.16
A-17(f)		36.0		3.3*	3.6		18.0	18.75	13.6	27.08	27.13	2.303
A-17(g)		48.0		3.6*	4.7		22.75	23.75	17.7	28.89	28.61	2.428
A-17(h)		56.0		3.7*	5.4		26.1	27.2	23.5	29.62	29.12	2.472
A-17(i)		64.0		3.95*	5.7		29.5	30.6	28.1	30.86	30.07	2.552
A-17(j)		66.5		4.0*	5.8		31.0	31.75	30.3	31.15	30.23	2.566

TABLE V-1 Continued

Run No.	Material	Weight lb.	Flow Metering Section				Test Column Section			Air Flow Rate		
			Inlet Dia. D _i , in.	Rotameter [@] Tube Reading cm.	Down- stream Air Pres. in. Hg.	Down- stream Air Temp. °F	Static Bed Height H, in.	Bed Ht. at Min. Spouting in.	Pressure Drop Across Bed in. CCl ₄ .	S.C.F.M.	C.F.M. at Average Bed Pres. and Temp.	V _s ft./sec.
A-18(a)	10% Alundum A +90% Alundum B	10	0.75	7.3	0.9	73	7.5	7.5	2.6	11.56	11.88	1.01
A-18(b)		15		9.2	1.2		9.75	9.75	5.1	13.85	14.16	1.2
A-18(c)		20		10.7	1.6		12.0	12.1	7.4	15.68	15.95	1.35
A-18(d)		25		11.1	1.9		14.1	14.25	9.8	16.26	16.48	1.4
A-18(e)		30		11.4	2.25		16.25	16.5	11.3	16.7	16.86	1.43
A-18(f)		35		11.9	2.4		18.6	19.0	14.1	17.35	17.43	1.48
A-18(g)		45		13.1	3.0		23.0	23.5	18.9	19.05	18.96	1.61
A-18(h)		55		13.7	3.8		27.25	28.0	24.6	19.91	19.6	1.66
A-18(i)		60		13.7	4.1		29.5	30.5	26.6	20.14	19.36	1.68
A-18(j)		65		13.8	4.4		31.75	32.75	29.1	20.38	19.91	1.69
A-18(k)		70		14.0	4.6		34.0	35.0	31.7	20.71	20.12	1.71
A-18(l)		75		14.1	5.0		36.5	37.5	34.8	21.0	20.29	1.72

@ All readings are of rotameter-1 except those marked with *.

* Rotameter-2 tube readings.

A mixture of 90% alundum A, 5% alundum B and 5% alundum C was spouted in the column fitted with 5/8" diameter inlet. Beds up to 20" high only were spoutable. With the mixture composed of 75% alundum A, 20% alundum B and 5% alundum C, beds up to 14" high only were spoutable.

The minimum spouting velocity data pertaining to the mixtures of alundum A, B and C was also included in the Table V-1.

V-2. RESULTS OF SPOUTED BEDS OF OTTAWA SAND, SILICA SAND AND CRYSTOLON

(a) OTTAWA SAND

Ottawa sand of the physical properties shown in Table IV-1 was spouted in the test column at different bed heights. The 5/8" and 1/2" diameter inlets were used. Minimum spouting velocity data is given in Table V-2.

It is of interest to note here than Mathur and Gishler (1) have reported that Ottawa sand, of approximately the same physical properties as used in the present investigation, could not be spouted in a 6" I.D. column fitted with a 1/2" standard pipe as inlet ($D_1 = 0.622"$, i.e., about 5/8"). But, in the present experimental set up, beds of Ottawa sand as high as 35" were spouted in the 6" I.D. column fitted with 5/8" diameter inlet. It is assumed that the increased spoutability thus obtained is due to the better design of inlet to the column.

(b) SILICA SAND

The silica sand (Tyler screen range -10 +28, see Table IV-1) was spouted at different heights in the test column fitted with a 3/4" diameter inlet. The minimum spouting velocity data obtained was given in Table V-3.

Beds up to 37" high were spoutable.

TABLE V-2

DATA FOR MINIMUM SPOUTING VELOCITY OF OTTAWA SAND

$$D_c = 6''$$

$$\text{Cone Angle} = 60^\circ$$

(See Table IV-1 for Physical Properties of the Material)

Run No.	Material	Weight lb	Flow Metering Section				Test Column Section			Air Flow Rate		V_s ft./sec.
			Inlet Dia. D_1 , in.	Rotameter [@] Tube Reading cm.	Down- Stream Air Pres. in. Hg.	Down- stream Air Temp. °F.	Static Bed Height H, in.	Bed Ht. at Min. Spouting in.	Pressure Drop [†] Across Bed in. CCl_4 .	S.C.F.M.	C.F.M. at Average Bed Pres. and Temp	
0-1 (a)	Ottawa Sand		0.5	5.1	0.9	72	11.0	11.0	3.9	9.07	9.3	0.789
0-1 (b)				6.0	1.3		14.6	14.75	6.6	10.2	10.41	0.884
0-1 (c)				6.8	1.6		18.5	19.25	9.2	11.1	11.28	0.957
0-1 (d)				7.2	2.1		23.0	23.5	12.3	11.64	11.76	0.998
0-1 (e)				7.8	2.5		27.0	27.8	15.5	12.0	12.05	1.023
0-1 (f)				8.1	2.8		30.0	31.0	18.0	12.87	12.86	1.092
0-1 (g)				9.0	3.1		36.3	35.3	20.9	13.67	13.58	1.153
0-1 (h)				8.8	3.4		36.0	37.0	22.7	13.87	13.7	1.163
0-2 (a)			0.625	5.0	0.8	73	9.6	9.75	3.4	8.96	9.21	0.782
0-2 (b)				6.5	1.2		14.4	14.5	7.1	10.73	10.95	0.929
0-2 (c)				7.8	1.5		18.25	18.5	9.7	12.27	12.46	1.06
0-2 (d)				8.4	2.0		23.5	24.0	13.4	13.09	13.2	1.12
0-2 (e)				8.9	2.3		26.0	26.75	15.6	13.8	13.85	1.18
0-2 (f)				9.1	2.5		29.0	30.0	17.8	14.02	14.02	1.19
0-2 (g)				8.8	2.9		31.5	32.5	20.3	13.74	13.67	1.16
0-2 (h)				9.5	3.1		34.2	35.5	22.4	14.62	14.49	1.23

[@] Rotameter-1 tube readings.

TABLE V-3

DATA FOR MINIMUM SPOUTING VELOCITY OF SILICA SAND

$D_c = 6''$

Cone Angle = 60°

(See Table IV-1 for Physical Properties of the Material)

Run No.	Material	Weight lb.	Flow Metering Section				Test Column Section			Air Flow Rate		V_s ft/sec.
			Inlet Dia. D_1 , in.	Rotameter [@] Tube Reading cm.	Down- stream Air Pres. in. Hg.	Down- stream Air Temp. °F.	Static Bed Height H, in.	Bed Ht. at Min. Spouting in.	Pressure Drop Across Bed in. CCl_4 .	S.C.F.M.	C.F.M. at Average Bed Pres. and Temp.	
S-1 (a)	Silica Sand	8.0	0.75	8.5	1.0	72	8.25	8.25	1.9	13.0	13.35	1.13
S-1 (b)		13.0		10.7	1.1		12.1	12.25	4.2	15.57	15.91	1.35
S-1 (c)		16.0		12.4	1.2		14.0	14.25	5.6	17.79	18.13	1.54
S-1 (d)		25.0		12.8	1.3		20.25	20.75	9.3	18.57	18.8	1.6
S-1 (e)		30.0		13.5	2.2		23.75	24.5	11.8	19.35	19.49	1.55
S-1 (f)		35.0		14.0	2.4		27.25	28.25	14.1	20.04	20.1	1.71
S-1 (g)		40.0		14.5	2.8		31.0	32.0	16.8	20.82	20.77	1.76
S-1 (h)		45.0		14.9	3.2		33.75	35.5	19.5	21.46	21.3	1.81
S-1 (i)		48.5		15.1	3.4		37.0	38.0	21.3	21.82	21.58	1.83

@ Rotameter-1 tube readings.

(c) CRYSTOLON

The minimum spouting velocity measurements at different bed heights were made of the beds of crystolon (see Table IV-1 for physical properties) in the test column fitted with a 3/4" diameter inlet. Stable spouting was observed in beds up to about 35" high. The experimental data is given in Table V-4.

V-3. RESULTS OF SPOUTED BEDS OF POLYSTYRENE A, POLYSTYRENE B AND MIXTURES OF POLYSTYRENE A AND B.

As mentioned earlier in Chapter IV-1, the polystyrene A and B are pellet-shaped. Each one of these is composed of uniform granules.

The minimum spouting velocity data obtained with the beds of polystyrene A, B and mixtures of polystyrene A and B is given in Table V-5.

The beds of polystyrene A were spouted at different heights in the column fitted with the 3/4", 5/8", 1/2" and 3/8" diameter inlets. The channelling tendencies of these beds even at heights as low as 20" were marked. This might be due to the high porosity and low density of the bed. By careful control of air flow, however, stable spouting was obtained in beds as high as 35".

The beds of various proportions of polystyrene A and B were spouted in the test column fitted with a 1/2" diameter inlet. The presence of polystyrene B in polystyrene A did not affect the spoutability of A or vice versa. Both fractions are individually spoutable in the system. The size of polystyrene A, as shown in Tables IV-1 and IV-3, is only about twice that of polystyrene B. Therefore, any mixture of these two is a narrow-cut fraction.

Beds of polystyrene B alone were also spouted in the column fitted with the 1/2" diameter inlet.

TABLE V-4

DATA FOR MINIMUM SPOUTING VELOCITY OF CRYSTOLON

$$D_c = 6''$$

$$\text{Cone Angle} = 60^\circ$$

(See Table IV-1 for Physical Properties of the Material)

Run No.	Material	Weight lb.	Inlet Dia. D_1 , in.	Flow Metering Section			Test Column Section			Air Flow Rate		V_s ft./sec.
				Rotameter [@] Tube Reading cm.	Down- stream Air Pres. in. Hg.	Down- stream Air Temp. °F.	Static Bed Height H, in.	Bed Ht. at Min. Spouting in.	Pressure Drop Across Bed in. CCl_4 .	S.C.F.M.	C.F.M. at Average Bed Pres. and Temp.	
C-1 (a)	Crystolon	10	0.75	6.3	0.8	70	9.0	9.25	2.7	10.47	10.7	0.908
C-1 (b)		15		8.2	1.1		11.75	12.0	4.9	12.62	12.84	1.09
C-1 (c)		20		9.2	1.4		14.6	15.0	7.2	13.92	14.09	1.196
C-1 (d)		25		10.1	1.7		17.25	18.0	9.1	15.02	15.15	1.236
C-1 (e)		35		11.2	2.4		23.25	24.0	13.9	16.53	16.53	1.403
C-1 (f)		40		11.5	2.6		26.25	27.0	16.2	16.97	16.89	1.434
C-1 (g)		45		12.0	2.8		29.25	30.0	19.1	17.55	17.46	1.482
C-1 (h)		50		12.3	3.2		32.0	33.0	21.7	18.13	17.85	1.515
C-1 (i)		55		12.6	3.5		34.75	36.0	23.8	18.62	18.26	1.55

[@] Rotameter-1 tube readings.

TABLE V-5

DATA FOR MINIMUM SPOUTING VELOCITY OF POLYSTYRENE A, B

AND MIXTURES OF A AND B

$$D_c = 6''$$

$$\text{Cone Angle} = 60^\circ$$

(See Table IV-1 for Physical Properties of the Material)

Run No.	Material	Weight lb.	Inlet Dia. D_i , in.	Flow Metering Section			Test Column Section			Air Flow Rate		
				Rotameter [@] Tube Reading cm.	Down- stream Air Pres in. Hg.	Down- stream Air Temp. °F	Static Bed Height H, in.	Bed Ht. at Min. Spouting in.	Pressure Drop Across Bed in. CCl_4 .	S.C.F.M.	C.F.M. at Average Bed Pres. and Temp.	V_s ft./sec.
P-1 (a)	Polystyrene A	5.0	0.75	4.0*	1.7	72	11.8	12.3	3.0	29.29	30.04	2.55
P-1 (b)		7.7		4.3*	2.0		16.9	17.5	3.5	30.73	31.5	2.674
P-1 (c)		10.2		4.5*	2.5		21.25	22.0	4.9	31.83	32.53	2.761
P-1 (d)		11.7		4.7*	2.7		24.0	25.5	5.5	32.79	33.48	2.842
P-1 (e)		12.75		5.0*	2.8		26.0	27.6	5.9	34.17	34.86	2.959
P-2 (a)		4.0	0.625	18.0	1.7		10.0	10.5	1.33	25.06	25.8	2.19
P-2 (b)	5.75	19.8		2.15		13.25	13.75	2.4	27.77	28.53	2.422	
P-2 (c)	7.2	20.3		2.4		15.75	16.5	3.1	28.7	29.45	2.5	
P-2 (d)	8.75	21.3		2.7		18.75	19.25	3.7	29.96	30.7	2.606	
P-2 (e)	11.3	4.4*		3.1		23.25	24.5	5.1	31.7	32.4	2.75	
P-2 (f)	12.6	4.9*		3.55		25.5	27.25	5.7	34.12	34.83	2.956	
P-2 (g)	14.2	5.2*		3.6		28.5	30.0	6.9	35.47	36.12	3.066	
P-2 (h)	16.6	5.5*		3.9		32.75	33.25	6.8	36.73	37.33	3.169	
P-3 (a)		4.75	0.50	17.5	2.6		11.5	12.0	1.3	24.73	25.46	2.161
P-3 (b)	6.1	19.5		3.4		14.0	14.5	1.9	27.69	28.43	2.417	
P-3 (c)	8.6	20.5		3.9		18.5	19.25	3.1	29.37	30.15	2.559	
P-3 (d)	10.0	21.0		4.1		21.0	21.75	3.8	30.19	30.94	2.626	
P-3 (e)	11.7	21.5		4.5		24.0	25.5	7.0	31.07	31.63	2.685	
P-3 (f)	15.0	4.8*		5.7		30.0	32.0	6.4	34.73	35.41	3.006	

TABLE V-5 Continued

Run No.	Material	Weight lb.	Flow Metering Section				Test Column Section			Air Flow Rate		
			Inlet Dia. D _i , in.	Rotameter [®] Tube Reading cm.	Down- stream Air Pres. in. Hg.	Down- stream Air Temp. °F	Static Bed Height H, in.	Bed ht. at Min. Spouting in.	Pressure Drop Across Bed in. CCl ₄ .	S.C.F.M.	C.F.M. at Average Bed Pres. and Temp.	V _B ft./sec.
P-4 (a)	Polystyrene A	5.1	0.375	17.0	6.0	71	12.0	12.4	1.4	25.35	26.05	2.211
P-4 (b)		7.17		18.5	7.5		16.75	17.25	2.8	27.99	28.68	2.434
P-4 (c)		10.6		19.7	8.9		22.0	22.75	4.3	30.27	30.92	2.624
P-4 (d)		12.6		21.0	10.3		25.6	26.4	5.1	32.89	33.55	2.848
P-4 (e)		17.2		22.45	12.8		34.0	35.0	7.3	36.34	36.91	3.133
P-5 (a)	90% Polystyrene A +10% Polystyrene B	5.0	0.50	14.7	1.9	73	11.0	11.5	1.4	20.78	21.39	1.816
P-5 (b)		7.5		16.8	2.5		15.1	15.75	2.6	23.78	24.42	2.073
P-5 (c)		10.0		17.9	3.0		19.1	20.25	3.8	25.38	26.0	2.207
P-5 (d)		12.5		19.5	3.5		23.5	25.0	4.8	27.75	28.37	2.408
P-5 (e)		16.25		21.4	4.3		30.0	32.25	6.6	30.84	31.42	2.667
P-5 (f)		20.0		22.8	5.0		36.25	39.25	8.3	33.08	33.58	2.85
P-6 (a)	80% Polystyrene A +20% Polystyrene B	5.0		13.8	2.3	74	11.25	11.5	1.4	19.73	20.39	1.731
P-6 (b)		7.5		15.6	2.5		15.5	15.75	2.5	22.13	22.82	1.937
P-6 (c)		10.0		17.0	3.0		19.5	20.25	3.5	24.2	24.9	2.114
P-6 (d)		12.5		18.0	3.5		23.75	25.0	4.7	25.7	26.38	2.239
P-6 (e)		15.0		19.1	4.0		28.0	29.5	5.8	27.37	28.05	2.381
P-6 (f)		17.5		20.2	4.4		32.25	34.0	7.0	29.09	29.74	2.524
P-6 (g)		20.0		21.5	5.2		36.5	39.0	8.2	31.32	31.94	2.711
P-7 (a)	50% Polystyrene A +50% Polystyrene B	5.0		11.3	1.3	68	11.5	11.75	1.5	16.41	16.75	1.422
P-7 (b)		8.0		13.7	1.8		16.75	17.0	2.9	19.54	19.89	1.688
P-7 (c)		11.0		14.6	2.2		21.75	22.25	4.0	20.87	21.21	1.8
P-7 (d)		14.0		15.9	2.5		27.27	28.0	5.4	22.66	22.96	1.949
P-7 (e)		16.0		16.8	2.9		30.0	31.25	6.3	24.03	24.3	2.063
P-7 (f)		19.0		17.7	3.3		34.0	35.5	7.4	25.37	25.61	2.174
P-7 (g)		21.0		19.0	3.4		36.5	39.0	8.2	27.14	27.35	2.321

TABLE V-5 Continued

Run No.	Material	Weight lb.	Flow Metering Section				Test Column Section			Air Flow Rate		
			Inlet Dia. D ₁ , in.	Rotameter [@] Tube Reading cm.	Down- stream Air Pres. in. Hg.	Down- stream Air Temp. °F.	Static Bed Height H, in.	Bed Ht. at Min. Spouting in.	Pressure Drop Across Bed in. CCl ₄ .	S.C.F.M.	C.F.M. at Average Bed Pres. and Temp.	V _s ft./sec.
P-8 (a)	25% Polystyrene A +75% Polystyrene B	4.0	0.50	8.9	0.95	72	10.25	10.5	1.1	13.48	13.89	1.179
P-8 (b)		6.0		10.3	1.2		13.5	13.75	2.0	15.13	15.56	1.321
P-8 (c)		8.0		11.3	1.45		17.0	17.3	2.8	17.0	17.46	1.482
P-8 (d)		10.0		12.5	1.7		20.25	21.0	3.6	17.93	18.38	1.56
P-8 (e)		12.0		13.3	1.9		24.0	24.75	4.6	19.01	19.46	1.652
P-8 (f)		15.0		14.7	2.5		31.0	32.5	6.4	20.98	21.39	1.816
P-8 (g)		20.0		16.0	2.9		38.0	40.0	8.5	22.84	23.23	1.972
P-9 (a)		10% Polystyrene A +90% Polystyrene B	5.0	0.5	9.35	1.0	71	11.9	12.0	1.7	14.0	14.34
P-9 (b)	7.5			10.3	1.3		16.5	16.75	2.8	15.16	15.49	1.315
P-9 (c)	12.5			12.5	1.8		24.75	26.0	4.9	17.98	18.3	1.553
P-9 (d)	17.5			14.4	2.5		34.0	35.5	7.3	20.63	20.9	1.774
P-10(a)		34.0	0.75	15.4	1.7	71	34.0	35.5	7.9	21.63	21.88	1.857
P-11(a)		34.0	0.625	14.8	1.9	70	34.0	35.5	7.7	20.97	21.18	1.798
P-12(a)		33.0	0.375	13.0	4.0	70	33.0	34.5	6.6	19.24	19.48	1.653
P-13(a)	Polystyrene B	10.25	0.5	8.3	0.35	71	10.25	10.25	1.2	12.77	13.12	1.114
P-13(b)		13.75		9.8	1.1		13.75	14.0	2.0	14.57	14.95	1.269
P-13(c)		17.25		10.5	1.3		17.25	17.75	2.9	15.41	15.78	1.339
P-13(d)		20.5		11.1	1.5		20.5	21.5	3.7	16.18	16.54	1.404
P-13(e)		24.5		12.2	1.8		24.5	25.25	4.5	17.63	18.0	1.528
P-13(f)		28.0		12.9	1.9		28.0	29.0	5.6	18.48	18.83	1.598
P-13(g)		31.75		13.5	2.2		31.75	32.75	6.5	19.37	19.69	1.671

@ All readings are of rotameter-1 except those marked with *.

* Rotameter-2 tube readings.

V-4. SEGREGATION OF FINES IN THE BED

(a) GENERAL

When beds of alundum A, alundum B, alundum C, crystolon and Ottawa sand were spouted, no tendency of segregation of fines in any part of the column was observed. It will be noted that in none of these materials the size of the coarsest fraction is more than twice that of the finest fraction (see Table IV-1).

But, during the experimental runs with mixtures of alundum A and B, alundum A, B and C and silica sand, non-uniformity of the size distribution in the beds was pronounced. It will be noted that the size range in each of these beds is more than two-fold. The behaviour of the fines in these beds, as observed during the investigation, can be classified as follows:

(b) TIME DEPENDENCE OF THE SEGREGATION OF FINE PARTICLES AT THE TOP OF THE BED

During the experimental runs with mixtures of alundum A and B, and silica sand, part of the fine material was carried to the top of the bed after a few minutes' flow of air before spouting.

During the runs with mixtures of alundum containing alundum C also (Runs A-11(a) to (f), A-12(a) and (b), A-14(a) to (e) and A-15(a) to (c)), almost all the fine material, i.e., alundum C was carried to the top of the bed after a few minutes' flow of air.

In all the above cases, the top portions of the bed fluidized before the incipient spouting took place.

The spouted bed, containing 83 1/3% alundum A and 16 2/3% alundum B, was suddenly stopped after the run A-7 (f) and the material in every 3" high bed was analyzed for the weight percentage of -10 +14 Tyler screen fraction.

It was found that the composition of this particular fraction was almost the same along the entire height of the bed.

The spouted bed, containing 50% alundum A, 25% alundum B and 25% alundum C, was suddenly stopped after the run A-15(c) and the material in every 3" high bed was analyzed for the weight percentage of -42 +48 Tyler screen fraction. It was found that the percentage of this fraction at the top of the bed was far above the average.

From the two qualitative measurements, described above, it is evident that mixing takes place during spouting. Non-uniformity of size distribution, however, exists in the axial direction in beds composed of widely different sized-particles (e.g., mixtures of alundum A, B and C in which the particle size range is about 6-fold), whereas beds of mixtures containing particles within 4-fold size range (e.g., mixtures of alundum A and B), are well mixed up so that the size distribution is almost uniform along the entire bed height.

(c) SEGREGATION OF FINE PARTICLES IN POCKETS

Pockets of fine particles along the entire height of the bed were observed during the runs with beds of mixtures alundum A and B, alundum A, B and C and silica sand. With increasing air flow, particularly in beds composed of widely different size particles such as mixtures of alundum A, B and C, large cracks developed at places in the bed where a considerable amount of fines happened to segregate. This caused slugging of the beds.

V-5. RADIAL SIZE DISTRIBUTION OF SOLIDS DURING SPOUTING

When the spout fell back into the column due to gravity, radial classification of solids took place. Visual observations of the downward moving annulus and the top of the bed indicated that the concentration of the fines near the column wall was very high. During the runs with all the mixtures of alundum A and B, alundum A, B and C, and silica sand at bed heights over and above 15", it was observed that the outside of the annulus, i.e., the layer of material which travels

downwards touching the column wall, was completely made up of the finer fractions of the bed material.

Similarly, during all the runs (above 15" high beds) with mixtures of polystyrene A and B, the radial size distribution was visible. The ratio of the size of polystyrene A to that of B is less than two. But the actual sizes are comparatively higher. The density of polystyrene is much less than that of all other materials.

The radial size distribution of solids in a spouted bed is, thus, clearly a complex function of gravitational and potential forces acting on the particles and of the physical properties of the material. In addition, it may also depend upon the electrostatic potentials that exist in the spouted beds.

Size analysis of the material was not, however, performed to determine the extent of non-uniformity of the radial distribution due to the sampling difficulties.

V-6. ELECTROSTATIC EFFECTS IN SPOUTED BED

It was observed, during many experimental runs, that the spout does not stay in the centre of the column, but moves around the central axis of the column. The channelling of the spout towards the sides of the column was observed in beds higher than 30". These peculiarities were very marked in the spouted beds of polystyrene.

In spouted beds, as in fluidized beds, electrostatic potentials are likely to be developed by the interparticle collision and particle-wall contact.

A recent paper by Ciborowski and Wlodorski (25) describes the electrostatic effects in fluidized beds. The electrostatic charges accumulated on the solid particles were found to cause:

- (i) The adhesion of a layer of solid particles to the walls of the column;
- (ii) The agglomeration of particles into larger aggregates; and
- (iii) The change of fluidized bed into a channelling bed.

In the present work, during the spouting of polystyrene mixture containing 50% A and 50% B (Runs P-7(e) to P-7(g)), a stagnant layer of polystyrene B was formed along the entire inside of the column wall. After the run P-7(g), the bed was suddenly brought to the static condition by closing the air valve. The particle-layer along the column wall from the top of the static bed to the top of the bed at the minimum spouting condition (i.e., nearly 2 1/2") remained adhering to the wall. The particles fell into the bulk of the material slowly as the electric charges decayed. This took about 15 minutes.

During the same runs (P-7(e) to P-7(g)), the tendency of the spouts to channel towards the column wall was pronounced. Similar effects, to a lesser extent, were observed during many runs with the polystyrene beds.

These effects, obviously caused by the electrostatic potentials, are less pronounced in the spouted beds of materials other than polystyrene.

V-7. SOLIDS-ATTRITION IN SPOUTED BEDS

Solids in the spouted beds undergo attrition due to the interparticle collision and particle-wall contact. Qualitative measurements of the rates of attrition were made during this work.

(i) Alundum A fed to the column for the experimental runs, A-5(a) to A-5(f), (See Table V-1), was a fresh stock and it did not contain material finer than +14-mesh.

During all these runs, the bed was in spouted condition for about 40 minutes. The material was discharged from the column after the run A-5(f) and all this alundum A — about 75 lbs. — was sieved through a 14-mesh screen. The material that passed through the 14-mesh screen weighed about 4 lbs.

(ii) The material retained on the 14-mesh screen was fed to the column during the runs A-6(a) to A-6(f). The bed, during all these runs, was in spouted condition for about 40 minutes. All the material discharged after the run A-6(f) was again sieved through the 14-mesh screen. The material finer than 14-mesh was only about 10 gms.

These results indicate that the initial solids attrition rate in the spouted beds is very high and becomes negligible within a short period of time.

V-8. PRESSURE DROP-AIR FLOW DATA

The pressure drop across the bed during the increasing and decreasing air flow, for the run P-3(e) was also collected. The data so obtained were plotted against the air flow rate in S. C. F. M. as abscissa and the pressure drop in inches of water as ordinate in Figure II-1 to illustrate the spouting phenomena.

V-9. MINIMUM SPOUTING VELOCITY OBSERVED VS. MINIMUM SPOUTING VELOCITY PREDICTED BY MATHUR-GISHLER CORRELATIONS

The Mathur-Gishler Equations (Equation II-8 and II-9, see Chapter II-3) are the only ones available for directly calculating the minimum spouting velocity from the physical properties of the bed material and column geometry. The Mathur-Gishler Equations are given below:

$$V_s = \left(\frac{D_p}{D_c} \right) \left(\frac{D_i}{D_c} \right)^{1/3} \sqrt{\frac{2g H(\rho_s - \rho_f)}{\rho_f}} \quad (\text{II-8})$$

and

$$V_s = \left(\frac{D_p}{D_c} \right) \left(\frac{D_i}{D_c} \right)^n \sqrt{\frac{2g H(\rho_s - \rho_f)}{\rho_f}} \quad (\text{II-9})$$

where $n = 0.23$ for 45° cone
 $= 0.13$ for 85° cone

For 60° cone, the exponent n on the group $\frac{D_i}{D_c}$, as mentioned already in Chapter II-3, is about the same as for 45° cone, i.e., 0.23.

A comparison is made below between the minimum spouting velocity V_s observed for Runs A-10(a) to A-10(i) and the minimum spouting velocity V_s calculated by either Equations II-8 and II-9.

TABLE V-6

COMPARISON OF VALUES OF EXPERIMENTAL MINIMUM SPOUTING VELOCITY OF RUNS A-10(a) TO A-10(i) WITH VALUES PREDICTED BY EQUATIONS II-8 AND II-9

Run No.	Bed Height Inches	V_s (Observed)	$\frac{V_s(\text{Observed})}{V_s(\text{Predicted})}$ Eq. II-8	$\frac{V_s(\text{Observed})}{V_s(\text{Predicted})}$ Eq. II-9
A-10(a)	9.8	1.413	1.07	0.85
A-10(b)	13.3	1.542	1.01	0.805
A-10(c)	16.6	1.662	0.975	0.775
A-10(d)	19.9	1.703	0.90	0.72
A-10(e)	23.3	1.75	0.89	0.685
A-10(f)	25.0	1.844	0.845	0.695
A-10(g)	28.75	1.858	0.86	0.655
A-10(h)	30.3	1.867	0.825	0.64
A-10(i)	34.0	1.949	0.82	0.63

It is evident from the last two columns that the observed values deviate very much from the calculated values. The trend of the deviation of the observed values from those calculated with the bed height is similar to the deviation exhibited by the data of Buchanan and Mamurung (see Chapter II-6 and Figure II-3.) and Koyanagi (see Chapter II-7 and Figure II-3).

Thus it became apparent that the Mathur-Gishler correlation for minimum spouting velocity is not a satisfactory one.

In the next chapter, the details of the correlation of the minimum spouting velocity data are discussed.

CHAPTER VI

CORRELATION OF MINIMUM SPOUTING VELOCITY DATA

VI-1. GENERAL

The results of previous work (1,15) indicate that the superficial minimum spouting velocity can be correlated in terms of the physical properties of the bed materials, static bed height and column geometry through dimensional analysis. The variables upon which the minimum spouting velocity would be expected to depend are listed in Table IV-1 below.

TABLE VI-1

LIST OF VARIABLES

<u>Variable</u>	<u>Symbol</u>	<u>Dimension</u> (In absolute units)
Mean particle diameter	D_p	L
Inside column diameter	D_c	L
Inlet-orifice diameter	D_i	L
Static bed height	H	L
Solid density	ρ_s	ML^{-3}
Fluid density	ρ_f	ML^{-3}
Local acceration due to gravity	g	LT^{-2}

Thus $V_s = f(D_p, D_c, D_i, H, \rho_s, \rho_f, g)$

D_p, D_i, H and ρ_s have been varied throughout this investigation.

D_c and ρ_f have not been varied and g is constant.

A general relationship, between the minimum spouting velocity V_s and bed height H , of the form

$$V_s = a' H^m$$

has been found in which a' is a function of g , D_p , ρ_s and D_i and m is a function of D_i only, being independent of D_p and ρ_s .

The effects of D_p and ρ_s on V_s were then determined by the technique of cross-plotting of data.

By representing the data in terms of dimensionless groups, a dimensionless correlation has been derived.

The details of the treatment of data are discussed below.

VI-2. EFFECT OF BED HEIGHT ON MINIMUM SPOUTING VELOCITY

Logarithmic plots of minimum spouting velocity V_s against bed height H , have been made from all the experimental data. These are shown in Figures VI-1, VI-2, VI-3, VI-4, VI-5 and VI-6.

The mean particle diameter noted in the keys of these figures is the length mean diameter for mixtures of all materials and the geometric mean diameter, i.e., $\sqrt[3]{\text{width} \times \text{breadth} \times \text{length}}$, for uniform granular materials, namely polystyrene A and B.

Figure VI-1 was plotted to determine the relationship between the bed height H and minimum spouting velocity V_s with inlet diameter D_i ($= 3/4''$) and solid density ρ_s ($= 246.3 \text{ lb.}_m/\text{ft.}^3$) being held constant. For the family of straight lines in Figure VI-1, the parameter is the mean particle diameter.

The slopes of all these lines are the same and equal to 0.27. Therefore,

$$V_s \propto H^{0.27}$$

for constant D_i and ρ_s .

It will be noted that the slopes of these lines are independent of mean particle diameter D_p .

Figure VI-2 was plotted to determine the effect of bed height H on minimum spouting velocity V_s with inlet diameter D_i ($= 3/4''$) being held constant. As shown on Figure VI-2, particle diameter D_p and solid density ρ_s were variables. The slopes of these lines are also the same and equal to 0.27.

It can be concluded from these two figures, i.e., VI-1 and VI-2, that the slope m of the straight lines obtained when minimum spouting velocity V_s was plotted against bed height H is independent of the physical properties — i.e., particle diameter D_p and density ρ_s — of the bed material for a given column geometry.

Figure VI-3 was plotted to find the relationship between the minimum spouting velocity and bed height when the diameter of the inlet used was $5/8''$. Particle density and diameter are variables for the set of data plotted in Figure VI-3. The slopes of all the lines obtained are same and have a best value of 0.32.

Figure VI-4 was plotted to determine the relationship between the minimum spouting velocity and the bed height with inlet diameter D_i ($= 1/2''$) and solid density ρ_s ($= 65.8 \text{ lb.}_m/\text{ft.}^3$) being held constant. The parameter for the family of straight lines in Figure VI-4 is the mean particle diameter.

The data obtained using the 1/2" diameter inlet, — the particle density and diameter being varied — is shown in Figure VI-5.

The slopes of the lines on Figures VI-4 and VI-5 are the same and equal to 0.36.

Figure VI-6 represents the data obtained — the particle diameter and density being varied — with a 3/8" diameter inlet. The best slope of the parallel lines for the 100% fractions has a value of 0.39, while the lines for the remaining data were drawn with this same slope.

From all these plots (Figures VI-1 to VI-6), it is evident that the relationship between the minimum spouting velocity and the bed height can be represented by an equation of the form

$$V_s \propto H^m$$

$$\text{or } V_s = a'H^m \quad (\text{VI-1})$$

where a' is a function of D_p , e_s and D_i and m is a function of D_i alone, being independent of D_p and e_s .

VI-3. EFFECT OF MEAN PARTICLE DIAMETER ON MINIMUM SPOUTING VELOCITY FOR ALUNDUM MIXTURES.

Figure VI-1, the plot of V_s against H on logarithmic co-ordinates represents data obtained with alundum A, alundum B and mixtures of alundum A and Alundum B. (See Table IV-1 for the differential screen analyses of alundum A and B, Table IV-2 for the calculated values different mean D_p 's defined by Equations II-2 to II-7 and Figure II-2 for a plot of mean D_p 's against % alundum B in alundum A) using a 3/4" diameter inlet.

Since all the lines on Figure VI-1 are parallel, a cross-plot of V_s against mean D_p at constant H will show a relation between V_s and mean D_p .

V_s read from each line on Figure VI-1 at a bed height of 20" was plotted against the mean D_p of the corresponding bed mixture on logarithmic co-ordinates. Such a plot is shown in Figure VI-7. The abscissae of the points through which a straight line can be drawn are the values of the length mean D_p of the mixtures. The slope of this line is equal to 1. The abscissae of the points on the dotted curve and the solid curve (Figure VI-7) are the values of surface mean and weight mean D_p respectively of the mixtures. It is, therefore, concluded that, all the other variables, i.e., D_i , ρ_s and H , being constant,

$$V_s \propto D_p \quad \text{(VI-2)}$$

if length mean D_p is used to represent the average diameter of the bed mixture.

VI-4. EFFECT OF MEAN PARTICLE DIAMETER ON MINIMUM SPOUTING VELOCITY FOR POLYSTYRENE MIXTURES

Figure VI-4 — a plot of V_s against H on logarithmic co-ordinates — represents the data obtained with beds of polystyrene A, polystyrene B and mixtures of polystyrene A and B, (See Table IV-1 for the dimensions of polystyrene A and B, Table IV-3 for the geometric mean D_p 's of the individual fractions of polystyrene A and B and the calculated values of the length mean D_p 's of mixtures of polystyrene A and B), using a 1/2" diameter inlet.

The effect of mean D_p on V_s is shown in Figure VI-8 — a cross-plot of V_s at $H=20$ " (from Figure IV-4) against mean D_p of the corresponding mixture — on logarithmic co-ordinates.

It will be observed that there are two straight lines obtained on Figure VI-8.

The abscissae of the points through which a solid straight line was drawn (Figure VI-8) are values of the geometric mean of three dimensions i.e., width d_1 , breadth d_2 and length d_3 for individual fractions of polystyrene A and B ($3\sqrt{d_1d_2d_3} = 0.104$ " for polystyrene A, $3\sqrt{d_1d_2d_3} = 0.0572$ " for polystyrene B) and the length mean diameters for mixtures of polystyrene A and B calculated thereof.

The abscissae of the points through which a dotted line was drawn (Figure VI-8) are values of the geometric mean of two smaller dimensions, namely width d_1 and breadth d_2 for polystyrene A and B ($\sqrt{d_1d_2} = 0.0884$ " for polystyrene A, and $\sqrt{d_1d_2} = 0.048$ " for polystyrene B) and the length mean diameters for mixtures of polystyrene A and B calculated thereof.

Both the lines on Figure VI-8 have a slope equal to 1, and therefore, P_s , D_i and H being constant, the relationship between V_s and D_p for polystyrene mixtures, as in the case of alundum mixtures, can be written as

$$V_s \propto D_p \quad \text{(VI-2(a))}$$

The two lines on Figure VI-8 are separate because of the difference between the values of $\sqrt{d_1d_2}$ and $3\sqrt{d_1d_2d_3}$ of either fraction of polystyrene.

The geometric mean of the three dimensions i.e., $3\sqrt{d_1d_2d_3}$ for polystyrene A and B and the length mean diameters calculated thereof were used in the final correlation, since this will take into account the influence of all the three dimensions on mean D_p for each single fraction and consequently on mean D_p of the mixtures as well.

VI-5. EFFECT OF SOLID DENSITY ON MINIMUM SPOUTING VELOCITY

It is recalled that Figure VI-2 is a plot of V_s against H (log-log co-ordinates) with mean D_p and ρ_s as variables. (All the lines of Figure VI-2 have the same slope).

It is clear from the foregoing analysis (Chapter VI-3 and VI-4) that $V_s \propto D_p$, all other variables being kept constant. Therefore, a cross-plot of $\frac{V_s}{D_p}$ at a constant bed height against ρ_s will show the dependence of V_s on ρ_s .

V_s read from each line on Figure VI-2 at $H = 20''$ was divided by the mean D_p of the corresponding bed material and the value of $\frac{V_s}{D_p}$ as ordinate was plotted against the corresponding solids density ρ_s as abscissa in Figure VI-9. The slope of the straight line obtained is 0.50. Thus, all other variables being kept constant,

$$V_s \propto \rho_s^{0.5} \quad \text{(VI-3)}$$

In making this plot, Figure VI-9, if the geometric mean of the two smaller dimensions of polystyrene A (i.e., $\sqrt{d_1 d_2} = \sqrt{0.073 \times 0.107} = 0.088''$) were used instead of the geometric mean of three dimension ($3\sqrt{d_1 d_2 d_3} = 3\sqrt{0.073'' \times 0.107'' \times 0.144''} = 0.104$), the value of $\frac{V_s}{D_p}$ corresponding to polystyrene ($\rho_s = 65.8 \text{ lb}_m/\text{ft}^3$) would deviate more from the line drawn on Figure VI-9.

If Equations VI-1, VI-2 and VI-3 are combined, there results

$$V_s \propto H^m D_p \rho_s^{0.5}$$

or $\frac{V_s}{D_p \rho_s^{0.5}} = a'' H^m \quad \text{(VI-4)}$

VI-6. DIMENSIONAL ANALYSIS

The data can be represented in terms of dimensional groups as shown in the following analysis.

From the variables D_p , D_i , D_c , H , ρ_s , ρ_f and g on which V_s is assumed to depend, the following dimensionless groups can be formed by dimensional analysis:-

$$\frac{V_s}{gD_p}, \frac{D_c}{D_p}, \frac{D_i}{D_c}, \frac{\rho_s}{\rho_f}, \frac{H}{D_c}$$

Though D_c and ρ_f have not been varied independently, these are included to form dimensionless groups for the sake of completeness and convenience.

By multiplying both sides of the Equation VI-4 by $\left(\frac{D_c \rho_f}{g}\right)^{0.5}$,

the equation

$$\left(\frac{V_s}{D_p}\right) \left(\frac{D_c \rho_f}{\rho_s g}\right)^{0.5} = a'' \left(\frac{D_c \rho_f}{g}\right)^{0.5} \frac{H^m}{D_c^m} \quad (VI-5)$$

is obtained.

By multiplying and dividing the right hand side of Equation VI-5 by D_c^m , the equation

$$\left(\frac{V_s}{D_p}\right) \left(\frac{D_c \rho_f}{\rho_s g}\right)^{0.5} = a'' \left(\frac{D_c \rho_f}{g}\right)^{0.5} D_c^m \left(\frac{H}{D_c}\right)^m \quad (VI-6)$$

is obtained.

After rearrangement, Equation VI-6 becomes

$$\sqrt{\left(\frac{V_s^2}{gD_p}\right) \left(\frac{D_c}{D_p}\right) \left(\frac{\rho_f}{\rho_s}\right)} = a'' \left(\frac{D_c \rho_f}{g}\right)^{0.5} D_c^m \left(\frac{H}{D_c}\right)^m \quad (\text{VI-7})$$

$$= A \left(\frac{H}{D_c}\right)^m$$

where $A = a'' \left(\frac{D_c \rho_f}{g}\right)^{0.5} D_c^m$ (VI-8)

and a'' and m are functions of D_i only. A is a dimensional constant. Since D_c , ρ_f and g were not varied in the experiments, they could be dropped out and A can be represented as a product of a dimensionless constant and some function of $\frac{D_i}{D_c}$, e. g.,

$$A = C \cdot f\left(\frac{D_i}{D_c}\right) \quad (\text{VI-9})$$

The exact form of Equation VI-9 can only be determined from the experimental data.

In Equation VI-7, ρ_s can be replaced by $(\rho_s - \rho_f)$ since ρ_f is negligibly small in comparison with ρ_s and a form which is hydrodynamically more realistic is obtained, viz.,

$$\sqrt{\left(\frac{V_s^2}{gD_p}\right) \left(\frac{D_c}{D_p}\right) \left(\frac{\rho_f}{\rho_s - \rho_f}\right)} = A \left(\frac{H}{D_c}\right)^m \quad (\text{VI-10})$$

$$= C \cdot f\left(\frac{D_i}{D_c}\right) \left(\frac{H}{D_c}\right)^m \quad (\text{VI-10a})$$

Denoting the left hand side of Equation VI-10 as Y, the same can be rewritten as :

$$Y = A \left(\frac{H}{D_c} \right)^m \quad \text{(VI-11)}$$

$$= C. f \left(\frac{D_i}{D_c} \right) \left(\frac{H}{D_c} \right)^m \quad \text{(VI-11a)}$$

Equation VI-11 suggests that a plot of Y against $\frac{H}{D_c}$ on logarithmic co-ordinates, for a constant $\frac{D_i}{D_c}$, should result in a straight line with slope m and intercept A.

Figure VI-10 is a plot of Y against $\frac{H}{D_c}$ on log-log co-ordinates for $D_i = 3/4"$, i.e., $\frac{D_i}{D_c} = 1/8$.

Figure VI-11 is a plot of Y against $\frac{H}{D_c}$ for 5/8" diameter inlet.

Y against $\frac{H}{D_c}$ for $D_i = 1/2"$ was plotted on Figure VI-12.

Figure VI-13 is an another plot of Y against $\frac{H}{D_c}$ for 3/8" diameter inlet.

The slopes m, of the lines in Figures VI-10, 11, 12 and 13 and their intercepts A at $\frac{H}{D_c} = 1$ are given in Table VI-2 below, together with the corresponding values of $\frac{D_c}{D_i}$.

TABLE VI-2

SLOPE m , INTERCEPT A AND $\frac{D_c}{D_i}$

$\frac{D_c}{D_i}$	Slope m	Intercept A
8	0.274	1.06
9.6	0.32	0.92
12	0.36	0.825
16	0.39	0.745

VI-7. CORRELATION OF SLOPE m WITH $\frac{D_i}{D_c}$

A plot of m against $\frac{D_i}{D_c}$, as shown in Figure VI-14, was made on arithmetic co-ordinates. A linear relationship is seen between m and $\frac{D_i}{D_c}$.

The equation of the straight line in Figure VI-14 is given by

$$m = 0.50 - 1.76 \left(\frac{D_i}{D_c} \right) \tag{VI-12}$$

The maximum deviation of the experimental value from Equation VI-12 is 2.16%.

VI-8. CORRELATION OF INTERCEPT A WITH $\frac{D_i}{D_c}$

A plot of A against $\frac{D_i}{D_c}$ on arithmetic co-ordinates, shown in

Figure VI-15, suggests that a correlation might be possible of the form

$$A - x \equiv B \left(\frac{D_i}{D_c} \right)^a$$

An excellent correlation, as shown in Figure VI-16, is obtained by plotting $\text{Log } (A-0.64)$ against $\text{Log } \left(\frac{D_i}{D_c} \right)$ giving

$$A = 0.64 + 26.8 \left(\frac{D_i}{D_c} \right)^2 \quad (\text{VI-13})$$

The maximum deviation of the experimental values from Equation VI-13 is 1.33%.

VI-9. DIMENSIONLESS CORRELATION

Elimination of A and m from Equation VI-11 through substitution of Equations VI-12 and VI-13 results in the final dimensionless correlation which can be written as :

$$Y = \sqrt{\left(\frac{v_s^2}{gD_p} \right) \left(\frac{D_c}{D_p} \right) \left(\frac{\rho_f}{\rho_s - \rho_f} \right)}$$

$$= \left[0.64 + 26.8 \left(\frac{D_i}{D_c} \right)^2 \right] \left(\frac{H}{D_c} \right)^{0.50 - 1.76 \left(\frac{D_i}{D_c} \right)} \quad (\text{VI-14})$$

All the experimental data obtained in the present work on minimum spouting velocity have been plotted in Figure VI-17 with Y as ordinate and

$A \left(\frac{H}{D_c} \right)^m$ as abscissae on arithmetic co-ordinates. A 45° straight line

was drawn through the points.

The average deviation, standard deviation and maximum deviation of the experimental values from Equation VI-14 are 5.33%, 6.87% and 32% respectively.

VI-10. DIMENSIONAL CORRELATION

Equation VI-14 predicts that for a given bed of material

$$V_s \propto \frac{1}{D_c^{0.5}} \quad \text{for constant} \quad \frac{H}{D_c} \quad \text{and} \quad \frac{D_i}{D_c}$$

The use of Equation VI-14 for predicting V_s of mixed particle-size beds in columns other than 6" diameter is not recommended because reliable data are not available for larger or smaller columns to test the dependence of V_s on D_c as stipulated by Equation VI-14.

Equation VI-14 can be reduced to dimensional form by substituting 0.50 for D_c and simplifying the expression, viz,

$$\begin{aligned} V_s &= \left[\frac{D_p \left(1.28 + 214.4 D_i^2 \right)}{(2H) 3.52 D_i} \right] \sqrt{\frac{g H (\rho_s - \rho_f)}{\rho_f}} \\ &= \left[\frac{D_p \left(0.905 + 152 D_i^2 \right)}{(2H) 3.52 D_i} \right] \sqrt{\frac{2g H (\rho_s - \rho_f)}{\rho_f}} \end{aligned} \quad \text{(VI-15)}$$

$$= C' \sqrt{\frac{2g H (\rho_s - \rho_f)}{\rho_f}} \quad \text{(VI-16)}$$

where C' is a function of D_p , D_i and H .

Equation VI-15 is applicable for columns of 0.50' diameter only.

A comparison between V_s predicted by Equation VI-14 or VI-15 and V_s observed at different bed heights is shown in Figure VI-18 in which

$\frac{V_s \text{ (predicted)}}{V_s \text{ (observed)}}$ as ordinate was plotted against bed height for all the

experimental runs.

All the calculated data used in plotting Figures VI-10, VI-11, VI-12, VI-13, VI-17 and VI-18 can be found in Appendix 3.

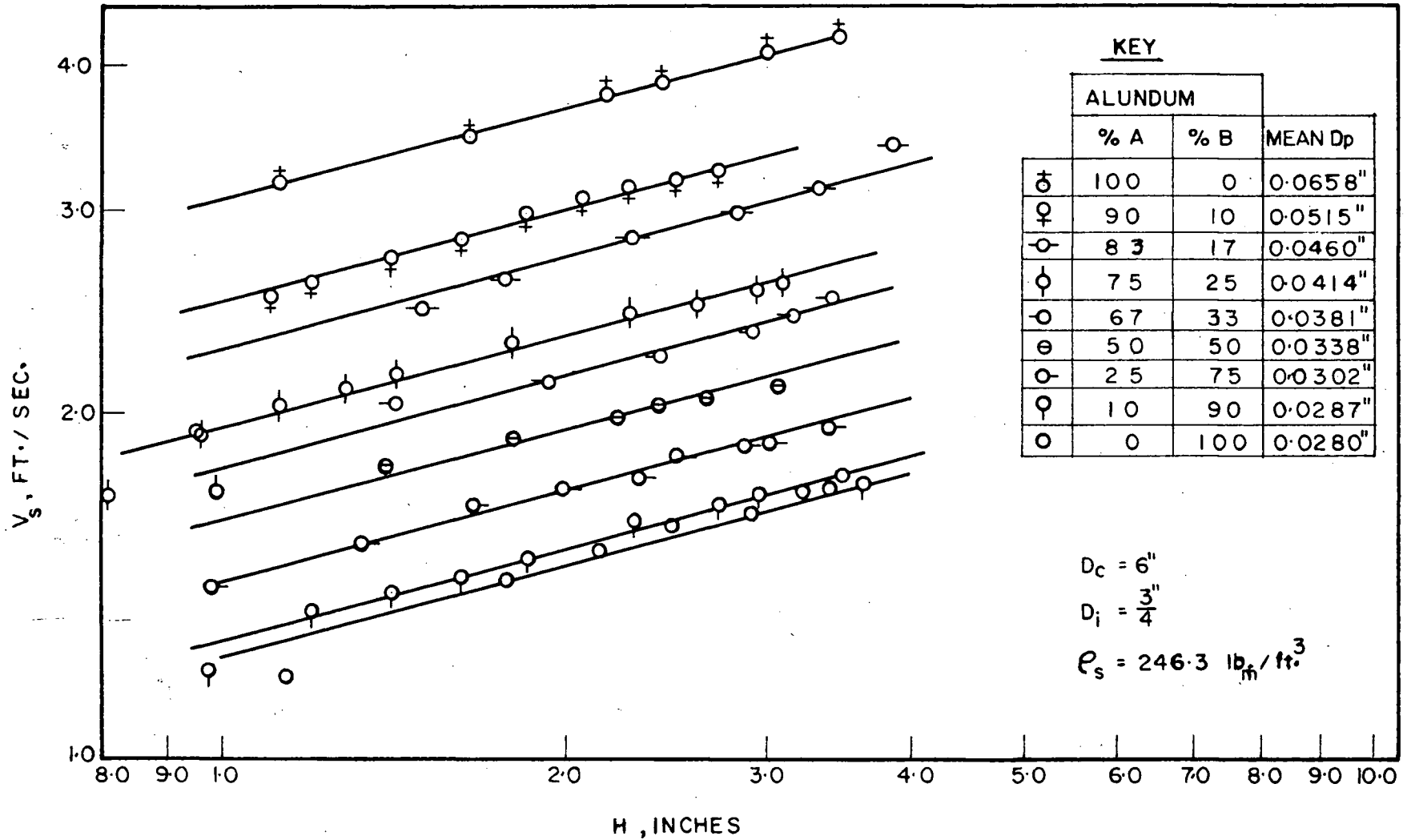


FIGURE VI-1. MINIMUM SPOUTING VELOCITY — BED HEIGHT RELATIONSHIP FOR ALUNDUM MIXTURES

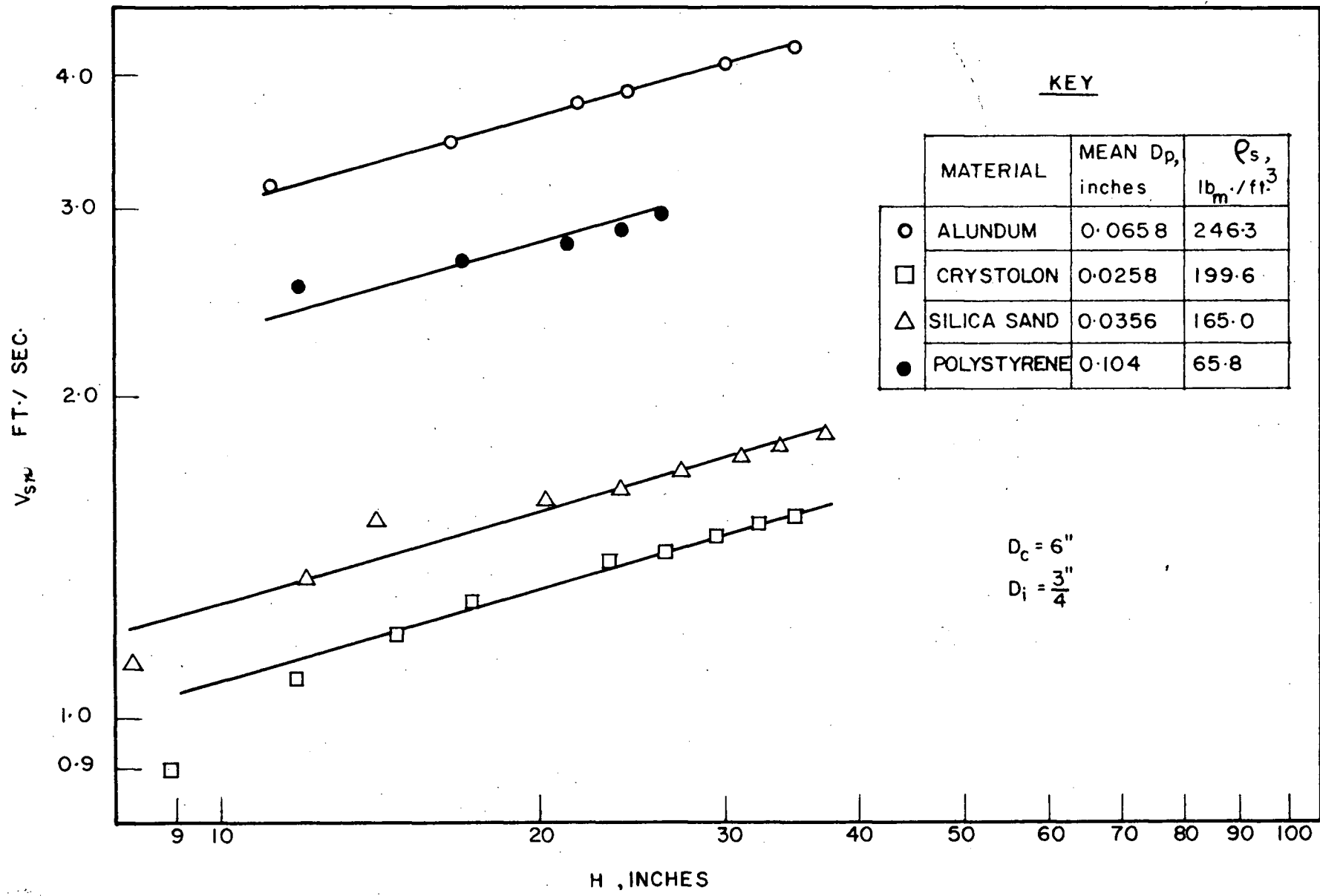


FIGURE VI-2. MINIMUM SPOUTING VELOCITY — BED HEIGHT RELATIONSHIP FOR ALUNDUM B, CRYSTOLON, SILICA SAND AND POLYSTYRENE A

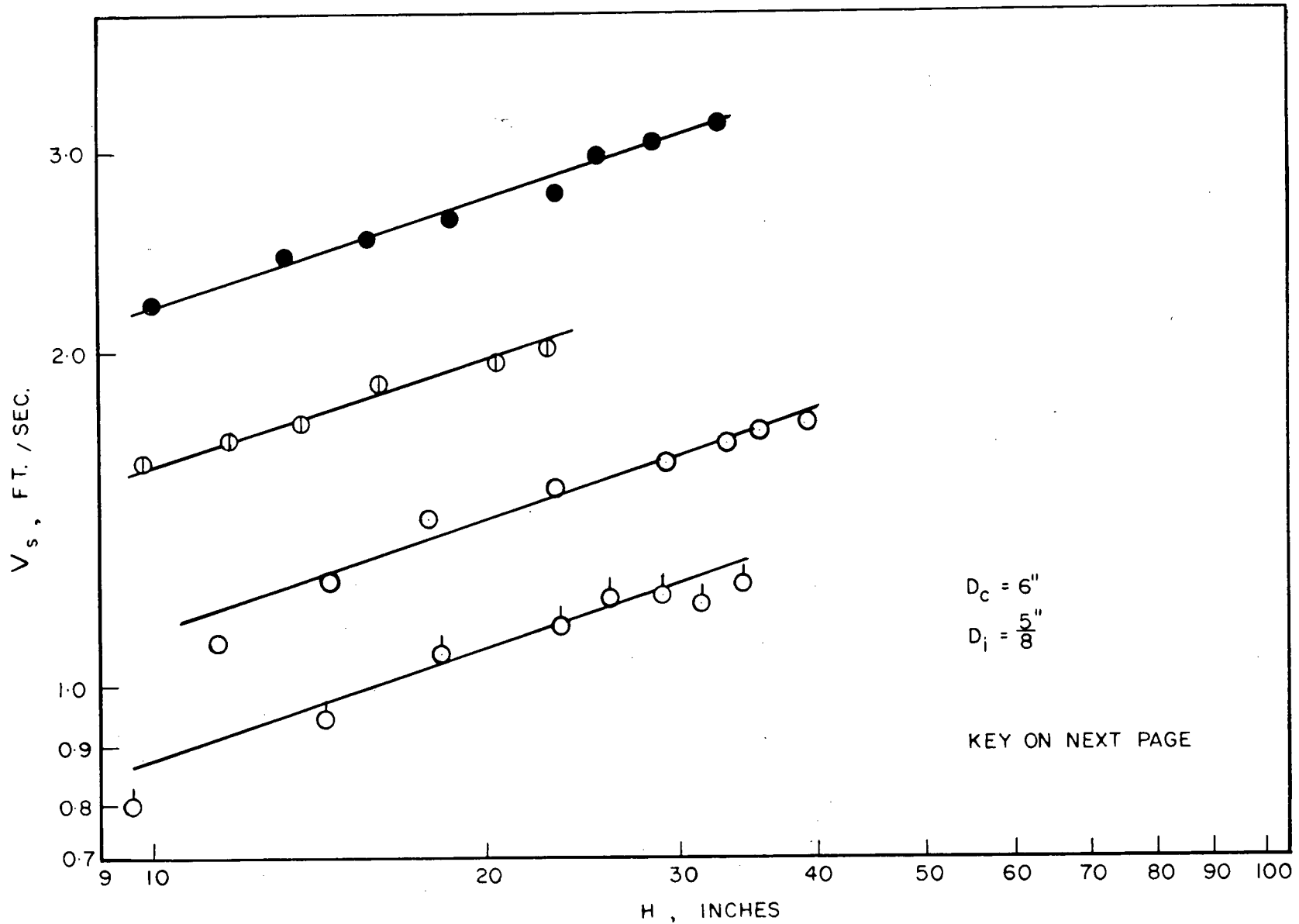


FIGURE VI-3. MINIMUM SPOUTING VELOCITY — BED HEIGHT RELATIONSHIP FOR ALUNDUM MIXTURES OTTAWA SAND AND POLYSTYRENE A

TABLE VI-3

KEY TO FIGURE VI-3

	Material	Mean D_p inches	e_s lb. _m /ft. ³
○	Alundum B	0.028	246.3
⊖	Alundum 90%A+5%B+5%C	0.0348	246.3
○	Ottawa Sand	0.025	166.4
●	Polystyrene A	0.104	65.8

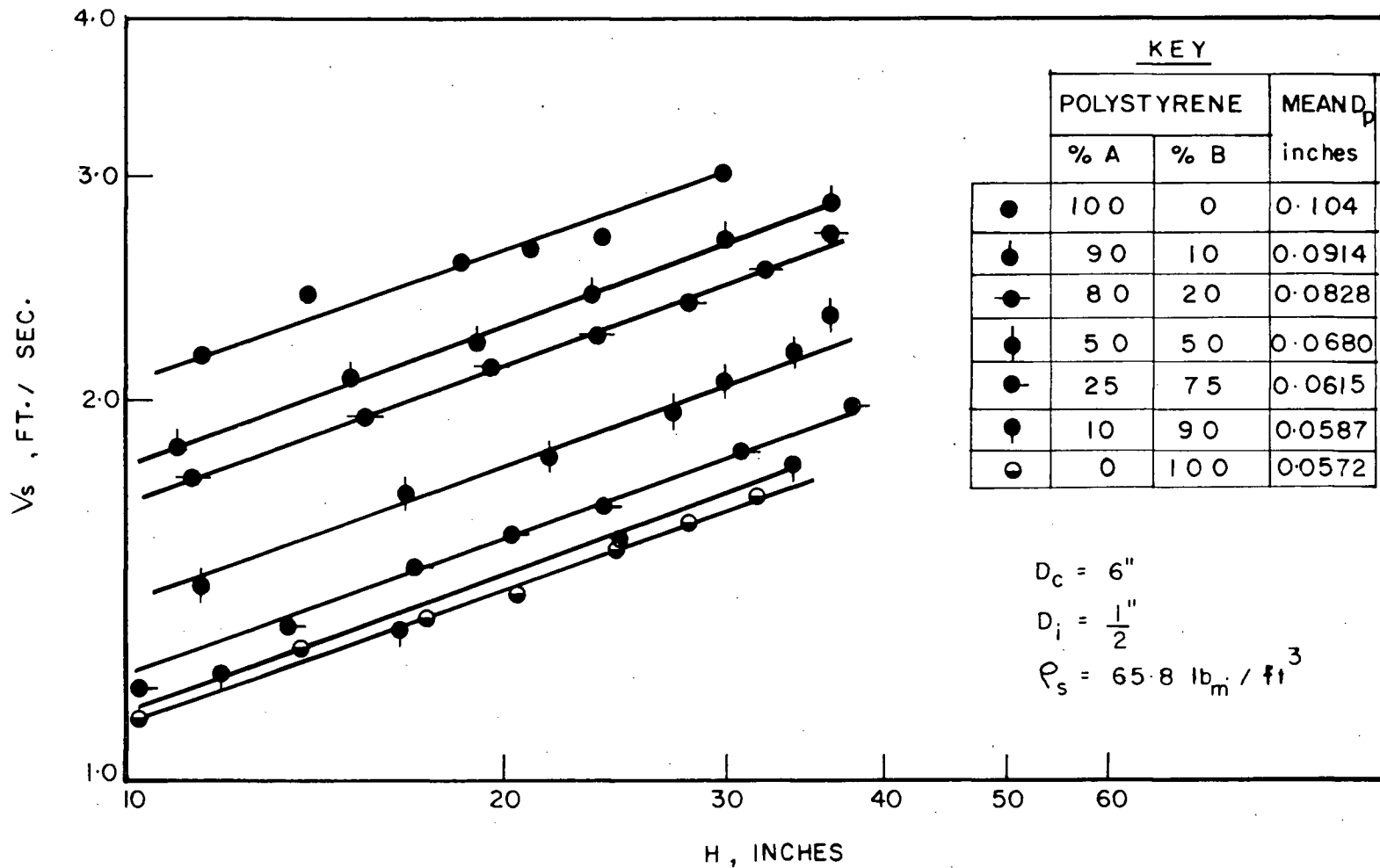


FIGURE VI-4. MINIMUM SPOUTING VELOCITY — BED HEIGHT RELATIONSHIP FOR POLYSTYRENE A, B AND MIXTURES OF POLYSTYRENE A AND B

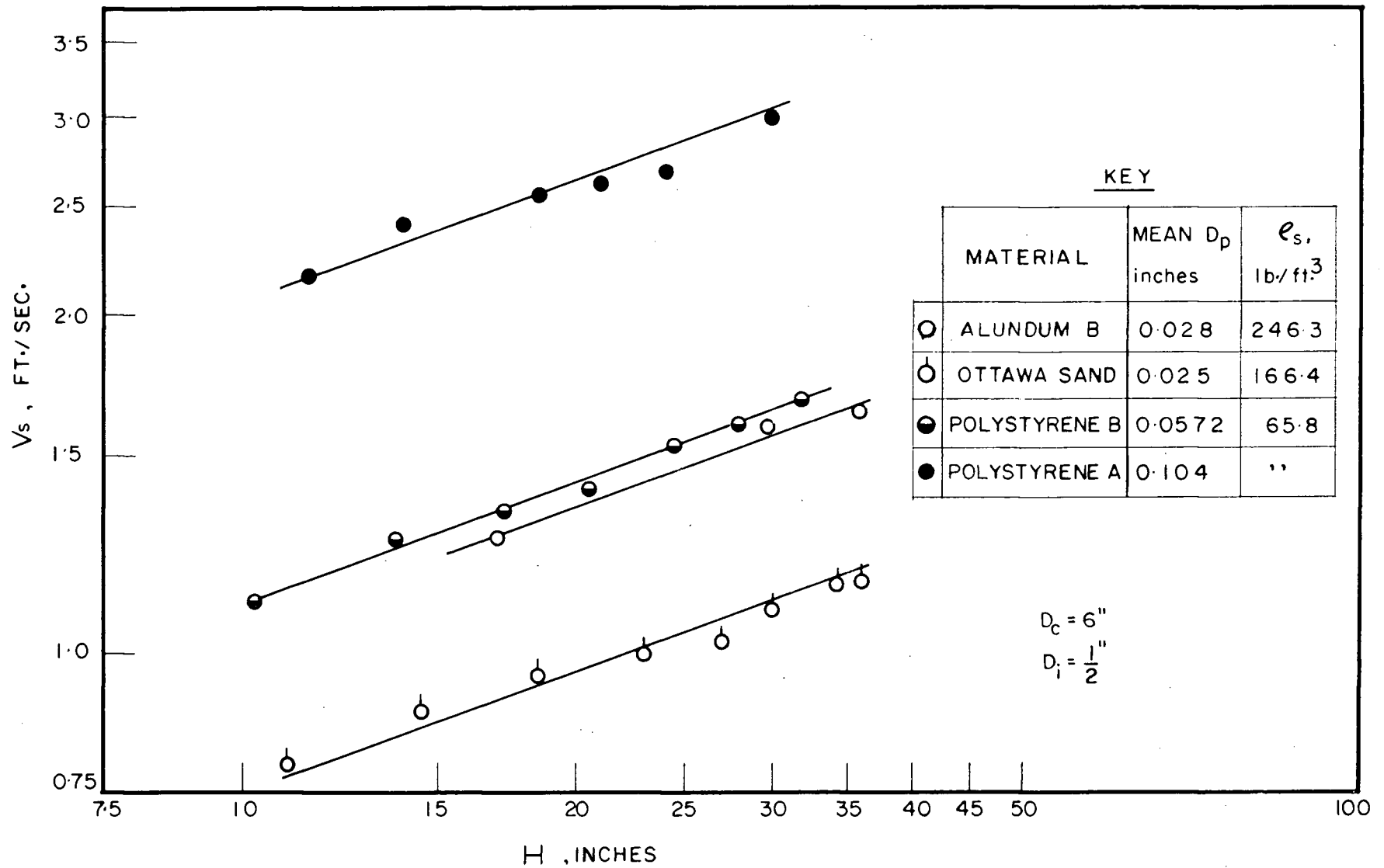


FIGURE VI-5. MINIMUM SPOUTING VELOCITY — BED HEIGHT RELATIONSHIP FOR ALUNDUM B, OTTAWA SAND, POLYSTYRENE A AND B

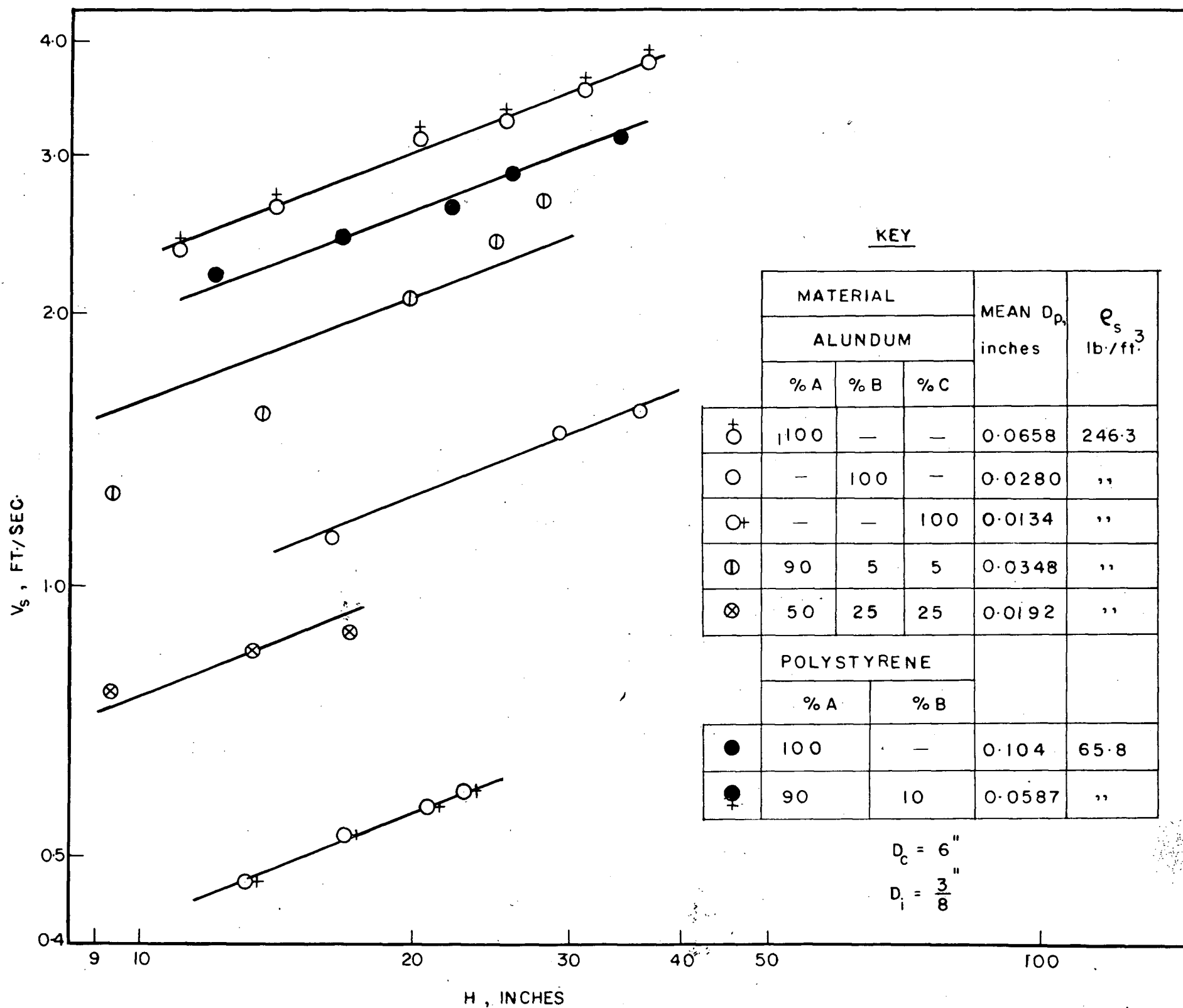


FIGURE VI-6. MINIMUM SPOUTING VELOCITY — BED HEIGHT RELATIONSHIP FOR ALUNDUM MIXTURES AND POLYSTYRENE A

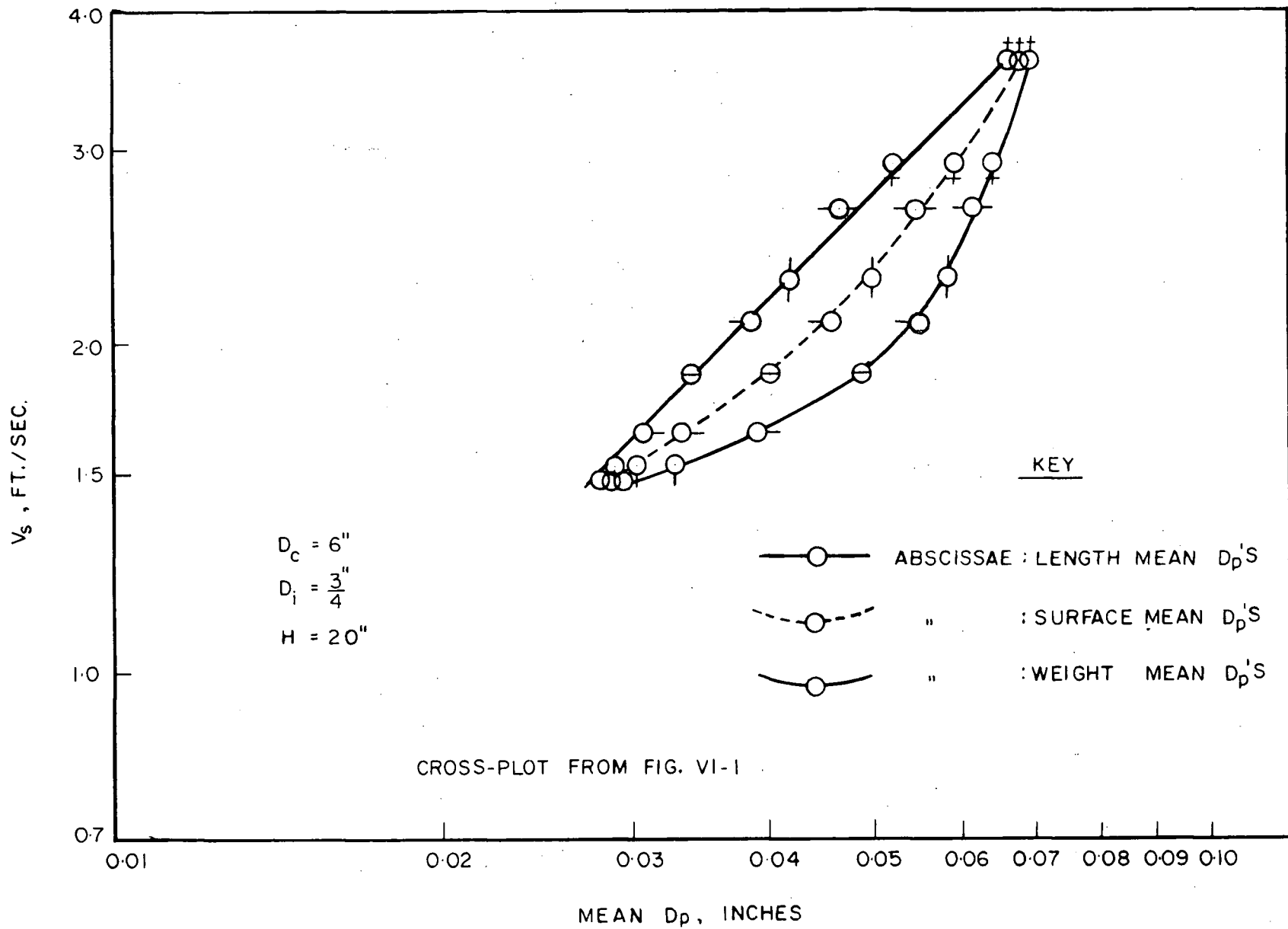


FIGURE VI-7. EFFECT OF MEAN PARTICLE DIAMETER OF ALUNDUM MIXTURES ON MINIMUM SPOUTING VELOCITY

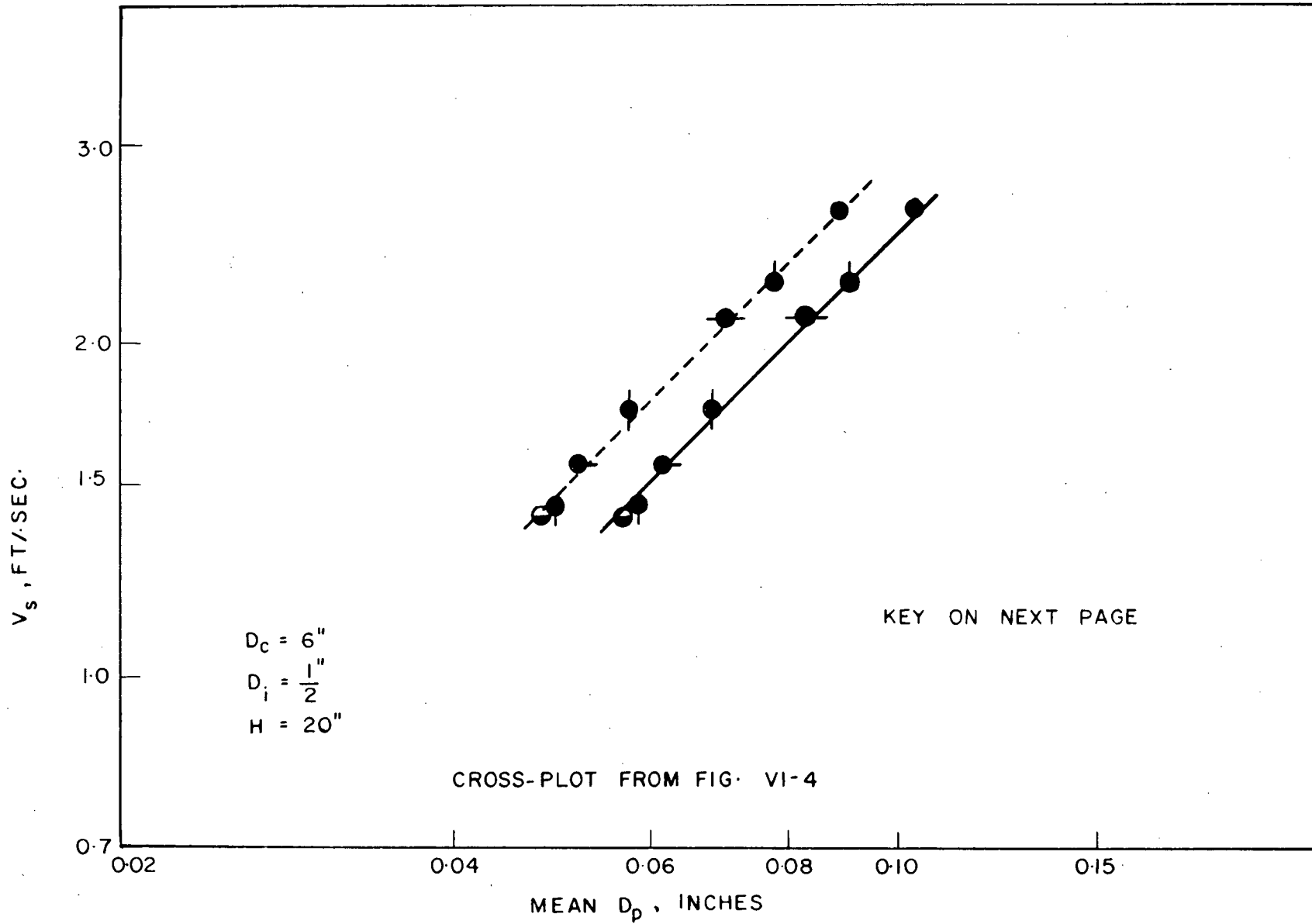


FIGURE VI-8. EFFECT OF MEAN PARTICLE DIAMETER OF POLYSTYRENE ON MINIMUM SPOUTING VELOCITY

TABLE VI-4

KEY TO FIGURE VI-8

<u>Line</u>	<u>Abscissa</u>
	Geometric mean of d_1 , d_2 and d_3 i.e., $\sqrt[3]{d_1 d_2 d_3}$, for polystyrene A and B and the length mean calculated there of, for mixtures of polystyrene A and B.
	Geometric mean of d_1 and d_2 , i.e., $\sqrt{d_1 d_2}$, for Polystyrene A and B and the length mean calculated there of, for mixtures of polystyrene A and B.

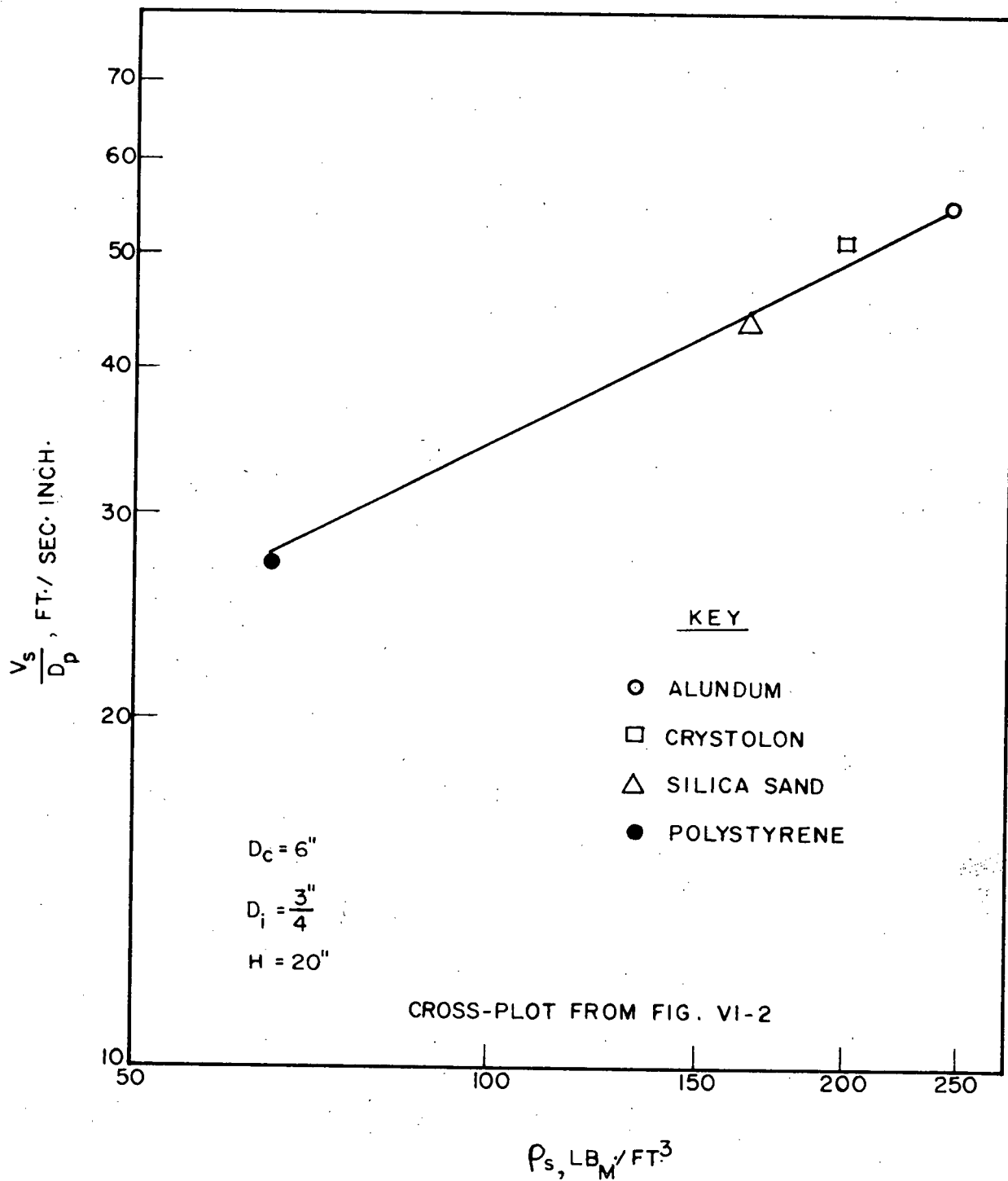


FIGURE VI-9. EFFECT OF SOLID DENSITY ON MINIMUM SPOUTING VELOCITY

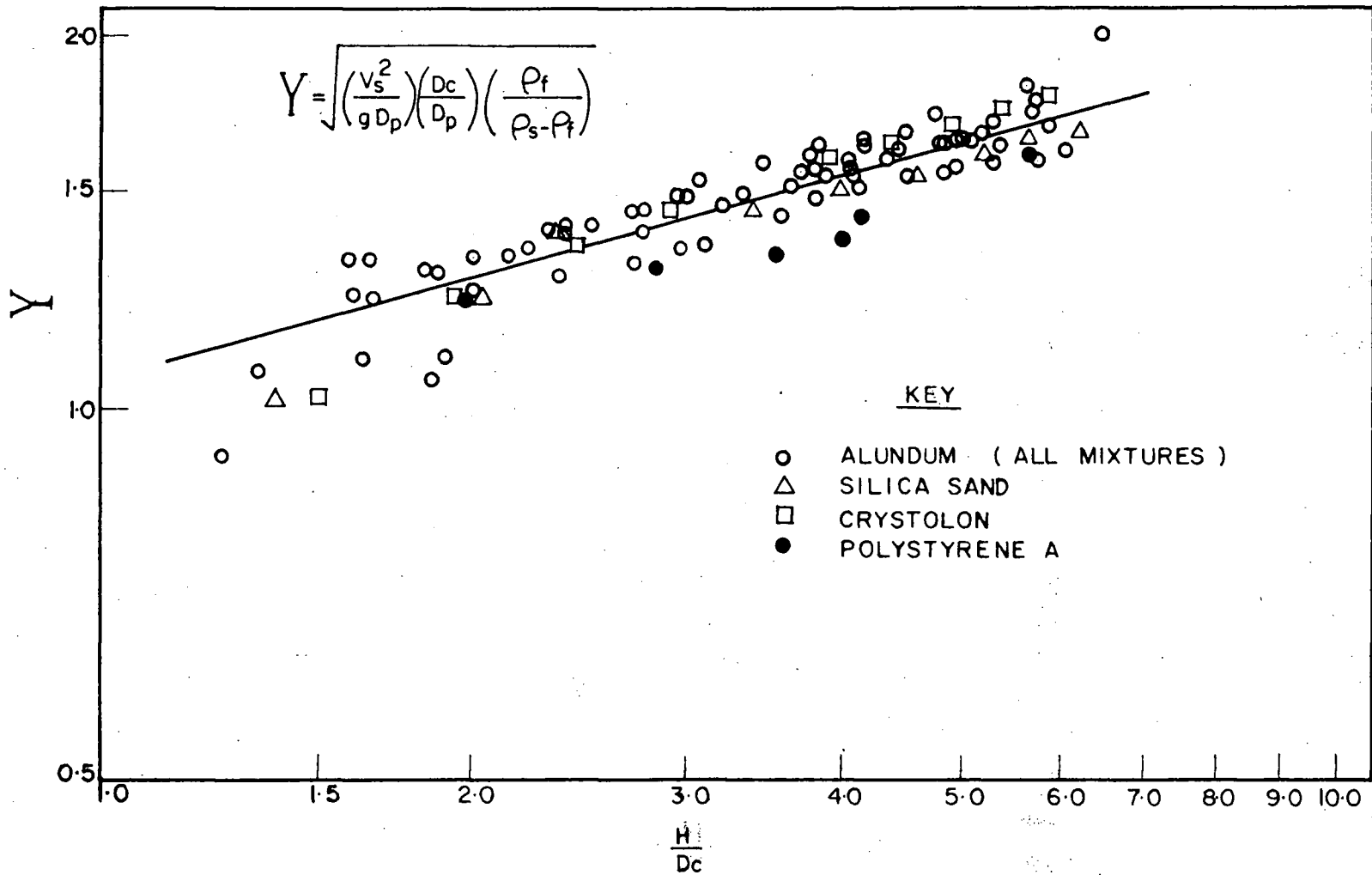


FIGURE VI-10. PLOT OF Y AGAINST $\frac{H}{D_c}$ FOR 3/4-INCH INLET

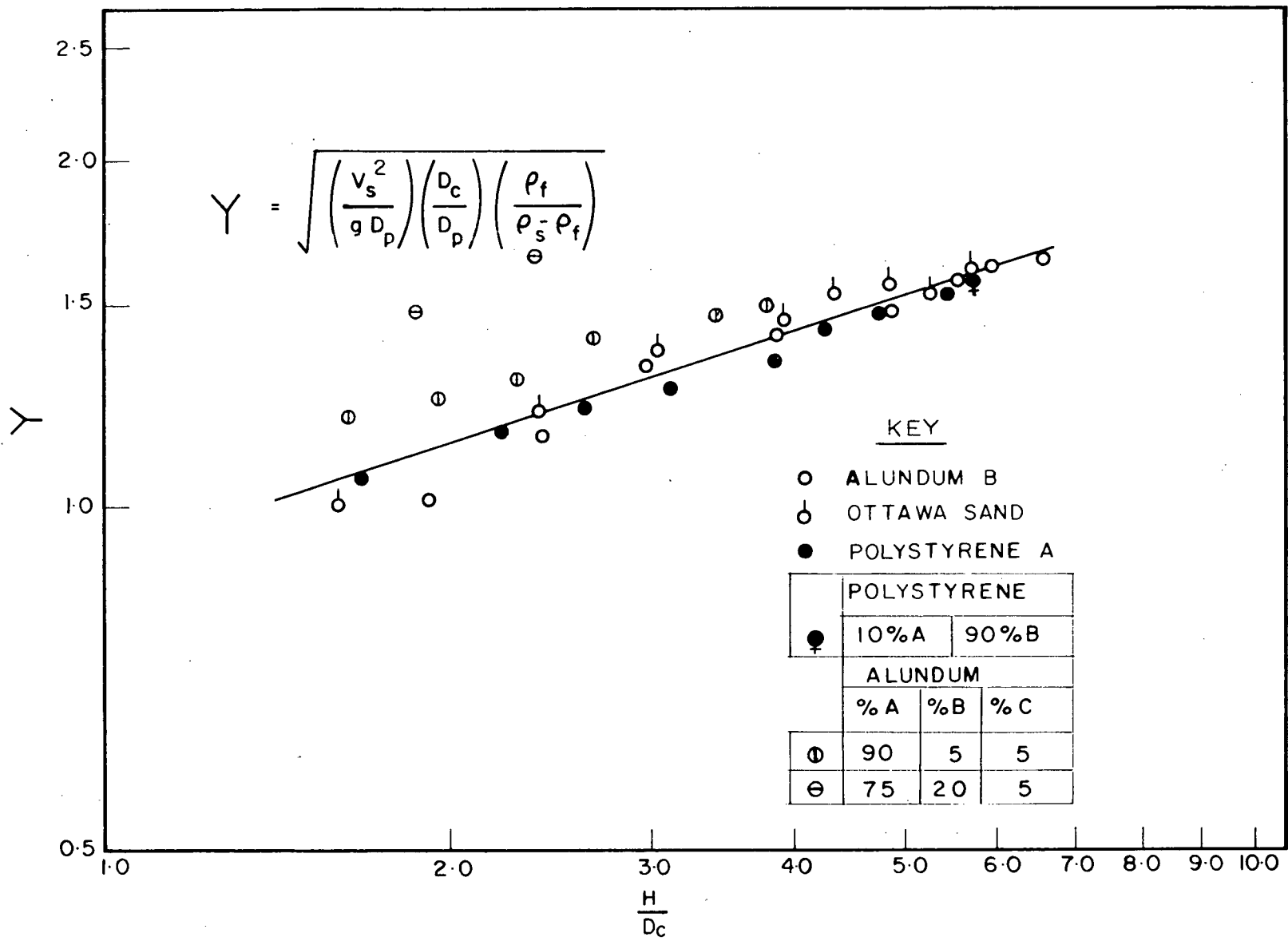


FIGURE VI-11. PLOT OF Y AGAINST $\frac{H}{D_c}$ FOR 5/8-INCH INLET

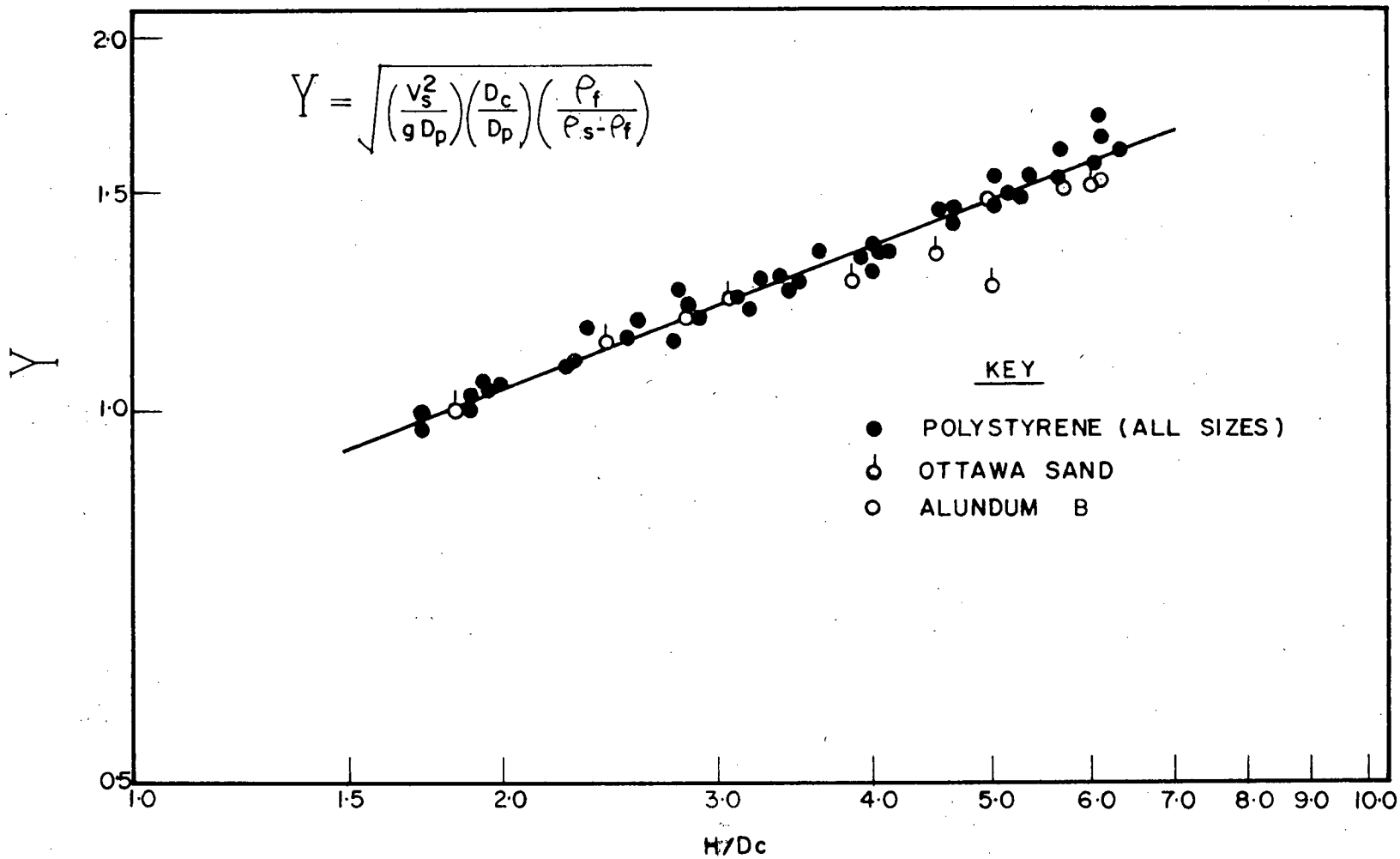


FIGURE VI-12. PLOT OF Y AGAINST $\frac{H}{D_c}$ FOR 1/2-INCH INLET

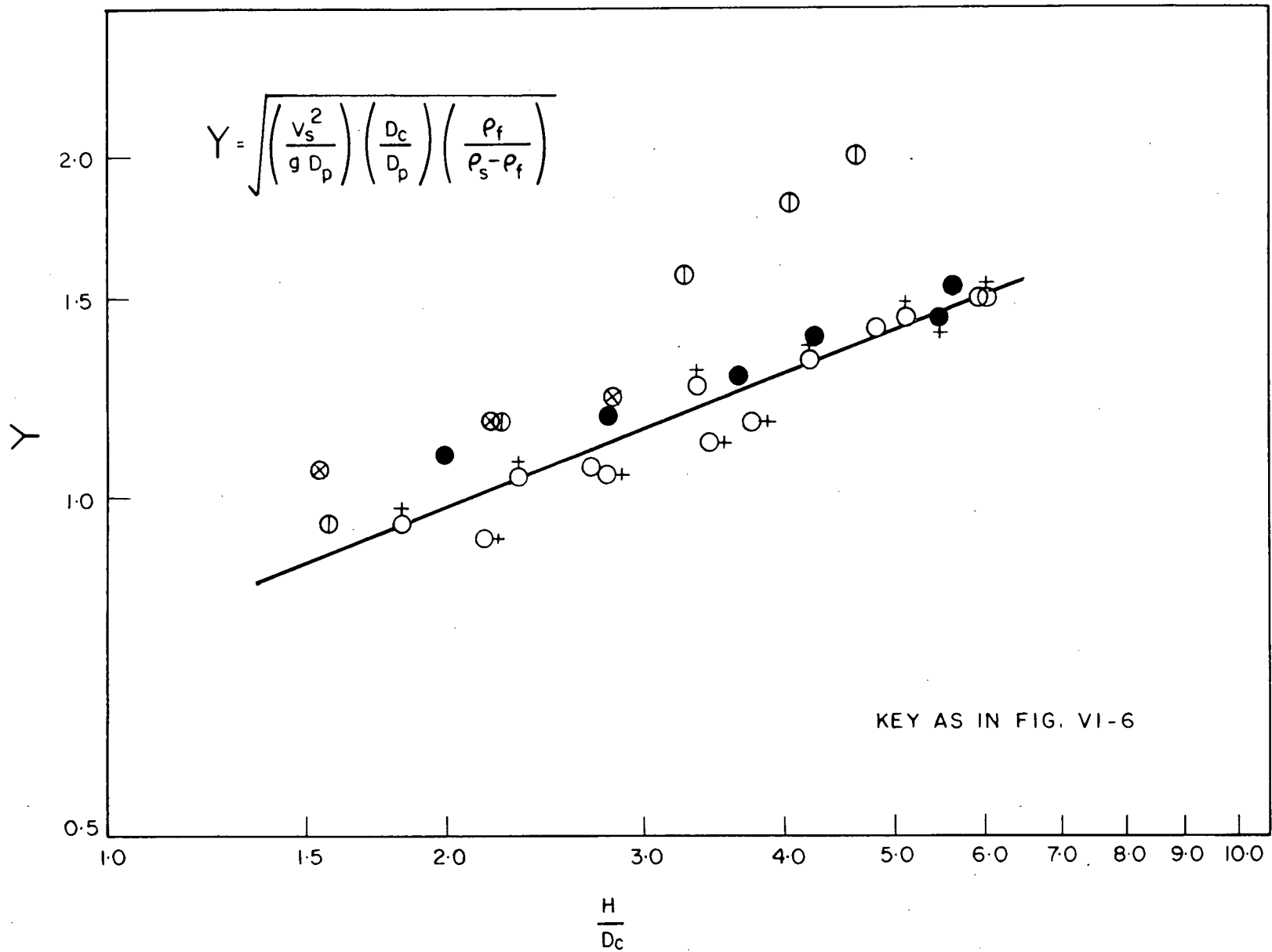


FIGURE VI-13. PLOT OF Y AGAINST $\frac{H}{D_c}$ FOR 3/8-INCH INLET

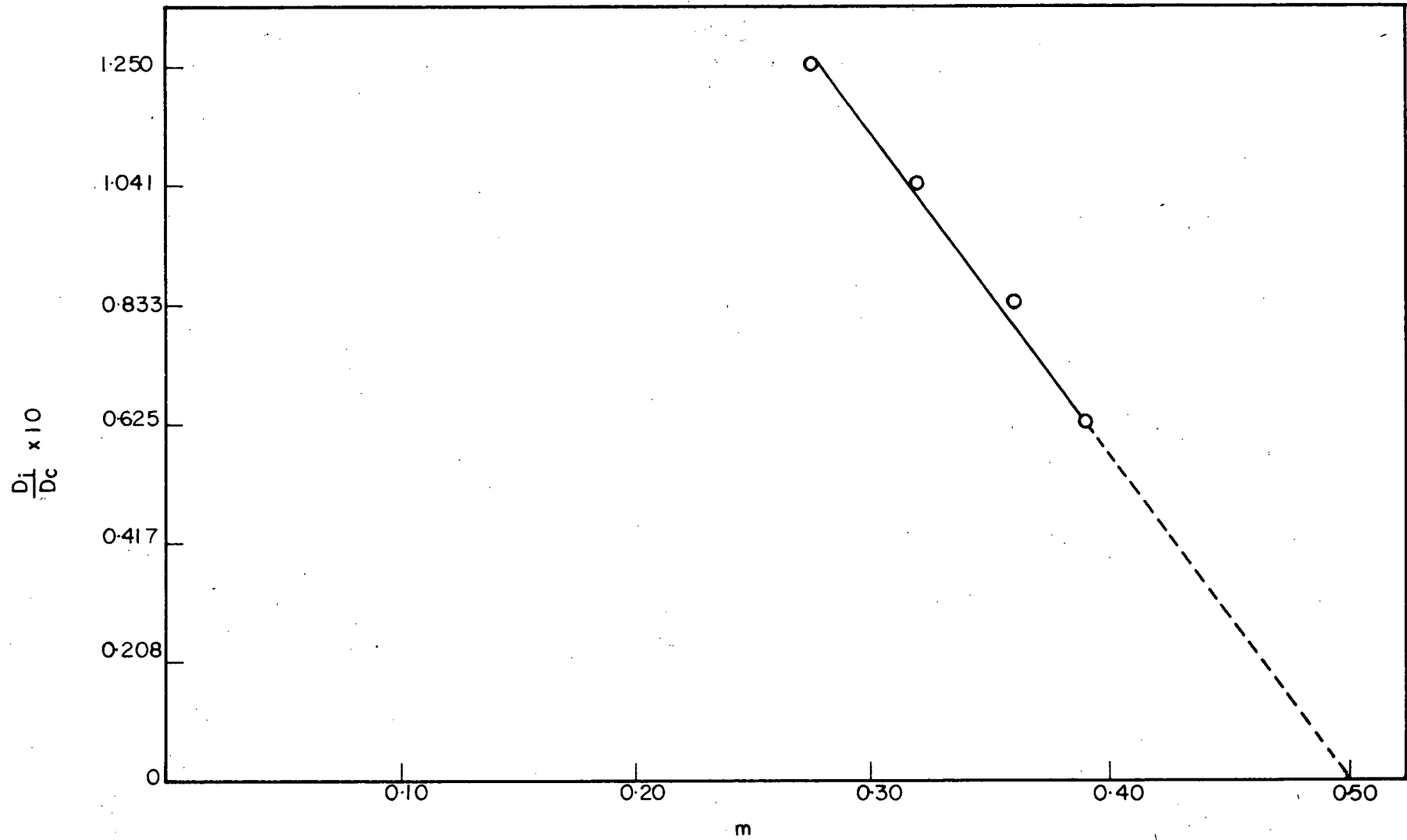


FIGURE VI-14. CORRELATION OF SLOPE m WITH $\frac{D_i}{D_c}$

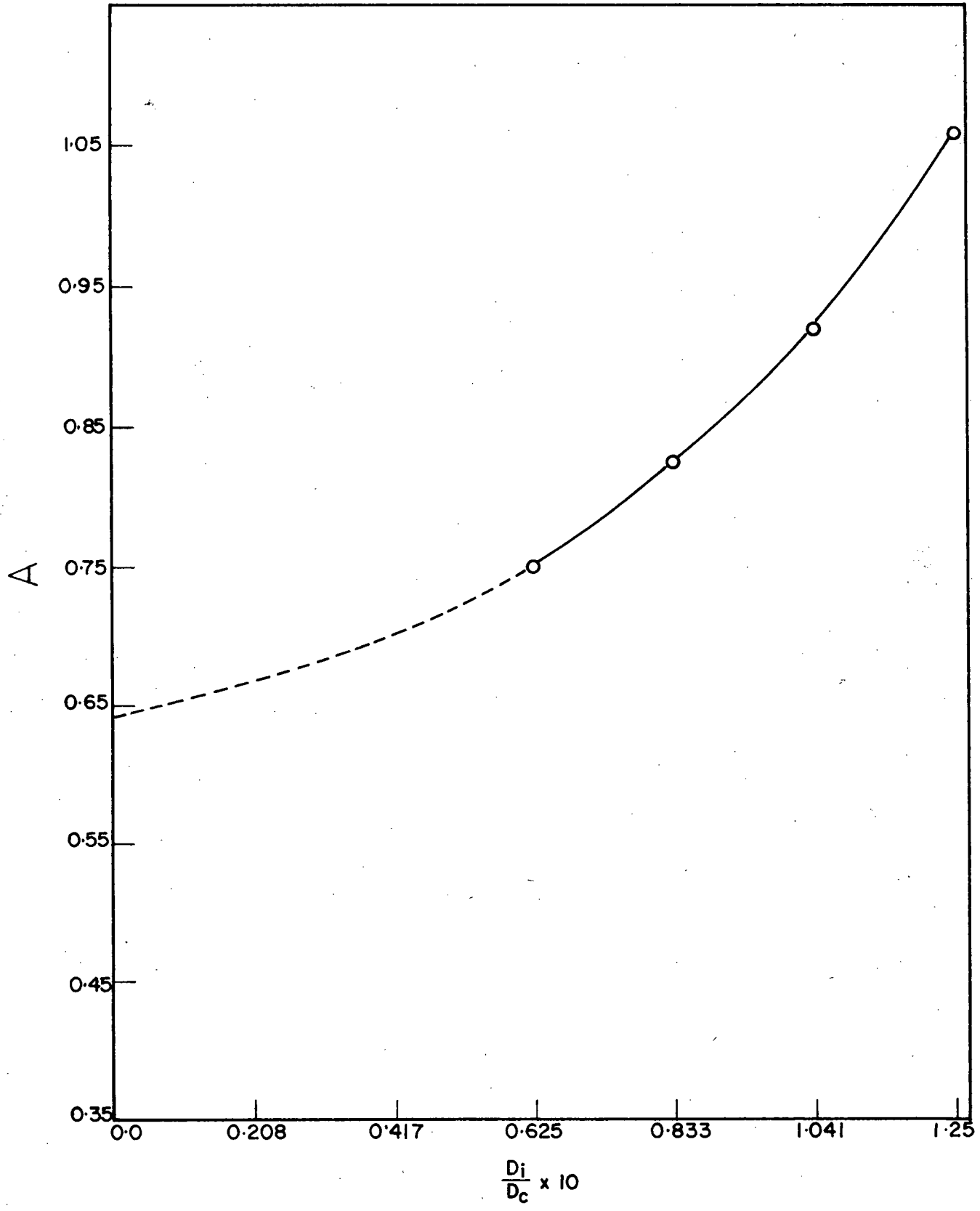


FIGURE VI-15. PLOT OF INTERCEPT A AGAINST $\frac{D_i}{D_c}$

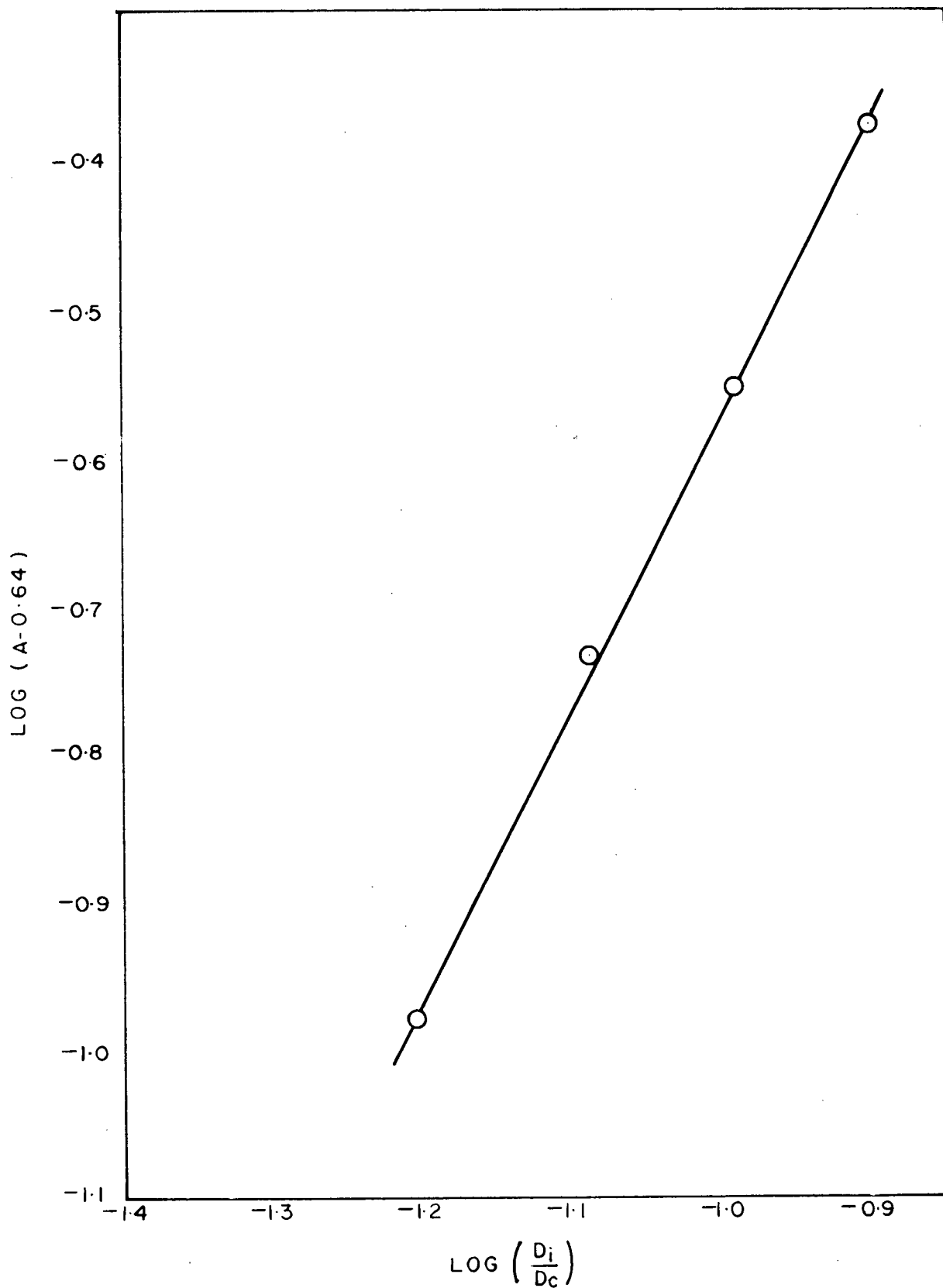


FIGURE VI-16. CORRELATION OF INTERCEPT A WITH $\frac{D_i}{D_c}$

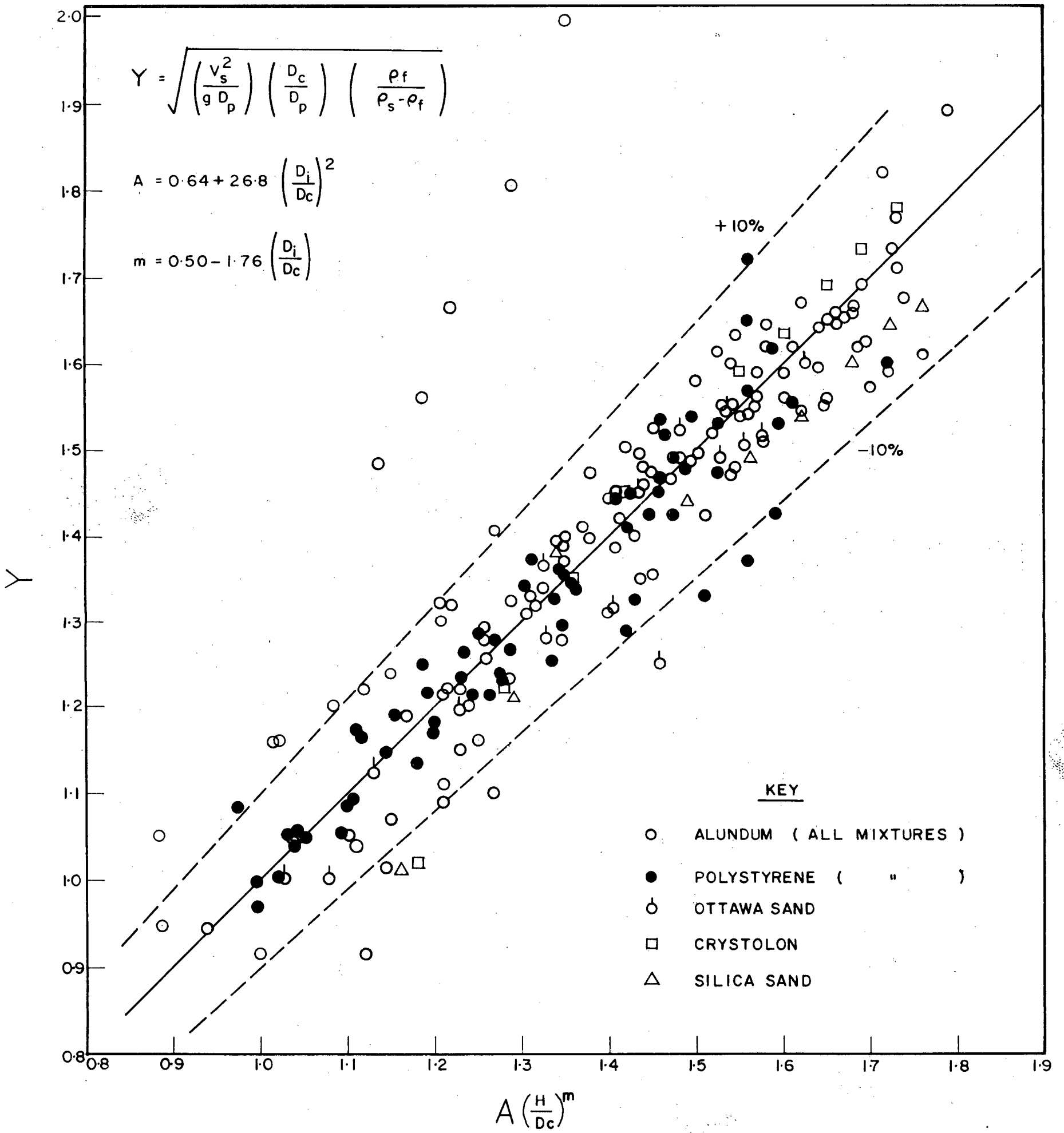


FIGURE VI-17. CORRELATION OF MINIMUM SPOUTING VELOCITY DATA

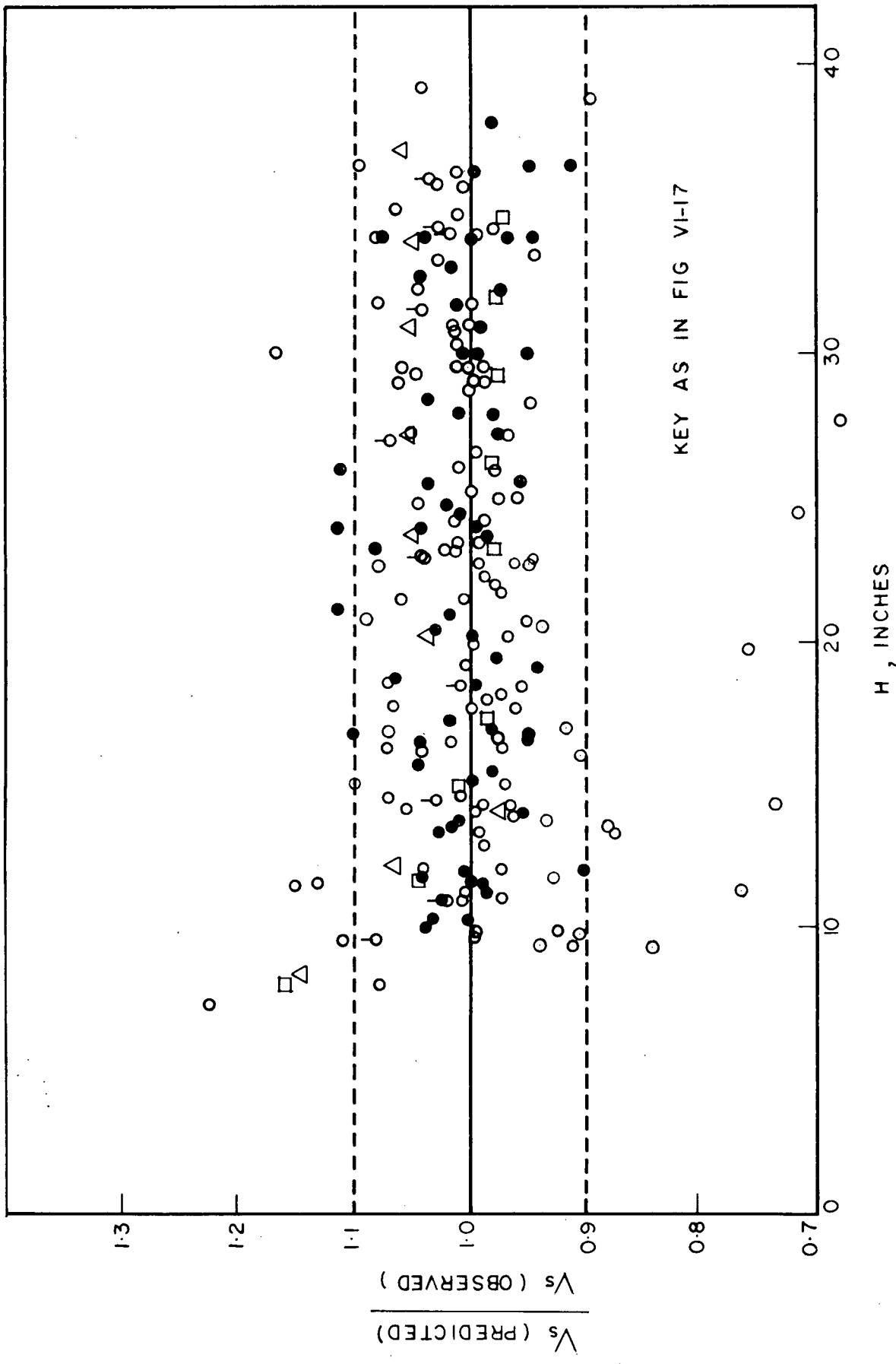


FIGURE VI-18. RATIO OF PREDICTED TO OBSERVED MINIMUM SPOUTING VELOCITY AGAINST BED HEIGHT

CHAPTER VII

DISCUSSION OF RESULTS

VII-1. MINIMUM SPOUTING VELOCITY MEASUREMENTS

Minimum spouting velocity measurements have been made with air as spouting medium in a 6" I.D. column fitted with a 60° conical bottom. Mean particle diameter, solid density, bed height and inlet-orifice diameter were varied.

The results of minimum spouting velocity even for uniform size particles have shown deviations from the values predicted by the Mathur-Gishler correlations, Equations II-8 and II-9. For a typical set of data, the trend and extent of the deviations have been shown in Table V-6. The % difference of the experimental value from the value predicted by the Mathur-Gishler correlations decreases with increase in bed height. Similar deviations, as shown in Figure II-3, have been exhibited by the data of Buchanan and Manurung (14) and Koyanagi (21).

The minimum spouting velocity data for these experiments have been correlated to within + 10% by dimensionless Equation VI-14:

$$\sqrt{\left(\frac{v_s^2}{gD_p}\right)\left(\frac{D_c}{D_p}\right)\left(\frac{\rho_f}{\rho_s - \rho_f}\right)} = \left[0.64 + 26.8 \left(\frac{D_1}{D_c}\right)^2\right] \left(\frac{H}{D_c}\right)^{0.50} - 1.76 \left(\frac{D_1}{D_c}\right)$$

A dimensional correlation, Equation VI-15, which may be used only for 0.50 diameter columns, has also been presented.

The correlation, Equation VI-14, was obtained by using the Tyler screen size as the characteristic diameter for individual fractions of particulate materials and by assuming a geometric mean diameter, i.e., $\sqrt[3]{d_1 d_2 d_3}$, for uniform granular materials and the length mean diameter for mixtures of any material.

For beds containing small proportions of very fine particles in very coarse material Runs A-11(a) to (f), A-14(a) to (e), A-15(a) to (c) , the values predicted by Equation VI-14 or VI-15 are much less than the experimental. This is so, because the length mean diameters for mixtures containing a small percentage of fines is very much less than that of the coarse material. For instance, the length mean diameter for a mixture containing 90% alundum A, 5% alundum B and 5% alundum C is 0.0348" whereas the length mean diameter of alundum A is 0.0658" (see Table IV-2).

For all mixtures of alundum A and B in which the coarsest fraction is about 3 1/2 times larger in diameter than the finest fraction the correlation fits the experimental data very well. But, in mixtures containing alundum A, B and C, the size of the coarser fraction is about 6 times that of the finest. It is reasonable, therefore, to conclude that the correlation is applicable to all beds of mixed particle sizes in which the size range is less than five-fold.

VII-2. COMPARISON OF EQUATION VI-14 WITH THE MATHUR-GISHLER CORRELATION, EQUATION II-8.

The Mathur-Gishler correlation, Equation II-8, is given below:

$$V_s = \left(\frac{D_p}{D_c} \right) \left(\frac{D_i}{D_{cd}} \right)^{1/3} \sqrt{\frac{2gH(\rho_s - \rho_f)}{\rho_f}} \quad (\text{II-8})$$

The simplest way to compare the two correlations (Equation VI-14 and Equation II-8) is by finding the deviations of V_s predicted by either equations from the observed values for typical sets of runs. Such a comparison is made in Table VII-1 below, for Runs A-10(a) to A-10(i) and P-13(a) to P-13(g).

TABLE VII-1

DEVIATIONS OF V_s , PREDICTED BY EQUATIONS II-8 AND VI-14, FROM THE EXPERIMENTAL:

RUNS A-10(a) to A-10(i) AND RUNS P-13(a) to P-13(g)

Run No.	Bed Height H, in.	V_s (Observed) ft./sec.	Equation II-8		Equation VI-14 or 15	
			V_s (Predicted) ft./sec.	% Deviation from Exptl. Value	V_s (Predicted) ft./sec.	% Deviation from Exptl. Value
A-10(a)	9.8	1.413	1.32	- 6.5	1.405	- 0.5
A-10(b)	13.3	1.542	1.56	+ 1.0	1.527	- 1.0
A-10(c)	16.6	1.662	1.73	+ 4.0	2.094	+ 2.6
A-10(d)	19.9	1.703	1.91	+12.0	1.713	+ 0.6
A-10(e)	23.3	1.75	2.065	+18.0	1.747	- 0.8
A-10(f)	25.0	1.844	2.14	+16.0	1.891	+ 2.6
A-10(g)	28.75	1.858	2.27	+22.0	1.858	0.0
A-10(h)	30.3	1.867	2.35	+26.0	1.886	+ 1.0
A-10(i)	34.0	1.949	2.48	+27.0	1.937	- 0.6
P-13(a)	10.25	1.114	0.758	-32.0	1.118	+ 0.4
P-13(b)	13.75	1.269	0.888	-30.0	1.28	+ 0.9
P-13(c)	17.25	1.339	0.991	-26.0	1.36	+ 1.7
P-13(d)	20.5	1.404	1.095	-22.0	1.440	+ 2.8
P-13(e)	24.5	1.528	1.192	-22.0	1.540	+ 0.8
P-13(f)	28.0	1.598	1.27	-20.5	1.610	+ 0.9
P-13(g)	31.75	1.671	1.345	-19.5	1.690	+ 0.9

The Mathur-Gishler correlation, Equation II-8, makes use of the weight mean diameter as particle size for particulate materials. The weight mean diameter is higher than any other mean for a given particle size distribution. So, the values predicted by the Mathur-Gishler correlation are higher than the experimental, as shown in Table VII-1 for runs from A-10(a) to A-10(i).

On the other hand, the smaller dimension has been suggested by Mathur-Gishler (1) as the characteristic diameter for granular material. So, the values predicted by the Mathur-Gishler correlation, as shown in Table VII-1, are always less than the observed.

Further, the deviation of values predicted by Equation II-8 from the experimental increases with increase in bed height. This is true, as shown in Table VII-1, for both types of materials and both inlets. But, the rate of deviation is higher for 3/4" diameter inlet (Runs A-10(a) to A-10(i), Table VII-1) than for 1/2" diameter inlet (Runs P-13(a) to P-13(g), Table VII-1).

The values predicted by Equation VI-14 or VI-15, i.e., the present proposed correlation, do not show any such trend or deviation from the experimental.

The difference between the present correlation, Equation VI-14 and the Mathur-Gishler correlation, Equation II-8, is clearly a function of

$\frac{H}{D_c}$, $\frac{D_i}{D_c}$, and the ratio of length mean diameter to the weight mean diameter

in the case of mixed particle-size materials; the ratio of geometric mean diameter to the smaller dimension in the case of uniform granular materials.

The present correlation, Equation VII-14, predicts reasonably well data of Buchanan and Manurung (14) and Mathur and Gishler (1) .

VII-3. COMPARISON OF V_s PREDICTED BY EQUATION VI-14 WITH PREVIOUS DATA

(a) DATA OF BUCHANAN AND MANURUNG (14)

Measurements of minimum spouting velocity of Buchanan and Manurung in a 5.75" I.D. column fitted with a 45° cone and 1/2" I.D. inlet have shown good agreement with the values predicted by Equation VI-14 (see Appendix 4). The results of Buchanan and Manurung have been discussed in detail in Chapter II-6.

Deviations were observed, as shown in Appendix 4, for runs 45, 46, 47, 48, 49, 51 and 53 of Buchanan and Manurung. These runs were with beds containing wide size fractions of coal (93.4% of -6 +28 mesh, 6.8% of -28 mesh size coal, Ref. 14). As explained already in Chapter VII-1, these deviations are due to the lower values of length mean diameter for wide size fractions. (Length mean diameter being equal to $\frac{\sum x_1/d_1}{\sum x_1/d_1^2}$, with decreasing d , the denominator increases more rapidly than numerator and consequently very low values of mean diameters are obtained).

(b) DATA OF MATHUR AND GISHLER (1)

The correlation, Equation VI-14, cannot be checked against most of the data of Mathur and Gishler (1) since neither the size distribution of particulate materials nor all the three dimensions of the granular materials were reported.

However, some of the experimental V_s values of Mathur and Gishler are compared in Appendix 4(b) with the values predicted by Equation VI-14.

In calculating V_s by Equation VI-14, the values of D_p reported by Mathur and Gishler (1) were used. The standard deviation of the predicted V_s from the experimental is 20.7%. It is to be noted that V_s predicted by Equation VI-14 is always higher than the experimental. (Appendix 4b). It is assumed that this is due to the higher values of D_p . On the other hand, for the same experimental values (Appendix 4b), the deviation of the values predicted by Equation II-8 was found to be 11.87%.

Thus, given the accurate values of the particle diameter, V_s predicted by Equation VI-14 would be much closer to the experimental values of Mathur and Gishler.

It is, therefore, concluded that the correlation, Equation VI-14, is valid for 6" diameter columns irrespective of the inlet configuration. (The inlet set-up used by Mathur-Gishler (1) was different from the one used in the present investigation. See chapter III-6c).

VII-4. CRITICAL RATIO OF $\frac{D_i}{D_c}$

The Equation VI-14, shows that $V_s \propto H^m$, (all other variables being held constant) where m is a function of $\frac{D_i}{D_c}$, viz.,

$$m = 0.50 - 1.76 \left(\frac{D_i}{D_c} \right) \quad (\text{II-12})$$

Only at very low values of D_i or $\frac{D_i}{D_c}$, m approaches 0.50.

On the other hand, m becomes zero at a value of $\frac{D_i}{D_c} = 0.284$. This means that V_s becomes independent of bed height at $\frac{D_i}{D_c} = 0.284$. Probably

at this high value of $\frac{D_1}{D_c}$, the gas distribution through the column becomes more or less uniform and so the bed is likely to fluidize or slug directly, with no spouting.

The ratio, $\frac{D_1}{D_c} = 0.284$, therefore, is probably a critical one beyond which no spouting can be achieved. This is further supported, as shown in Table VII-2 below, by comparing the calculated minimum spouting velocities of typical bed materials at $\frac{D_1}{D_c} = 0.284$ with the minimum fluidization velocities predicted by Leva's generalized correlation (16).

TABLE VII-2

COMPARISON OF VALUES OF V_s AT $\frac{D_1}{D_c} = 0.284$ WITH V_{mf}

Material	V_s , ft./sec. Predicted by Eq. VI-14, for $\frac{D_1}{D_c} = 0.284$.	V_{mf} ft./sec. Calculated by Leva's generalized correlation
Alundum A	6.9	9.3
Alundum B	2.96	1.98
Alundum C	1.45	0.50
Polystyrene A	5.86	4.55
Polystyrene B	3.17	1.5

As can be seen from Table VII-2, V_{mf} is always less than V_s at

$\frac{D_1}{D_c} = 0.284$, except for alundum A. This indicates that fluidization will probably

take place before the minimum spouting velocity is reached.

Leva's generalized correlation (16) for minimum fluidization velocity

is not applicable for gas-fluidized systems in which the surface mean diameter of the particulate materials is more than about 0.50". This fact may explain why the V_{mf} for Alundum A (Surface mean $D_p = 0.0665"$) is far higher than V_s as shown in Table VII-2. Even though V_s at $\frac{D_i}{D_c} = 0.284$ for alundum A is apparently lower than V_{mf} (Table VII-2), it may be assumed that alundum A will not spout, because at these high gas flow rates (i.e., $V_s \approx 7$ ft./sec.), the bed is more likely to slug than spout.

Hence, it can, reasonably, be assumed that no spouting takes place if $\frac{D_i}{D_c} \approx 0.28$, even in beds composed of very large (i.e., coarse) particles.

VII-5. EFFECT OF COLUMN DIAMETER ON MINIMUM SPOUTING VELOCITY

The present correlation, Equation VI-14, was derived from data obtained in a 6" diameter column. An examination of Equation VI-14 indicates that V_s is proportional to $D_c^{-0.5}$ for a given bed of material at constant

$\frac{D_i}{D_c}$ and $\frac{H}{D_c}$. The Mathur-Gishler correlation, Equation II-8, also indicates

the same relationship between V_s and D_c .

The possibility of applying Equation VI-14 to columns of diameter other than 6" has been checked by comparing the values of minimum spouting velocity predicted by Equation VI-14 with the experimental values of Koyanagi (21) in Table VII-3 below. Koyanagi (21), as mentioned in Chapter II-7, obtained data in a 4" diameter column fitted with a 60° cone and a 0.364" I.D. inlet. The inlet set-up used by Koyanagi (21) was similar to the one used by Mathur-Gishler (1).

TABLE VII-3

COMPARISON OF V_s PREDICTED BY EQUATION VII-14, WITH KOYANAGI'S (21) DATA

$$D_c = 4''$$

$$D_i = 0.364''$$

$$\text{Cone Angle} = 60^\circ$$

Bed Height in.	V_s , ft./sec. Predicted by Eq. VI-14.	V_s , ft./sec. Experimental	% Deviation of Predicted Value from Experimental
4.8	0.89	0.766	+16
6.0	0.96	0.826	+17
8.8	1.11	0.948	+16
10.8	1.19	0.994	+20
12.8	1.26	1.06	+19
16.8	1.39	1.16	+20
20.8	1.49	1.24	+20
24.3	1.58	1.31	+20

The values predicted by present correlation, Equation VI-14, as shown in Table III-3, are constantly higher by about 18% than the experimental values of minimum spouting velocity of Koyanagi. The difference between the predicted value from the experimental, as is evident from Table VII-3, is not dependent on bed height (i.e., $\frac{H}{D_c}$) and consequently the data of Koyanagi can be represented by an equation of the form

$$V_s \propto H^m$$

where m is correlated by Equation II-12.

Rewriting the present correlation, Equation II-14, one gets

$$V_s = D_p \times \sqrt{\frac{g(\rho_s - \rho_f)}{\rho_f}} \times H^m \left[\left| \frac{1}{D_c^{0.50+m}} \right| \left\{ 0.64 + 26.8 \left| \frac{D_i}{D_c} \right|^2 \right\} \right] \quad (\text{VII-1})$$

Since the effects of the variables D_p , e_s and H on V_s were independently studied in the present investigation, the deviation of values predicted by Equation VI-14 from the experimental values of Koyanagi can only be accounted for by a change in the term within the square brackets of Equation VII-1 above.

Reliable experimental data with D_c as variable are not available to determine the exact form of the term within the square brackets of Equation VII-1.

VII-6. EFFECT OF INLET DESIGN

The spoutability of any bed is dependent on the physical properties of the material and the column geometry, i.e., $\frac{D_i}{D_c}$.

As explained in Chapter III-6(c), the design of inlet also has an important effect on the spoutability.

The results of the present investigation with the beds of Ottawa Sand ($D_p = 0.025"$, $D_i = 0.625"$, $D_c = 6"$ and $H = 35"$) as detailed in Chapter V-2 (a), clearly indicated the increased spoutability of this material compared to the observations of Mathur and Gishler (1).

Beds of Alundum C of mean particle diameter equal to $0.0134"$ were spouted well up to a height of 23 inches (see Chapter V-1). This is the finest material ever spouted in any system.

These observations indicate that the design of the inlet adopted in the present investigation is a better one compared to the set-up used by Mathur and Gishler (1) and Thorley, Mathur, Klassen et al (15).

VII-7. SOME CHARACTERISTICS OF THE SPOUTED BEDS OF MIXED-SIZE PARTICLES

Alundum A and B (see Table IV-1 for physical properties) are in the spoutable size range. The experimental runs with the mixtures of alundum A and B (Runs A-6 to Runs A-12) indicated that the spoutability of the mixtures was not affected. The size range in any mixture of alundum A and B is 3 1/2-fold.

Alundum C was spoutable only with inlets up to 3/8" diameter. For inlets larger than 3/8" diameter, alundum C can be considered as fine non-spoutable material.

It was observed that the spoutability of the mixtures of alundum A, B and C decreased with increasing proportions of alundum C and any mixture containing more than about 25% alundum C cannot be spouted even with 3/8" diameter inlet. Since each one of these materials, i.e., alundum A, B or C is in spoutable size range for 3/8" inlet, the decrease in the spoutability of the mixtures of these materials indicated that a wide variation in the size range of the bed material may make a mixture unspoutable. Thus, a mixture of alundum A, B and C, in which there is about 6-fold difference in the size range will not spout well.

It is reasonable, therefore, to conclude that mixtures in which there is about 5-fold difference in size range (each individual fraction being spoutable) will spout well.

An interesting observation made was that the presence of even a small proportion (about 10%) of alundum A, which is coarse, in alundum C (fine) completely destroyed the spoutability of alundum C.

Furthermore, in systems which alundum C could not be spouted (for instance, 5/8" diameter inlet), any mixture containing 10% or more of alundum C, the balance being alundum A and B could not be spouted.

The observed segregation of fines in mixtures of alundum A and B and silica sand, previously mentioned in Chapter V-4(a), (b) and (c), which occurred initially in the beds as the air flow was increased was apparently almost completely destroyed during spouting. This resulted in near uniformity of the beds in the axial direction. But, in beds composed of wide size fractions (mixtures of alundum A, B and C), the proportion of the fines at the top of the bed even during spouting was observed to be higher than the average. Thus, mixing in axial direction is not very effective in beds of widely different sized particles.

On the other hand, it was observed that there was a regular radial size classification during spouting. Finer particles drift more towards the column wall. As mentioned in Chapter V-5, radial size distribution was clearly visible in spouted beds of all mixtures in which there was more than two-fold size difference (beds of mixtures of alundum A and B, alundum A, B and C and silica sand). The radial size classification of solids in spouted beds of mixtures of polystyrene A and B ($\rho_s = 65.8 \text{ lb.}_m/\text{ft.}^3$) was also pronounced even though the size difference was less than two. This indicates that the degree of radial classification of solids is inversely proportional to the density of the material. However, as mentioned in Chapter V-5, the radial classification of solids may also depend on the electrostatic potentials existing in the spouted beds.

The adhesion of a layer of fine particles to the column wall, the tendency of the spout to channel towards the column wall and the movement

of the spout around the central axis of the column — all observed markedly in spouted beds of polystyrene — are believed to be caused by electrostatic potentials in the bed created by interparticle and particle-wall collisions.

The qualitative experiments on attrition described in Chapter V-7 indicate that the initial solids-attrition in spouted beds is very high. This initial high rates of solids-attrition appears to be due to the presence of defects, cracks etc. in the particles produced by the comminution process. The attrition after few minutes' runs seems to be very low being caused almost entirely by shearing forces.

CHAPTER VIII

CONCLUSIONS AND RECOMMENDATIONS

Conclusions of the present investigation are listed below:

- (1) The length mean diameter is best suited to represent the data on minimum spouting velocity of mixed size particles. This diameter is suitable for mixtures of granular as well as particulate materials.
- (2) When the length mean diameter of mixed size particles of granular materials, is evaluated, the geometric mean i.e. $3\sqrt{\text{width} \times \text{breadth} \times \text{length}}$ should be used as the characteristic mean diameter of granular materials; and Tyler screen size is sufficient to represent the characteristic diameter of a single size fraction.
- (3) The new dimensionless correlation, Equation VI-14, or dimensional correlation, Equation VI-15, should permit prediction of minimum spouting velocity in a 6" I.D. column, with a degree of accuracy of $\pm 10\%$ for all mixtures in which the size range is not more than 5-fold.
- (4) The Mathur-Gishler correlations, Equation II-8 and II-9, are not quite as accurate in predicting the minimum spouting velocity.
- (5) The new design of inlet adopted permits spouting of material (Ottawa sand, $D_p = 0.025''$) in a system ($D_i = 0.625''$, $D_c = 6''$) in which it was not hitherto spoutable.

Stable spouting at considerably higher bed depths ($\approx 25''$) with very fine particles (mean $D_p = 0.0134''$) was obtained. However, since the same is spoutable with $3/8''$ diameter inlet only in the 6" diameter column, the agitation is feeble. The new design of inlet is recommended because it increases the spoutable size range and stable

spouting even at higher bed depths.

- (6) It appears that spouting is unlikely to occur beyond a critical ratio $\frac{D_1}{D_c}$ of about 0.28.
- (7) The spoutability of mixed particle-size beds decreases with increasing proportions of fine material. Mixtures containing Tyler screen fractions of 10% or greater which differ more than about 5-fold in size do not spout well.
- (8) The observed radial classification of solids in spouted beds with fine particles concentrating near the walls is a complex function of gravitational potential and electrostatic forces and of the physical properties of the bed material.
- (9) Thorough and uniform mixing can be obtained in spouted beds of narrow cut fractions. However, in beds of widely different sized particles, finer particles tend to segregate at the top of the beds during spouting.
- (10) Electrostatic potentials were created during spouting due to inter-particle and particle-wall collisions.
- (11) The solids-attrition rate is initially very high and the same decreases after few minutes' spouting. However, slow and continuous attrition is likely to take place which results in creation of fines in the bed.

It is recommended that

- (1) The effect of column diameter on minimum spouting velocity be investigated and a generalized correlation for predicting the minimum spouting velocity be attempted;
- (2) The effect of mixing, on spoutability, of fine non-spoutable materials with coarse spoutable materials be further studied;
- (3) Quantitative measurements on the effect of electrostatic potentials in the spouted beds be made;
- (4) Quantitative measurements of the solids-attrition rates in spouted beds be conducted, and
- (5) Studies in axial and radial distribution of solids in mixed-size spouted beds be made.

NOMENCLATURE

- a' = dimensional constant, Eq. VI-13
- \hat{a}' = dimensional constant, Eq. VI-4
- A = intercept obtained when Y is plotted against $\frac{H}{D_c}$, dimensionless
- A_1 = Cross-sectional area of the rotameter tube on the downstream side of the float, ft.²
- A_2 = Area of the annulus between the float and the tube, ft.².
- A_c = Cross-sectional area of the column, ft.².
- A_F = Maximum cross-sectional area of the float in a horizontal plane, ft.².
- C = Constant, Eq. VI-9.
- C' = dimensional constant, Eq. VI-15.
- C_D = discharge coefficient, Eqs. III-2 and III-7.
- C_D = drag coefficient, Eq. II-16.
- d_1, d_2, d_3 = particle diameter of uniform size fractions 1,2,3 when referred to particulate materials; ft. or in., width, breadth, and length of granular materials.
- D_c = inside column diameter, ft. or in.
- D_i = inlet-orifice diameter, ft. or in.
- D_d = length mean diameter, ft. or in.; Eq. II-4.
- D'_2 = mean length diameter, ft. or in.; Eq. II-7.
- D_s = surface mean diameter, ft. or in.; Eq. II-3.
- D'_s = mean surface diameter, ft. or in.; Eq. II-6.
- D_w = weight or volume mean diameter, ft. or in. Eq. II-2.
- D'_v = mean volume diameter, ft. or in.; Eq. II-6.
- g = acceleration due to gravity, ft./sec.².
- H = static bed height, ft. or in.
- H_m = maximum spoutable bed height, ft. or in.
- k, k_v, k_s = constants
- m = slope obtained when Y is plotted against $\frac{H}{D_c}$

NOMENCLATURE Continued

- n = exponent on $\frac{D_1}{D_c}$ in Eq. II-9.
- P_1 = standard absolute pressure, lb._F/in.² or in. Hg. , Eq. III-10.
- P_2 = absolute pressure of rotameter downstream air lb._F/in.² or in. Hg. Eq. III-10.
- T_1 = standard temperature °R, Eq. III-10.
- T_2 = temperature of rotameter downstream air, °R, Eq. III-10.
- $(-\Delta P)$ = frictional pressure drop, lb._F/ft.² or in. H₂O.
- Re_m = particle Reynolds Number, $D_p V_p \rho / \mu$
- \dot{v}_1 = volumetric flow rate from Fig. IV-3 or III-4, standard ft.³/minute.
- \dot{v}_2 = volumetric flow rate calculated using Equation III-10 and Fig. III-3 or III-4, standard ft.³/minute.
- V_F = volume of float, ft³.
- V_i = velocity through inlet, ft./sec.
- V_m = superficial minimum spouting velocity at maximum spoutable bed bed depth, ft./sec.
- V_{mf} = minimum fluidization velocity, ft./sec.
- V_s = superficial minimum spouting velocity, ft./sec.
- W = mass rate of flow, lb._m/minute or sec.
- W_1 = mass rate of air flow through rotameter at standard conditions lb._m¹/ft.³
- W_2 = mass rate of air flow when air pressure and temperature are P_2 and T_2 lb._m/ft.³.
- x = weight fraction
- x_1, x_2 = weight fraction of component 1,2.
- Y = $\sqrt{\left| \frac{V_s^2}{gD_p} \right| \left| \frac{D_c}{D_p} \right| \left| \frac{\rho_s}{\rho_s - \rho_f} \right|}$, dimensionless
- s_1 = surface area of a particle of diameter d_1 , ft.² or in.²

NOMENCLATURE Continued

Greek Letters

- μ = air viscosity, $\text{lb}_m./\text{ft}.\text{sec}.$
- θ = included angle of cone at the bottom of cone, degrees.
- α = coefficient of friction between solids and column material.
- ϵ = porosity
- ρ_f = air density, $\text{lb}_m./\text{ft}^3.$
- ρ_{f1} = air density at the standard conditions, $\text{lb}_m./\text{ft}^3.$
- ρ_{f2} = air density at T_2 and P_2 , $\text{lb}_m./\text{ft}^3.$
- ρ_F = density of the material of float, $\text{lb}_m./\text{ft}^3.$
- ρ_s = solid density, $\text{lb}_m./\text{ft}^3.$
- $f(\theta)$ = experimental particle shape factor

REFERENCES

- (1) Gishler, P.E., and Mathur, K.B., A.I. Ch. E. J. 1, 157 (1955).
- (2) Mathur, K.B., and Gishler, P.E., J. Appl. Chem., 5, 620 (1955).
- (3) Becker, H.A., and Sallans, H.R., Chem. Eng. Sci., 13, 97 (1961).
- (4) Klassen, J., and Gishler, P.E., Can. J. Chem. Eng., 36, 12, (1958).
- (5) Ghosh, B., and Osberg, G.L., Can. J. Chem. Eng., 37, 205, (1959).
- (6) Cowan, C.B., Peterson, W.S., and Osberg, G.L., Pulp and Paper Mag. Can., 12, 139, (1957).
- (7) Cowan, C.B., Peterson, W.S., and Osberg, G.L., Can. Eng. J., 41, 60, (1958).
- (8) Thorley, B., Saunby, J.B., Mathur, K.B., and Osberg, G.L., Can. J. Chem. Eng., 37, 184, (1959).
- (9) Becker, H.A., Chem. Eng. Sci., 13, 245, (1961).
- (10) Madonna, L.A., Lama, R.F., and Brisson, W.L., Brit. Chem. Eng., 6, 524, (1961).
- (11) Madonna, L.A., Lama, R.F., Ind. Eng. Chem. 52, 169, (1960).
- (12) Peterson, W.S., Can. J. Chem. Eng., 40, 226, (1962).
- (13) Buchanan, R.H., and Manurung, F., Brit. Chem. Eng., 6, 402, (1961).
- (14) Buchanan, R.H., and Manurung, F., Private Communication.
- (15) Thorley, B., Mathur, K.B., Klassen, J., and Gishler, P.E. (Not Published) N. R. C. Progress Report.
- (16) Leva, M., Shirai, T., and Wen, C.Y., Genie Chimique 75, 33, (1956).
- (17) Liang-Tseng Fan., and Charles.J. Swartz., Can. J. Chem. Eng., 37, 204 (1955).
- (18) Leva, M., "Fluidization", pp 48-61, McGraw Hill Book Co. Ltd., New York, (1959).
- (19) Ibid., pp 180-269.
- (20) Rausch, J.M. Ph.D. Thesis, Princeton University, 1948, As quoted by Leva, M., "Fluidization", pp 158-159, McGraw Hill Book Co. Ltd., New York (1959).
- (21) Koyanagi, M., B.A.Sc., Thesis, Univ. Brit. Col. (1955).
- (22) Lowrie-Fairs, G., Trans. Inst. Chem. Eng. 28, 110 (1940).
- (23) Coulson, J.M., and Richardson, J.F., "Chemical Engineering", Vol. 1, pp 93-95, Pergamon Press, London (1954).

REFERENCES Continued

- (24) Linford, A., "Flow Measurement and Meters" (Spon, 1949), As quoted by Coulson, J.M., and Richardson, J.F., "Chemical Engineering", Vol. 1, 94, Pergamon Press, London, (1954).
- (25) Ciborowski, J., and Wlodarski, W., Chem. Eng. Sci., 17, 23 (1962).

APPENDIX 1

EQUIPMENT DETAILS

(a) PRESSURE REGULATING VALVE

Type: Masoneilan

Manufacturer: Masoneilan

Division of Worthington Corporation

Mass., U. S. A.

Size: 1 1/4"

Operation: Direct operated, spring loaded. Operated directly by reduced pressure acting on the underside of the diaphragm. An increase in pressure closes the valve. A decrease permits the spring to open the valve.

Specifications:

Body:

Connections: Screwed

Material: Bronze

Rating: 150 p.s.i. @ 100°F

Valve: Renewable Composition Disc.

Diaphragm: Neoprene

Capacity:

Inlet Pressure p.s.i.g.	Outlet Pressure p.s.i.g.	Air Flow S.C.F.M.
50	10 - 20	185
	30	170
	40	130

(b) ROTAMETER-1

Manufacturer: Rotameter Manufacturing Co., England

Type: 907

Tube Size (Metric): 35

Float Type: K, Korannite

Full Capacity: 32 cu. ft./minute air at 14.7 p.s.i.a. pressure and
59°F temperature

Minimum Reading: 1/10 of the full capacity

Pressure Loss: 8.2 cm. Water

Tolerances:

Tube: 1%

Float: 2%

Accuracy: 3% of full scale

Maximum deviation at any scale reading: 2.30%

(c) ROTAMETER-2

Manufacturer: Rotameter Manufacturing Co., England

Type: 907

Tube Size (Metric): 65

Float Type: K, Korannite

Full Capacity: 124 cu. ft./minute air at 14.7 p.s.i.a. pressure and
59°F temperature

Minimum Reading: 1/10 of the full capacity

Pressure Loss: 13 cm. water

Tolerances:

Tube: 1%

Float: 2%

Accuracy: 3% of full scale reading

Maximum deviation at any scale reading, (below 9 cm.): 3.10%

APPENDIX 2

CALIBRATION DATA

(a) ROTAMETER-1

Air Temperature: 71°F

Tube Reading cm.	Downstream Air Pressure (gauge)		Volume in S.C.F.M. Calculated using Eq. III-10 and Calibration Chart Fig. III-3:	Volume in S.C.F.M. Measured by Dia- phragm Meter/Vane Anemometer	% Deviation of the Value Cal- culated from the Measured
	in.Hg.	p.s.i.			
1	0.2		4.84	4.84	0.0
1	0.2		4.84	4.79	+1.28
2	0.2		5.90	5.96	-1.00
2		28	10.20	10.10	+1.00
3	0.2		6.89	6.89	0.00
3		19	10.45	10.45	0.00
4.5	0.3		8.02	7.98	+0.50
4.9		5	9.95	10.20	-0.70
5	0.4		9.04	9.07	-0.33
5	15.0		11.05	11.15	-0.90
5		10	11.72	11.68	+0.34
6	0.4		10.15	10.25	-0.98
6	13.0		12.20	12.25	-0.41
7	0.5		11.30	11.30	0.00
8	0.7		12.45	12.50	-0.40
10	0.7		14.80	14.80	0.00
10		20	22.80	23.10	-1.30
15	1.5		21.40	21.95	-2.50
19	2.5		27.20	27.40	-0.73
20		10	35.60	34.80	+2.30

APPENDIX 2 Continued

(b) ROTAMETER-2

Air Temperature: 71°F

Tube Reading cm.	Downstream Air Pressure (gauge)		Volume in S.C.F.M. Calculated using Eq. III-10 and Calibration Chart Fig. III-4.	Volume in S.C.F.M. Measured by Dia- phragm Meter/Vane Anemometer	% Deviation of the Value Cal- culated from the Measured
	in.Hg.	p.s.i.			
1.5		10	23.9	24.1	-0.83
2	12.8		24.4	25.1	-2.79
2.9	2.4		27.0	26.2	+3.05
3	6.6		27.0	26.4	+2.27
4	3.8		30.4	31.0	-1.98
4	17.4		36.4	35.3	+3.10
5		14	46.6	47.0	-0.85
7.1		5	49.2	49.6	-0.81
9		6	60.6	61.0	-0.66

APPENDIX 3

CALCULATED DATA

(a) DATA OF 3/4" INLET.

$$Y = \sqrt{\left(\frac{V_s^2}{gD_p}\right) \left(\frac{D_c}{D_p}\right) \left(\frac{e_f}{e_s - e_f}\right)}$$

$$A = 0.64 + 26.8 \left(\frac{D_i}{D_c}\right)^2$$

$$m = 0.50 - 1.76 \left(\frac{D_i}{D_c}\right)$$

Run No.	Y	$\frac{H}{D_c}$	$A \left(\frac{H}{D_c}\right)^m$	$\frac{V_s \text{ (Predicted)}}{V_s \text{ (Observed)}}$
A-2 (a)	1.10	1.90	1.268	1.15
A-2 (b)	1.348	2.958	1.437	1.066
A-2 (c)	1.426	3.583	1.51	1.059
A-2 (d)	1.509	4.125	1.576	1.044
A-2 (e)	1.551	4.833	1.647	1.06
A-2 (f)	1.624	5.367	1.696	1.044
A-2 (g)	1.674	5.833	1.737	1.038
A-6 (a)	1.258	1.867	1.262	1.003
A-6 (b)	1.386	2.75	1.408	1.015
A-6 (c)	1.517	3.625	1.521	1.003
A-6 (d)	1.549	4.042	1.567	1.012
A-6 (e)	1.659	5.0	1.66	1.00
A-6 (f)	1.714	5.8	1.73	1.009

APPENDIX 3(a) Continued

Run No.	Y	$\frac{H}{D_c}$	$A \left \frac{H}{D_c} \right ^m$	$\frac{V_s \text{ (Predicted)}}{V_s \text{ (Observed)}}$
A-7 (a)	1.412	2.50	1.37	0.97
A-7 (b)	1.496	2.95	1.435	0.959
A-7 (c)	1.635	3.817	1.543	0.944
A-7 (d)	1.728	4.717	1.637	0.947
A-7 (e)	1.819	5.567	1.714	0.942
A-7 (f)	2.002	6.467	1.79	0.895
A-8 (a)	1.322	1.583	1.205	0.911
A-8 (b)	1.401	2.375	1.351	0.964
A-8 (c)	1.465	3.208	1.47	1.003
A-8 (d)	1.56	4.042	1.57	1.006
A-8 (e)	1.648	4.875	1.65	1.001
A-8 (f)	1.694	5.292	1.69	0.998
A-8 (g)	1.768	5.708	1.73	0.979
A-9 (a)	1.319	1.65	1.219	0.924
A-9 (b)	1.396	2.317	1.341	0.96
A-9 (c)	1.482	3.0	1.442	0.973
A-9 (d)	1.552	3.708	1.53	0.986
A-9 (e)	1.593	4.033	1.57	0.986
A-9 (f)	1.621	4.433	1.61	0.993
A-9 (g)	1.662	5.133	1.68	1.011
A-10(a)	1.222	1.633	1.216	0.995
A-10(b)	1.339	2.217	1.325	0.99
A-10(c)	1.448	2.767	1.41	0.974
A-10(d)	1.489	3.317	1.48	0.994
A-10(e)	1.537	3.883	1.55	1.008
A-10(f)	1.623	4.167	1.58	0.974
A-10(g)	1.64	4.792	1.64	1.0
A-10(h)	1.653	5.05	1.67	1.01
A-10(i)	1.733	5.667	1.723	0.994
A-16(a)	1.292	1.833	1.256	0.972
A-16(b)	1.325	2.0	1.287	0.971
A-16(c)	1.392	2.35	1.347	0.968
A-16(d)	1.446	2.708	1.401	0.969
A-16(e)	1.525	3.083	1.452	0.952
A-16(f)	1.583	3.458	1.50	0.948
A-16(g)	1.603	3.791	1.54	0.961
A-16(h)	1.645	4.167	1.58	0.96
A-16(i)	1.673	4.533	1.62	0.968

APPENDIX 3(a) Continued

Run No.	Y	$\frac{H}{D_c}$	$A \left(\frac{H}{D_c} \right)^m$	$\frac{V_s \text{ (Predicted)}}{V_s \text{ (Observed)}}$
A-17(a)	1.068	1.333	1.15	1.077
A-17(b)	1.215	1.60	1.21	0.995
A-17(c)	1.28	1.875	1.26	0.984
A-17(d)	1.329	2.133	1.31	0.987
A-17(e)	1.369	2.375	1.35	0.987
A-17(f)	1.464	3.0	1.44	0.984
A-17(g)	1.544	3.791	1.54	0.991
A-17(h)	1.588	4.35	1.60	1.008
A-17(i)	1.646	4.917	1.66	1.009
A-17(j)	1.658	5.167	1.68	1.013
A-18(a)	0.914	1.25	1.12	1.226
A-18(b)	1.092	1.625	1.21	1.11
A-18(c)	1.233	2.0	1.28	1.04
A-18(d)	1.277	2.35	1.347	1.055
A-18(e)	1.308	2.71	1.40	1.07
A-18(f)	1.355	3.1	1.45	1.07
A-18(g)	1.452	3.833	1.54	1.04
A-18(h)	1.54	4.541	1.62	1.05
A-18(i)	1.556	4.917	1.65	1.06
A-18(j)	1.571	5.292	1.696	1.08
A-18(k)	1.591	5.67	1.72	1.08
A-18(l)	1.609	6.03	1.76	1.094
P-1 (a)	1.23	1.97	1.28	1.04
P-1 (b)	1.29	2.82	1.42	1.10
P-1 (c)	1.33	3.54	1.51	1.135
P-1 (d)	1.37	4.0	1.56	1.140
P-1 (e)	1.425	4.133	1.59	1.116
P-10(a)	1.60	5.667	1.72	1.075
S-1 (a)	1.01	1.375	1.158	1.147
S-1 (b)	1.21	2.017	1.29	1.066
S-1 (c)	1.38	2.373	1.34	0.971
S-1 (d)	1.44	3.375	1.49	1.035
S-1 (e)	1.49	3.958	1.56	1.047
S-1 (f)	1.54	4.542	1.62	1.052
S-1 (g)	1.60	5.167	1.68	1.05
S-1 (h)	1.645	5.625	1.72	1.046
S-1 (i)	1.665	6.167	1.76	1.057

APPENDIX 3(a) Continued

Run No.	Y	$\frac{H}{D_c}$	$A \left(\frac{H}{D_c} \right)^m$	$\frac{V_s \text{ (Predicted)}}{V_s \text{ (Observed)}}$
C-1 (a)	1.018	1.5	1.18	1.159
C-1 (b)	1.228	1.925	1.28	1.042
C-1 (c)	1.351	2.433	1.36	1.006
C-1 (d)	1.45	2.88	1.42	0.979
C-1 (e)	1.59	3.88	1.55	0.975
C-1 (f)	1.633	4.38	1.60	0.98
C-1 (g)	1.691	4.88	1.65	0.976
C-1 (h)	1.734	5.33	1.69	0.975
C-1 (i)	1.782	5.8	1.73	0.971

(b) DATA OF 5/8" INLET

Run No.	Y	$\frac{H}{D_c}$	$A \left(\frac{H}{D_c} \right)^m$	$\frac{V_s \text{ (Predicted)}}{V_s \text{ (Observed)}}$
A-1 (a)	1.012	1.197	1.144	1.13
A-1 (b)	1.15	2.417	1.231	1.07
A-1 (c)	1.317	2.967	1.314	0.998
A-1 (d)	1.404	3.867	1.43	1.019
A-1 (e)	1.472	4.883	1.539	1.046
A-1 (f)	1.559	5.542	1.602	1.028
A-1 (g)	1.595	5.967	1.64	1.028
A-1 (h)	1.62	6.517	1.686	1.041
A-11(a)	1.20	1.625	1.084	0.903
A-11(b)	1.24	1.958	1.15	0.927
A-11(c)	1.299	2.292	1.209	0.931
A-11(d)	1.406	2.667	1.269	0.903
A-11(e)	1.472	3.417	1.377	0.935
A-11(f)	1.502	3.80	1.42	0.945
A-12(a)	1.485	1.875	1.135	0.765
A-12(b)	1.665	2.375	1.223	0.735

Run No.	Y	$\frac{H}{D_c}$	$A \left(\frac{H}{D_c} \right)^m$	$\frac{V_s \text{ (Predicted)}}{V_s \text{ (Observed)}}$
P-2 (a)	1.055	1.667	1.095	1.038
P-2 (b)	1.168	2.21	1.197	1.025
P-2 (c)	1.212	2.63	1.264	1.043
P-2 (d)	1.255	3.13	1.336	1.064
P-2 (e)	1.325	3.88	1.43	1.08
P-2 (f)	1.425	4.25	1.473	1.034
P-2 (g)	1.475	4.76	1.526	1.035
P-2 (h)	1.528	5.46	1.594	1.043
P-11(a)	1.552	5.667	1.61	1.037
0-2 (a)	1.0	1.6	1.08	1.08
0-2 (b)	1.195	2.4	1.229	1.028
0-2 (c)	1.365	3.04	1.325	0.971
0-2 (d)	1.45	3.92	1.434	0.989
0-2 (e)	1.522	4.333	1.482	0.974
0-2 (f)	1.545	4.833	1.533	0.992
0-2 (g)	1.515	5.25	1.575	1.04
0-2 (h)	1.60	5.7	1.626	1.016

(c) DATA OF 1/2" INLET

Run No.	Y	$\frac{H}{D_c}$	$A \left(\frac{H}{D_c} \right)^m$	$\frac{V_s \text{ (Predicted)}}{V_s \text{ (Observed)}}$
P-3 (a)	1.041	1.92	1.039	0.998
P-3 (b)	1.165	2.33	1.114	0.956
P-3 (c)	1.235	3.09	1.229	0.995
P-3 (d)	1.266	3.5	1.286	1.016
P-3 (e)	1.293	4.0	1.347	1.042
P-3 (f)	1.449	5.0	1.458	1.006

APPENDIX 3(c) Continued

Run No.	Y	$\frac{H}{D_c}$	$A \left(\frac{H}{D_c} \right)^m$	$\frac{V_s \text{ (Predicted)}}{V_s \text{ (Observed)}}$
P-5 (a)	1.0	1.835	1.023	1.023
P-5 (b)	1.147	2.52	1.144	0.997
P-5 (c)	1.215	3.185	1.243	0.941
P-5 (d)	1.326	3.92	1.338	1.009
P-5 (e)	1.47	5.0	1.458	0.992
P-5 (f)	1.568	6.04	1.559	0.994
P-6 (a)	1.05	1.875	1.032	0.983
P-6 (b)	1.179	2.583	1.155	0.98
P-6 (c)	1.286	3.25	1.253	0.974
P-6 (d)	1.363	3.96	1.343	0.985
P-6 (e)	1.45	4.667	1.423	0.981
P-6 (f)	1.539	5.375	1.496	0.972
P-6 (g)	1.65	6.083	1.562	0.947
P-7 (a)	1.056	1.917	1.039	0.984
P-7 (b)	1.251	2.792	1.187	0.949
P-7 (c)	1.34	3.625	1.302	0.972
P-7 (d)	1.447	4.542	1.409	0.974
P-7 (e)	1.535	5.0	1.458	0.95
P-7 (f)	1.614	5.667	1.524	0.944
P-7 (g)	1.72	6.083	1.562	0.908
P-8 (a)	0.967	1.708	0.998	1.032
P-8 (b)	1.033	2.25	1.1	1.016
P-8 (c)	1.218	2.833	1.193	0.979
P-8 (d)	1.277	3.375	1.269	0.994
P-8 (e)	1.355	4.0	1.347	0.994
P-8 (f)	1.491	5.167	1.475	0.989
P-8 (g)	1.618	6.313	1.585	0.98
P-9 (a)	1.048	1.98	1.052	1.004
P-9 (b)	1.132	2.75	1.181	1.043
P-9 (c)	1.338	4.125	1.362	1.018
P-9 (d)	1.529	5.667	1.524	0.997
P-13(a)	0.998	1.708	0.998	1.00
P-13(b)	1.097	2.29	1.097	1.009
P-13(c)	1.18	2.875	1.18	1.017
P-13(d)	1.24	3.417	1.24	1.028
P-13(e)	1.347	4.08	1.347	1.008
P-13(f)	1.41	4.67	1.41	1.009
P-13(g)	1.474	5.29	1.474	1.009

Run No.	Y	$\frac{H}{D_c}$	$A \left(\frac{H}{D_c} \right)^m$	$\frac{V_s \text{ (Predicted)}}{V_s \text{ (Observed)}}$
A-3 (a)	1.187	2.873	1.166	0.982
A-3 (b)	1.472	4.933	1.451	0.986
A-3 (c)	1.542	6.04	1.559	1.011
O-1 (a)	1.0	1.833	1.023	1.023
O-1 (b)	1.122	2.433	1.131	1.008
O-1 (c)	1.221	3.08	1.23	1.007
O-1 (d)	1.28	3.833	1.328	1.038
O-1 (e)	1.315	4.5	1.404	1.068
O-1 (f)	1.25	5.0	1.458	1.166
O-1 (g)	1.49	5.717	1.529	1.026
O-1 (h)	1.505	6.0	1.555	1.033

(d) DATA OF 3/8" INLET

Run No.	Y	$\frac{H}{D_c}$	$A \left(\frac{H}{D_c} \right)^m$	$\frac{V_s \text{ (Predicted)}}{V_s \text{ (Observed)}}$
A-4 (a)	1.056	2.7	1.097	1.039
A-4 (b)	1.397	4.833	1.377	0.986
A-4 (c)	1.486	5.96	1.494	1.005
A-5 (a)	0.938	1.833	0.943	1.005
A-5 (b)	1.043	2.33	1.037	0.994
A-5 (c)	1.24	3.37	1.196	0.965
A-5 (d)	1.31	4.217	1.306	0.997
A-5 (e)	1.42	5.167	1.413	0.995
A-5 (f)	1.495	6.05	1.503	1.005
A-13(a)	0.915	2.167	1.007	1.10
A-13(b)	1.038	2.79	1.111	1.07
A-13(c)	1.11	3.46	1.209	1.09
A-13(d)	1.16	3.78	1.252	1.08
A-14(a)	0.947	1.567	0.887	0.937
A-14(b)	1.16	2.25	1.022	0.881
A-14(c)	1.56	3.29	1.186	0.76
A-14(d)	1.805	4.08	1.289	0.714
A-14(e)	1.99	4.63	1.354	0.68

APPENDIX 3(a) Continued

Run No.	Y	$\frac{H}{D_c}$	$A \left(\frac{H}{D_c} \right)^m$	$\frac{V_s \text{ (Predicted)}}{V_s \text{ (Observed)}}$
A-15(a)	1.05	1.55	0.884	0.842
A-15(b)	1.16	2.21	1.015	0.875
A-15(c)	1.22	2.833	1.118	0.916
P-4 (a)	1.085	2.0	0.976	0.90
P-4 (b)	1.171	2.79	1.112	0.95
P-4 (c)	1.265	3.67	1.236	0.977
P-4 (d)	1.372	4.27	1.312	0.956
P-4 (e)	1.517	5.67	1.465	0.966
P-12(a)	1.425	5.5	1.448	1.016

APPENDIX 4DATA OF PREVIOUS WORKERS(a) DATA OF BUCHANAN AND MANURUNG (14)

Run No.	V_s Predicted by Eq. VI-14 (ft./sec.)	V_s Experimental (ft./sec.)	% Deviation of the V_s Predicted from the Experimental
40	2.175	2.13	+ 2.0
40a	2.49	2.26	+10.0
40b	2.80	2.82	- 0.7
40c	2.98	3.02	- 1.3
40d	3.12	3.16	- 1.3
40e	3.19	3.22	- 1.0
43	1.86	1.58	+18.0
43a	2.28	2.02	+12.0
43b	2.60	2.34	+11.0
43c	2.75	2.41	+14.0
43d	2.85	2.50	+14.0
43e	3.0	2.52	+19.0
43f	3.1	2.70	+14.0
44	0.69	0.76	- 0.9
44a	0.86	1.0	-14.0
44b	0.98	1.06	- 7.0
44c	1.07	1.18	- 9.3
44d	1.15	1.24	- 7.0
44e	1.22	1.29	- 5.0
52	0.726	0.85	-14.6
53	0.735	0.94	-22.0
45	0.746	0.92	-19.0
46	0.765	0.99	-23.0
47	0.794	1.12	-29.0
48	0.869	1.29	-33.0
49	1.04	1.51	-31.0
51	1.30	1.87	-30.0
50	2.29	2.26	+ 1.4

APPENDIX 4 Continued

(b) DATA OF MATHUR AND GISHLER (1)

$$D_c = 6''$$

$$D_i = 0.493''$$

$$\text{Cone Angle} = 85^\circ$$

Material	Bed Height in.	V_s Predicted by Eq. VI-14 (ft./sec.)	V_s Experimental (ft./sec)	% Deviation of V_s Pre- dicted for the Experimental
Mustard Seeds	34.0	2.72	2.57	+ 6.0
Rape Seeds	30.0	2.01	2.01	0.0
Peas	12.0	5.90	5.31	+11.1
Ottawa Sand	27.0	0.94	0.75	+25.33
Shale	36.0	1.65	1.21	+36.0
Gravel	25.0	5.87	4.31	+36.0
Gravel	46.0	3.63	3.27	+11.1
Peas	12.0	5.87	5.33	+10.0
Peas	10.0	5.53	4.76	+16.0
Peas	8.0	5.20	4.15	+25.0
Mustard Seeds	30.0	2.60	2.54	+ 2.0
Mustard Seeds	24.0	2.40	2.19	+ 9.6
Mustard Seeds	18.0	2.16	1.82	+18.6
Mustard Seeds	12.0	1.87	1.44	+29.8
Rape Seeds	30.0	2.01	2.02	- 0.5
Rape Seeds	24.0	1.85	1.72	+ 8.0
Rape Seeds	18.0	1.68	1.44	+17.0
Rape Seeds	12.0	1.46	1.15	+27.0
Ottawa Sand	24.0	0.90	0.74	+22.0
Ottawa Sand	20.0	0.85	0.68	+25.0
Ottawa Sand	16.0	0.79	0.61	+29.0
Ottawa Sand	12.0	0.71	0.55	+29.0
Gravel	24.5	5.95	4.67	+27.0
Gravel	35.6	3.30	3.18	+ 4.0
Gravel	48.5	2.07	1.72	+20.0

APPENDIX 5SAMPLE CALCULATIONS(a) MINIMUM SPOUTING VELOCITY

The minimum spouting velocity was calculated from the observed readings as follows:

- (i) The flow rate v_2 , in S. C. F. M. was calculated by making use of the calibration chart (Figure III-3 for rotameter-1, Figure III-4 for rotameter-2) and Equation III-10 derived in Chapter III-5(c).
- (ii) The flow rate v_2 was converted to the flow rate in C. F. M. at the average conditions of pressure and temperature in the test column.
- (iii) From the flow rate obtained in step (ii) above, the superficial minimum spouting velocity was then calculated.

For Run No. S-1(e), the calculations are given below.

Run No. S-1(e)

- | | |
|---|---------------------------------------|
| (i) Rotameter-1 tube reading | = 13.5 cm. |
| Flow rate from Figure III-3 at
the calibration conditions, i.e.,
14.7 p.s.i.a. and 59°F | = 18.93 C.F.M. = v_1 |
| Rotameter downstream air
pressure, gauge | = 2.2" Hg. |
| Barometric pressure | = 758 mm. Hg = 29.83" Hg. |
| Downstream air pressure, absolute | = 29.84 + 2.2"
= 32.04" Hg = P_2 |
| Rotameter downstream air temperature | = 72°F = 532°R = T_2 |

Pressure at which the calibration chart Fig. III-3 is applicable = 14.7 p.s.i.a.
 = 29.92" Hg. = P_1

Temperature at which the calibration chart, Fig. III-3, is applicable = 59°F
 = 519°R = T_1

$$V_2 = V_1 \sqrt{\frac{T_1 \cdot P_2}{T_2 \cdot P_1}} \quad \text{(III-10)}$$

Substituting the values of V_1 , T_1 , P_1 , P_2 and T_2 in Equation III-10 one gets

$$V_2 = 18.93 \sqrt{\frac{519 \times 32.04}{532 \times 29.92}} = \underline{\underline{19.35 \text{ S.C.M.}}}$$

(ii) Pressure drop across the bed = 11.8" CCl_4 = 1.38" Hg = ΔP
 Average air pressure in the bed = Barometric pressure + 1/2 ΔP
 = 29.84" + 1/2(1.38") = 30.53" Hg

Average air temperature is assumed to be equal to that of rotameter

downstream temperature = 532°R

Air flow rate obtained in (i) above = 19.35 S.C.F.M,

(Standard conditions are 29.92" Hg. pressure and 519°R. temperature)

Air flow rate at the average bed conditions, i.e., 30.53" Hg.

pressure and 532°R. temperature (Ideal gas-law was applied here)

$$= 19.35 \times \frac{29.92}{30.53} \times \frac{532}{519}$$

$$= \underline{\underline{19.42 \text{ C.F.M.}}}$$

(iii) Column diameter = 6" = 0.5'

Cross sectional area of the column = $\pi \times \frac{(0.5)^2}{4}$
 = 0.1963 ft.² = A_c

Minimum spouting velocity = $\frac{\text{C.F.M.}}{60} \times \frac{1}{A_c}$
 = $\frac{19.42}{60} \times \frac{1}{0.1963} = \underline{\underline{1.65 \text{ ft./sec.}}}$

(b) LENGTH MEAN DIAMETER

The length mean diameter is defined by

$$D_p = \frac{\sum \frac{x_1}{d_1}}{\sum \frac{x_1}{d_1^2}} \quad (\text{II-4})$$

For Run No. S-1(e), the material used is silica sand. From the screen analysis given in Table IV-1, the length mean D_p is calculated below.

$$D_p = \frac{\frac{0.091}{0.06} + \frac{0.263}{0.0505} + \frac{0.221}{0.0425} + \frac{0.163}{0.0359} + \frac{0.11}{0.0302} + \frac{0.152}{0.0254}}{\frac{0.091}{(0.06)^2} + \frac{0.263}{(0.0505)^2} + \frac{0.221}{(0.0425)^2} + \frac{0.163}{(0.0359)^2} + \frac{0.11}{(0.0302)^2} + \frac{0.152}{(0.0254)^2}}$$

= 0.0356"

(c) MINIMUM SPOUTING VELOCITY BY EQUATIONS VI-14 AND VI-15

(i) Rewriting Equation VI-14, one gets

$$V_s = D_p \times \sqrt{\frac{g(\rho_s - \rho_f)}{\rho_f} \cdot \frac{1}{D_c}} \times \left[0.64 + 26.8 \left(\frac{D_i}{D_c} \right)^2 \right]^{0.50-1.76} \left(\frac{D_i}{D_c} \right)$$

For Run No. S-1(e)

$$D_p = 0.0356'' = \left(\frac{0.0356}{12} \right) \text{ ft.}$$

$$\rho_s = 165.0 \text{ lb}_m/\text{ft.}^3$$

$$\rho_f = 0.0762 \text{ lb.}/\text{ft.}^3$$

(at average
bed conditions)

$$D_i = 3/4'' = 1/16'$$

$$D_c = 6'' = 0.5'$$

$$H = 23.75'' = \left(\frac{23.75}{12} \right) \text{ ft.}$$

$$g = 32.14 \text{ ft./sec.}^2$$

(at Vancouver)

Substituting all these values in the above equation, one gets,

$$V_s = \frac{0.0356}{12} \times \sqrt{\frac{32.14 (165.0 - 0.0762)}{0.0762 \times 0.5}} \times \left[0.64 + 26.8 \left(\frac{1}{8} \right)^2 \right] \\ \times \left(\frac{23.75}{12 \times 0.5} \right)^{0.50} - 1.76 \left(\frac{1}{8} \right)$$

Solution of the above yields,

$$V_s = \underline{1.725} \text{ ft./sec.}$$

Ratio of V_s predicted to V_s observed is

$$\frac{1.725}{1.65} = \underline{1.047} ;$$

i.e., the deviation of the predicted value is +4.7% from the experimental.

(ii) The dimensional Equation VI-15 is given below:-

$$V_s = \left[\frac{D_p \left(0.905 + 152 D_i^2 \right)}{(2H)^{3.52 D_i}} \right] \times \sqrt{\frac{2g H (e_s - e_f)}{\rho_f}}$$

Substitution of the values of D_p , D_i etc., in the above equation yields

$$V_s = \left[\frac{0.0356}{12} \times \frac{\left(0.905 + 152 \times \left(\frac{1}{16} \right)^2 \right)}{\left(\frac{2 \times 23.75}{12} \right)^{3.52 \times \frac{1}{16}}} \right] \times \sqrt{\frac{2 \times 32.14 \times 23.75 \times 165}{12 \times 0.0762}}$$

$$= \underline{1.725} \text{ ft./sec.}$$